

https://dspace.org/

Structural analysis and co-crystallization of neurotransmitter analogues

Reece, Hayley A.

2009-05-20T13:51:47Z
http://hdl.handle.net/10539/6959

Downloaded from a DSpace repository. https://dspace.org/

STRUCTURAL ANALYSIS AND CO–CRYSTALLIZATION OF NEUROTRANSMITTER ANALOGUES

By

Hayley A. Reece

A dissertation submitted to the Faculty of Science, University of the Witwatersrand, Johannesburg, in fulfillment of the requirements for the degree of

Master of Science

Johannesburg, January 2008

Declaration

I declare that this dissertation is my own, unaided work. It is being submitted for the degree of Master of Science in the University of the Witwatersrand, Johannesburg. It has not been submitted before for any degree or examination in any other university.

_____

(Signature of candidate)

_____ day of _____200_____.

Abstract

In recent years, the amino acid neurotransmitter γ-aminobutyric acid (GABA) has been widely studied for its significant inhibitory action in the central nervous system. Two polymorphs of GABA with different crystal systems have been reported in literature. A novel GABA solvate has been crystallized as thin needle-like single crystals. Through X-ray single crystal diffraction analysis, this solvate was found to have a hexagonal crystal system and contain disordered solvent molecules in the asymmetric unit, which are found in channels created by the GABA molecules. ^{1}H NMR allowed for the solvent to be identified as ethanol. This hexagonal GABA solvate is unique in that it is the first single amino acid to be crystallized in this form, where it has hexagonal channels which contain solvent molecules.

Gabapentin (1-(aminomethyl)cycloheaxaneacetic acid) is a drug compound which is structurally related to GABA. It has been extensively studied due to interest in possible polymorphs and gabapentin analogues. Gabapentin exists as a zwitterion in the solid state. The crystal structures and bonding networks of two new monoclinic polymorphs (β- and γ-gabapentin) were studied using x-ray powder and single crystal diffraction. These polymorphs were compared with a previously reported gabapentin polymorph (α-gabapentin). All three polymorphs have extensive hydrogen bonding between the NH_3^+ and COO^- groups of neighbouring molecules, with the β-gabapentin polymorph containing an additional weak intramoleular hydrogen bond.

There have also been a number of reported studies on the co-crystallization of amino acids with various carboxylic acids. A significant feature in the co-crystallization of amino-carboxylic acid complexes includes the ionization states of the individual compounds used. The co-crystallization of neurotransmitter amino acids and their analogues with oxalic acid were carried out. Co-crystals of GABA-oxalic acid, gabapentin-oxalic acid and β-alanine-oxalic acid-water were formed at specific pH values. The crystal structures and hydrogen bonding networks of the co-crystals were analysed using X-ray diffraction techniques.

Thermal analysis was carried out on all the structures as a means of comparing the melting points of different polymorphs and examining the possibility of phase transitions for each structure.

Acknowledgements

I would like to thank:

- My supervisor, Professor D. C. Levendis for all his continued assistance and guidance throughout this project.

- The following people for all their assistance:

  Dr. M. Fernandes
  Prof. D. Billing
  Gareth Morgans

- My parents Mike and Lyn for all their support.

Publication and Conferences

A part of this dissertation has been accepted for publication and presented at two conferences:

Reece, H.A., Levendis, D.C. (2008). Acta Cryst., C64 , 105-108.

24th European crystallographic meeting, Marrakech, Morroco, 22-27 August 2007.

2nd Annual Symposium of the Biomaterials Association of South Africa, University of the Witwatersrand, Johannesburg, 26th November 2007.

Table of Contents

Declaration i
Abstract ii
Acknowledgements iv
Publication and Conferences iv
Table of contents v
List of Figures ix
List of Tables xiii

Chapter 1- Introduction 1

1.1 Amino Acids 1
1.2 Neurotransmitters 2
1.3 Zwitterionic Form 3
1.4 Hydrogen Bonding 3
1.5 Polymorphism 4
1.6 Co-crystals 7
1.7 Aims of Project 8
1.8 Chapter 1 References 9

Chapter 2 - Experimental Techniques 12

2.1. Introduction 12
2.2. Crystallization techniques 12
2.3. X-ray Diffraction 13
2.3.1. X-ray Powder Diffraction 13
2.3.2. X-ray Single Crystal Diffraction 14
2.4. Thermal Analysis 16
2.4.1. Hot Stage Microscopy 16

2.4.2. Differential Scanning Calorimetry 16
2.5. ^{1}H Nuclear Magnetic Resonance (NMR) Spectroscopy 17
2.6. Chapter 2 References 18

Chapter 3 γ- Aminobutyric Acid(GABA) 20

3.1. Introduction and related work 20
3.2. Hexagonal GABA and published polymorphs 21
3.2.1. Experimental 21
3.2.2. Visual comparison of GABA forms 22
3.2.3. X-ray Powder Diffraction 23
3.2.4. X-ray Single Crystal Diffraction 24
3.2.5. Hydrogen Bonding 28
3.2.6. Thermal Analysis 32
3.3. Further Characterisation of the GABA Solvate 33
3.3.1. Hot Stage Microscopy 33
3.3.2. Nuclear Magnetic Resonance (^{1}H NMR) Spectroscopy 34
3.4. Further Experimentation 36
3.5. Discussion and Conclusion 38
3.6. Chapter 3 References 40

Chapter 4 Gabapentin 41

4.1. Introduction and related work 41
4.2. Hexagonal GABA and published polymorphs 43
4.2.1. Experimental 43
4.2.2. Visual comparison of gabapentin polymorphs 43
4.2.3. X-ray Powder Diffraction 44
4.2.4. X-ray Single Crystal Diffraction 46
4.2.5. Hydrogen Bonding 49
4.3. Thermal Analysis 53
4.4. Molecular Modeling 59

4.5. Discussion and Conclusion 60
4.6. Chapter 4 References 61

Chapter 5 Co-crystals 63

5.1. Introduction and related work 63
5.2. Co-crystals of Glycine and Oxalic acid 67
5.2.1. Introduction 67
5.2.2. Experimental 68
5.2.3. X-ray Powder Diffraction 69
5.2.4. Discussion and Conclusion 70
5.3. Co-crystals of GABA and Oxalic Acid 71
5.3.1. Introduction 71
5.3.2. Experimental 72
5.3.3. Microscopic analysis of crystals formed 72
5.3.4. X-ray Powder Diffraction 73
5.3.5. X-ray Single Crystal Diffraction 74
5.3.6. Hydrogen Bonding 76
5.3.7. Thermal Analysis 81
5.3.8. Discussion and Conclusion 82
5.4. Co-crystals of Gabapentin and Oxalic Acid 84
5.4.1. Introduction 84
5.4.2. Experimental 84
5.4.3. Microscopic analysis of crystals formed 85
5.4.4. X-ray Powder Diffraction 85
5.4.5. X-ray Single Crystal Diffraction 87
5.4.6. Hydrogen Bonding 90
5.4.7. Thermal Analysis 94
5.4.8. Discussion and Conclusion 95
5.5. Co-crystals of β-alanine and Oxalic Acid 97
5.5.1. Introduction 97
5.5.2. Experimental 98

5.5.3. Microscopic analysis of crystals formed 98
5.5.4. X-ray Powder Diffraction 99
5.5.5. X-ray Single Crystal Diffraction 100
5.5.6. Hydrogen Bonding 102
5.5.7. Thermal Analysis 107
5.5.8. Discussion and Conclusion 108
5.6. Chapter 5 References 110

Chapter 6 Conclusion 112

6.1. Conclusion 112
6.2. Chapter 6 References 115

Appendix 116

List of Figures

Figure 1.1: General structure of α-amino acids 1

Figure 1.2: Structures of (a) glycine and (b) β-alanine 2

Figure 1.3: Amino acid zwitterion 3

Figure 1.4: Channel in which the solvent molecules are found in L-valyl-L-alanine crystals 6

Figure 2.1: Vapour diffusion method set-up. 13

Figure 3.1: Structural formula of GABA 20

Figure 3.2: Optical microscope (Micro Met Scientific, 45x magnification) images of different crystalline forms of GABA. (a) GABA Monoclinic (exists as blocks and needles) (b) GABA tetragonal (c) New GABA solvate 22

Figure 3.3: X-ray powder diffraction pattern comparison of the three forms of GABA 23

Figure 3.4: An Ortep diagram of the two independent GABA molecules in the asymmetric unit with disordered solvate molecules. The non-hydrogen atoms of the two GABA molecules have the displacement ellipsoids drawn at 50% probability 25

Figure 3.5: The three torsion angles to be compared on the GABA molecules where α = O1-C4-C3-C2 and O4-C8-C7-C6; β = C4-C3-C2-C1 and C8-C7-C6-C5; γ = C3-C2-C1-N1 and C7-C6-C5-N2 for molecules 1 and 2 respectively 26

Figure 3.6: Molecular conformations of GABA in (a) Monoclinic GABA, (b) Tetragonal GABA and (c) GABA Chloride Salt where the formula is $HOOCCH_2CH_2CH_2NH_3^+$, Cl^- 27

Figure 3.7: A view of the hexagonal GABA solvate unit cell down the c-axis, showing the hydrogen bonding network 28

Figure 3.8: Space-filling model of the unit cell of the hexagonal GABA solvate viewed down the c-axis 30

Figure 3.9: View of the linking of the two different types of GABA chains present in the hydrogen bonding network 31

Figure 3.10: DSC curve of heat flow (mW) vs. temperature (°C) for the hexagonal GABA solvate grown in the presence of gabapentin 32

Figure 3.11: Optical microscope images of the release of solvate bubbles from the hexagonal GABA solvate crystals as the temperature is increased from 190 to 206° 34

Figure 3.12: ^1H NMR spectrum of the hexagonal GABA solvate (excluding D_2O solvent peak at 4.780ppm) 35

Figure 3.13: Visual indication of the effect of iodine saturated toluene on the hexagonal GABA solvate crystals 37

Figure 4.1: Structural formula of gabapentin 41

Figure 4.2: Optical microscope (Micro Met Scientific, 45x magnification) images of three different

crystalline forms of gabapentin. (a) α-gabapentin, (b) β-gabapentin, (c) γ-gabapentin..... 44
Figure 4.3: X-ray powder diffraction pattern comparison of α-, β- and γ-gabapentin 45
Figure 4.4: Ortep diagrams of (a) α-gabapentin, (b) β-gabapentin and (c) γ-gabapentin with the displacement ellipsoids drawn at the 50% probability level 47
Figure 4.5: Centrosymmetric dimers of (a) α-gabapentin, (b) β-gabapentin and (c) γ-gabapentin indicating the $C_2^2(14)$ graph set in each case 48
Figure 4.6: Hydrogen bonding networks of (a) α-gabapentin, (b) β-gabapentin and (c) γ-gabapentin where the α-form is viewed down the a-axis and the β- and γ-forms are viewed down the b-axis 51
Figure 4.7: Diagram representing the possible hydrogen bonds present for each structure (a) α-gabapentin, (b) β-gabapentin and (c) γ-gabapentin where the bold letters each represent a different individual hydrogen bond in each structure. Some of the first and second level graph set motifs, resulting from these bonds, are indicated in table 4.4 for α-gabapentin, β-gabapentin and γ-gabapentin. The single red dots refer to the oxygen atoms where the remainder of the molecule has been deleted for visual clarity 52
Figure 4.8: DSC curve of heat flow (mW) vs. temperature (°C) for β-gabapentin over the range 25 - 220°C 53
Figure 4.9: Plot of points obtained for the change in volume ($Å^3$) against the change in temperature (°C) of β-gabapentin. 54
Figure 4.10: DSC curve of heat flow (mW) vs. temperature (°C) for γ-gabapentin over the range 25 - 200°C 56
Figure 4.11: Hydrogen bonding contacts for γ-gabapentin at (a) -100°C, (b) 70°C and (c) 100°C respectively. 58
Figure 5.1.1: Three possible ionization states of an amino acid (a) zwitterionic form, (b) cationic form, (c) anionic form 65
Figure 5.1.2: Three possible forms of a carboxylic acid (a) neutral form, (b) carboxylate dianion, (c) semi-carboxylate anion 66
Figure 5.2.1: Speciation diagram of glycine 67
Figure 5.2.2: Speciation diagram of oxalic acid 68
Figure 5.2.3: X-ray powder diffraction patterns of glycine-oxalic acid at pH 3, 6 and 12 compared with patterns of the starting materials 69
Figure 5.3.1: Speciation diagram of GABA 71
Figure 5.3.2: Optical microscope images of crystals formed from a pH 6 solution at 45x magnification. 72
Figure 5.3.3: X-ray powder diffraction patterns of the products obtained at pH 4, 6 and 10, compared with the patterns of the starting materials and an additional known GABA polymorph..... 73
Figure 5.3.4: Ortep diagram of the molecular conformation of the GABA-oxalic acid co-crystal, with the

displacement ellipsoids at a 50% probability level 75
Figure 5.3.5: Unit cell of the GABA-oxalic acid co-crystal 76
Figure 5.3.6: Diagram indicating the numbering scheme of the hydrogen atoms present on the GABA molecule 77
Figure 5.3.7: Hydrogen bonding interactions between GABA and oxalic acid 79
Figure 5.3.8: Hydrogen bonds linking the GABA molecules along the b-axis in the hydrogen bonding network 79
Figure 5.3.9: The letters **a** - **d** refer to the four strongest individual hydrogen bonds which are present, where some of the first and second level graph set motifs resulting from these bonds are indicated in table 5.3.3 above. The single red dots refer to the oxygen atoms where the remainder of the molecule has been deleted for visual clarity 80
Figure 5.3.10: DSC plot of heat flow (mW) vs. temperature (°C) for the 2:1 GABA-oxalic acid co-crystals over the range 25 - 350°C 81
Figure 5.4.1: Speciation diagram for gabapentin 84
Figure 5.4.2: Optical microscope images of the crystals formed at pH4 using a 45x magnification 85
Figure 5.4.3: X-ray powder diffraction pattern comparison of the crystals obtained at pH 4 with the patterns of known polymorphs of gabapentin and the oxalic acid starting material 86
Figure 5.4.4: Ortep diagram of the molecular conformation of the gabapentin-oxalic acid structure with displacement ellipsoids at a 50% probability level 88
Figure 5.4.5: Unit cell of the gabapentin-oxalic acid co-crystal 90
Figure 5.4.6: Numbering scheme for the hydrogen atoms present on the gabapentin molecule 91
Figure 5.4.7: Hydrogen bonding interactions between gabapentin and oxalic acid 92
Figure 5.4.8: Hydrogen bonds linking the gabapentin molecules along the b-axis in the hydrogen bonding network 93
Figure 5.4.9: The letters **a** - **e** refer to five individual hydrogen bonds which are present, where some of the first and second level graph set motifs resulting from these bonds are indicated in table 5.4.4. The single red dots refer to the oxygen atoms where the remainder of the molecule has been deleted for visual clarity. Only a portion of the $C_1^1(7)$ chain motif is present. 94
Figure 5.4.10: DSC curve of heat flow (mW) vs. temperature (°C) for the 2:1 gabapentin-oxalic acid co-crystals over the range of 25 -200°C 95
Figure 5.5.1: Speciation diagram of β-alanine 97
Figure 5.5.2: Optical microscope images of the crystals formed at pH 3 using a 45x magnification 98
Figure 5.5.3: X-ray powder diffraction pattern comparison of the products obtained at the pH values of 3, 6 and 12 with the patterns of the starting materials, β-alanine and oxalic acid 99

Figure 5.5.4: Ortep diagram of the molecular conformation of the β-alanine-oxalic acid-water structure

with displacement ellipsoids at a 50% probability level 101
Figure 5.5.5: Unit cell of the β-alanine-oxalic acid-water co-crystal..... 102
Figure 5.5.6: Numbering scheme for the hydrogen atoms present on the molecules within the β-alanine-oxalic acid-water co-crystal 103
Figure 5.5.7: Hydrogen bonding interaction O1-H8---O2 forming a dimer 104
Figure 5.5.8: Hydrogen bonding interactions amongst the β-alanine, oxalic acid and water molecules . 105
Figure 5.5.9: The letters **a** – **f** refer to the six strongest individual hydrogen bonds which are present, where some of the first and second level graph set motifs resulting from these bonds are indicated in table 5.5.3 106
Figure 5.5.10: DSC scan of heat flow (mW) vs. temperature (°) for the 2:2:1β-alanine-oxalic acid-water co-crystals over the range 25-200°C 107
Figure 5.5.11: Images of the β-alanine-oxalic acid-water co-crystals: a.) Room temperature b.) 110°C c.) 147°C 108
Figure A1.1: DSC curve of heat flow (mW) vs. temperature (°C) for monoclinic GABA from 30 to 280°C 116
Figure A1.2: DSC curve of heat flow (mW) vs. temperature (°C) for tetragonal GABA from 30 to 280°C 116
Figure A1.3: DSC curve of heat flow (mW) vs. temperature (°C) for α-gabapentin from 30 to 300°C 129

List of Tables

Table 3.1: Crystallographic data of the new GABA solvate compared with data from two existing polymorphs 24

Table 3.2: Comparison of the torsion angles of the two GABA molecules within the hexagonal GABA asymmetric unit 26

Table 3.3: Comparison of the torsion angles for the hexagonal GABA molecules with the GABA chloride salt molecule 28

Table 3.4: ^{1}H NMR chemical shifts and assigned functional groups 35

Table 4.1: Crystallographic data of the gabapentin crystalline forms 46

Table 4.2: Selected torsion parameters of the gabapentin polymorphs 49

Table 4.3: Hydrogen bonding parameters of the gabapentin polymorphs 50

Table 4.4: Matrix of selected graph sets for the hydrogen bonding of the gabapentin polymorphs 52

Table 4.5: Changes in the unit cell parameters of β-gabapentin with temperature 54

Table 4.6: Comparison of the hydrogen bonding parameters of β-gabapentin at different temperatures (Å, °) 55

Table 4.7: Comparison of the torsion angles of β-gabapentin at different temperatures(°) 56

Table 4.8: Comparison of the hydrogen bonding parameters of γ-gabapentin at different temperatures(Å, °) 57

Table 4.9: Comparison of the torsion angles of γ-gabapentin at different temperatures(°) 58

Table 5.3.1: Crystallographic data for GABA-oxalic acid crystals 74

Table 5.3.2: Hydrogen bonding parameters for the GABA-oxalic acid co-crystal(Å, °) 78

Table 5.3.3: Matrix of selected graph sets for the hydrogen bonding of the GABA-oxalic acid co-crystal 80

Table 5.4.1: Crystallographic data for gabapentin-oxalic acid crystals 87

Table 5.4.2: Selected torsion angles of gabapentin from the co-crystal compared with other gabapentin polymorphs 89

Table 5.4.3: Hydrogen bonding parameters of the gabapentin-oxalic acid co-crystal(Å, °) 92

Table 5.4.4: Matrix of selected graph sets for the hydrogen bonding of the gabapentin-oxalic acid co-crystal 93

Table 5.5.1: Crystallographic data for the β-alanine-oxalic acid-water co-crystal 100

Table 5.5.2: Hydrogen bonding parameters of the β-alanine-oxalic acid-water co-crystal(Å, °) 104

Table 5.5.3: Matrix of selected graph sets for the hydrogen bonding of the of β-alanine-oxalic acid-water co-crystal. 106

Table A1.1.1: Fractional atomic coordinates and isotropic or equivalent isotropic displacement parameters for the hexagonal GABA solvate (Å^2) 117

Table A1.1.2: Atomic displacement parameters for the hexagonal GABA solvate (Å^2) 118

Table A1.1.3: Bond length parameters for the hexagonal GABA solvate (Å) 119
Table A1.1.4: Bond angle parameters for the hexagonal GABA solvate (°) 120
Table A1.1.5: Torsion angle parameters for the hexagonal GABA solvate (°) 123
Table A1.1.6: Hydrogen bonding parameters for the hexagonal GABA solvate (Å,°) 128
Table A1.2.1: Fractional atomic coordinates and isotropic or equivalent isotropic displacement parameters for β-gabapentin($Å^2$) 129
Table A1.2.2: Atomic displacement parameters for β-gabapentin ($Å^2$) 130
Table A1.2.3: Bond lengths of β-gabapentin (Å). 131
Table A1.2.4: Bond angles of β-gabapentin (°) 132
Table A1.2.5: Torsion angles of β-gabapentin (°) 133
Table A1.2.6: Hydrogen bonding parameters of β-gabapentin (Å, °) 133
Table A1.2.7: Fractional atomic coordinates and isotropic or equivalent isotropic displacement parameters for γ-gabapentin($Å^2$) 134
Table A1.2.8: Atomic displacement parameters for γ-gabapentin ($Å^2$) 135
Table A1.2.9: Bond lengths of γ-gabapentin (Å) 135
Table A1.2.10: Bond angles of γ-gabapentin (°) 136
Table A1.2.11: Torsion angles of γ-gabapentin (°). 137
Table A1.2.12: Hydrogen bonding parameters of γ-gabapentin (Å, °) 138
Table A1.3.1: Fractional atomic coordinates and isotropic or equivalent isotropic displacement parameters of the GABA-oxalic acid co-crystal ($Å^2$) 139
Table A1.3.2: Atomic displacement parameters of the GABA-oxalic acid co-crystal ($Å^2$) 140
Table A1.3.3: Bond lengths of the GABA-oxalic acid co-crystal (Å) 140
Table A1.3.4: Bond angles of the GABA-oxalic acid co-crystal (°) 141
Table A1.3.5: Torsion angles of the GABA-oxalic acid co-crystal (°) 141
Table A1.3.6: Hydrogen bonding parameters of the GABA-oxalic acid co-crystal (Å, °) 142
Table A1.3.7: Fractional atomic coordinates and isotropic or equivalent isotropic displacement parameters of the gabapentin-oxalic acid co-crystal ($Å^2$). 142
Table A1.3.8: Atomic displacement parameters of the gabapentin-oxalic acid co-crystal ($Å^2$) 143
Table A1.3.9: Bond lengths of the gabapentin-oxalic acid co-crystal (Å) 144
Table A1.3.10: Bond angles of the gabapentin-oxalic acid co-crystal (°) 145
Table A1.3.11: Torsion angles of the gabapentin-oxalic acid co-crystal (°). 146
Table A1.3.12: Hydrogen bonding parameters of the gabapentin-oxalic acid co-crystal (Å,°). 146
Table A1.3.13: Fractional atomic coordinates and isotropic or equivalent isotropic displacement parameters of the β-alanine-oxalic acid-water co-crystal ($Å^2$). 147
Table A1.3.14: Atomic displacement parameters of the β-alanine-oxalic acid-water co-crystal ($Å^2$) 148
Table A1.3.15: Bond lengths of the β-alanine-oxalic acid-water co-crystal (Å) 148

Table A1.3.16: Bond angles of the β-alanine-oxalic acid-water co-crystal (°) 149
Table A1.3.17: Torsion angles of the β-alanine-oxalic acid-water co-crystal (°) 149
Table A1.3.18: Hydrogen bonding parameters of the β-alanine-oxalic acid-water co-crystal (Å, °)..... 150

Chapter 1

Introduction

1.1 Amino Acids

Amino acids are a class of small biomolecules which are characterised by the presence of amine and carboxyl groups. This class of molecules can be divided into various categories, according to their function, availability, properties and uses. One vital category is the α-amino acids in which the amine group is found on a carbon atom adjacent to the carboxylic acid group. They have the alpha carbon in the centre and differ with respect to the -R side chain. The properties of these amino acids are generally attributed to the composition of their side chains, which can cause them to behave as weak acids or bases, as well as making them hydrophilic or hydrophobic (Brown *et al.*, 2003, 9th ed.). The general structure of these α-amino acids is presented in figure 1.1.

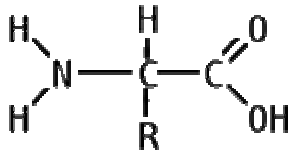


Figure 1.1 General structure of α-amino acids.

Within this group, there exist twenty standard amino acids which are used by the cells in the synthesis of proteins. Ten of these amino acids can be synthesized within the body and are referred to as non-essential amino acids; however the other ten, known as essential amino acids, must be taken in as part of the human diet as the body is unable to synthesize them. Some examples of standard amino acids include glycine, glutamic acid, aspartic acid, alanine, leucine and serine (Clugston *et al.*, 2002, 1st ed.).

Apart from glycine, the remaining nineteen standard amino acids are optically active and can exist as both D and L stereoisomers. In general, the naturally occurring amino acids

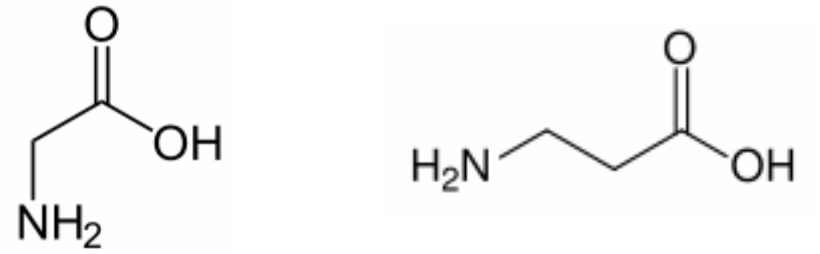
found in proteins, most often take on the levorotatory isomer form (www.micro.magnet.fsu.edu, 31/10/2007).

Apart from the standard amino acids, there are a number of other non-standard amino acids which can often be formed by modifying the standard amino acids. Both standard and non-standard amino acids can often function in non-protein roles in the cells, for example, as neurotransmitters and chemical messengers.

1.2 Neurotransmitters

Neurotransmitters are chemicals used in the body in order to relay, amplify and modulate signals between neurons and other cells. They are generally classified as either amino acids, peptides or monoamines. Neurotransmitters are used throughout the central nervous system and in the case of the various amino acid types; they act as either inhibitory or excitatory neurotransmitters. Some examples of monoamine neurotransmitters include serotonin, dopamine and melatonin. There are also over fifty peptide neurotransmitters including insulin and neurotensin. Four amino acids function as neurotransmitters, including glycine, γ-aminobutyric acid (GABA), glutamic acid and aspartic acid (www.web.indstate.edu, 31/10/2007).

Apart from these neurotransmitters, there exist a large number of neurotransmitter analogues which are structurally related to the neurotransmitters. An example of such an amino acid is β-alanine which is closely related in structure to glycine but contains one additional carbon in the backbone (figure 1.2).



(a) (b)

Figure 1.2 Structures of (a) glycine and (b) β-alanine.

β-alanine is the only naturally occurring β-amino acid in the brain and acts as a glycine receptor agonist which binds to the glycine receptor and triggers a response in the cell (Mori *et al.*, 2002).

Further neurotransmitter analogues often come in the form of amino acid drug compounds. Examples of these include gabapentin (Ibers, 2001), pregabalin (Venu *et al.*, 2007) and phenibut (Lapin, 2001), all of which have structural similarities to GABA. These three analogues also operate within the central nervous system.

1.3 Zwitterionic Form

For most amino acids, at a certain pH called the isoelectric point, the carboxyl group becomes deprotonated and the amine group, protonated. This is known as the zwitterionic form and the molecule has no net charge. Each amino acid will exist as a zwitterion at different specific pH values depending on the properties of the molecule. The zwitterionic form is shown in figure 1.3.

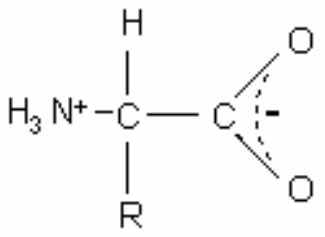


Figure 1.3 Amino acid zwitterion.

These protonated amino acid forms can generally be obtained from amino acid solutions, acidified with strong acids such as HCl (Mukhopadhyay *et al.,* 2004).

1.4 Hydrogen Bonding

In both the non-protonated and protonated forms of amino acid structures, there exists extensive hydrogen bonding due to the presence of the carboxyl and amine groups in each molecule.

The hydrogen bonding networks present for protonated amino acids are generally more complex and can often consist of mono-, bi- or trifurcated intermolecular C-COO^----^+H_3N-C hydrogen bonds. These refer to bonds in which for example, a hydrogen atom interacts with two other atoms, thus creating two hydrogen bonds with a single hydrogen atom(bifurcated) (www.cmt.dur.ac.uk, 15/06/2007). Another type of hydrogen bond which could exist for protonated amino acids is intramolecular hydrogen bonding which occurs between the N-H and O atoms of the same molecule. There is also weaker hydrogen bonding interactions which take place between C-H---N and C-H---O groups. An effective method of examining hydrogen bonding networks is by using a graph set method (Etter *et al.*, 1990) to find the similarities and differences in various hydrogen bonding networks. This divides the hydrogen bonding network up according to the patterns of hydrogen bonding present. The patterns can include intramolecular bonds(S), chains(C), rings(R) and finite hydrogen bond sets(D). The graph set symbol also describes the number of hydrogen bonding donors and acceptors which are present for a particular pattern. An example of a graph set symbol is $D_2^2(5)$, where D indicates a finite hydrogen bond set, the superscripted '2' refers to the number of hydrogen bond acceptors in the motif, the subscripted '2' refers to the number of hydrogen bond donors in the motif and the (5) indicates the number of atoms which make up the graph set motif (Bernstein, 2002).

1.5 Polymorphism

Amino acids can often exist as polymorphs, which is a characteristic of particular interest to the pharmaceutical industry. Polymorphism can occur as a result of a compound crystallizing into more than one structure. The chemical composition of the structures are the same, however, they have different crystal lattices. Each polymorph often has very different properties such as varying energies, thermal and chemical stabilities, and solubilities. This is particularly significant for polymorphs of drug compounds when examining the way in which each polymorph interacts with the body (Bernstein, 1993). Different polymorphs are generally obtained when altering the experimental conditions under which crystallization takes place. Some factors which can have an effect are

temperature, atmospheric changes, the use of different solvents and the rate and conditions of evaporation. An example of using different evaporation conditions is the case of using contact line crystallization in order to grow metastable polymorphs. This was carried out on the drug paracetamol where it was found that the more stable form crystallizes at the centre of the crystallization set-up whereas the metastable form grew in contact with the solution surface. The crystal nucleation of this form occurred at the edge of the meniscus and the crystals then grew in contact with the solution surface as evaporation occurred (Capes *et al.*, 2007).

In the case of temperature, it is often found that different polymorphs exist in different temperature ranges and some are more thermodynamically favoured while others are more kinetically favoured. The solvent used in crystallizations can play a vital role in forming a particular polymorph. An example which has been extensively studied in the past is the crystallization of α, β and γ forms of glycine. A mixture of ethanol or methanol and water as the solvent causes the formation of the least stable β-glycine form. When water is used as the solvent, α- and γ-glycine forms are produced (Weissbuch *et al*., 2005).

Another factor which has been examined in controlling crystal polymorphism is the use of additives to stabilize the formation of one form over another (www.xtal.gws.uky.edu/info_polymorph.htm l, 05/11/2007). An additive can have the effect of retarding the growth of one phase and allowing the nuclei of another phase to develop and form macroscopic crystals. Thus, the use of specific additives can allow for the growth of a less thermodynamically stable polymorph over a more stable one. Additives are able to effect the nucleation, growth, habit and texture of the crystals which are formed. The ability of amino acids to act as stereospecific nucleation inhibitors has been studied, again using glycine. It is shown that in the presence of certain amino acids, changes are obtained in the form of glycine which is crystallized. As mentioned in the paragraph above, α- and γ-glycine forms are produced when using an aqueous solution. In order to isolate the growth of γ-glycine, racemic hexafluorovaline can be added (Weissbuch *et al.*, 2003). The concentration of the amino acids also has an effect on

which form is crystallized (Torbeev *et al*., 2005). Additives are also able to affect the face growth rates of crystals. An example of this can be found in the case of γ-aminobutyric (GABA) acid where the effects of adding various additive types were studied. The different additives resulted in varying morphologies and growth rates of the crystal faces. One study carried out involved the addition of the ion Cr^{3+}, in the form of hydrated chromium nitrate to an aqueous solution containing GABA. When crystals were formed, the usual prism shaped GABA crystals were flattened due to the slowing down of the progression of one face (Lin *et al.*, 1996).

Another possible type of polymorphism is pseudo polymorphism or solvates in which the solvent used becomes incorporated into the crystals. An example of this is the monoclinic nanoporous crystal structure of L-valyl-L-alanine acetonitrile solvate (Görbitz, 2007). These crystals contain pores or channels in which solvent molecules are found. Figure 1.4 shows the channel in which the solvent molecules are found.

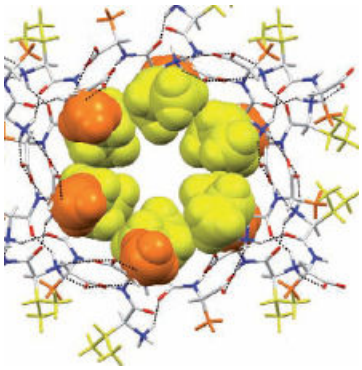


Figure 1.4 Channel in which the solvent molecules are found in L-valyl-L-alanine crystals (Görbitz, 2007).

If the crystals are dried out, they undergo a change in space group for this substance. Crystals of an L-valyl-L-serine trifluoroethanol solvate have also been produced. However in this case the solvent was more difficult to remove and its final removal did not result in a change in space group (Görbitz, 2005).

1.6 Co-crystals

A further aspect of interest in the pharmaceutical industry is the formation of co-crystals. These can be described as a homogenous crystalline material which contains two or more molecular species that are present in definite stoichiometric amounts (Aakeröy *et al.*, 2005). As is the case with different polymorphs, the co-crystallization of a drug compound with another substance will greatly affect the physical and chemical properties of the compound (Vishweshwar *et al.*, 2006). This is significant as the co-crystallization may allow for improved therapeutic utility and could also be useful in possibly reducing side effects (Wenger *et al*., 2006).

There are a number of cases in which co-crystallizations of two amino acids, as well as an amino acid with a carboxylic acid, have been performed. There are also a number of factors that need to be considered when attempting to design a co-crystal. One aspect which has been considered in the design of co-crystals is the examination of structural motifs and patterns, particularly within a hydrogen bonding network. Very often, there are specific hydrogen bonding motifs which are present for a group of co-crystals like amino acid/carboxylic acid co-crystals. When forming a co-crystal, the two or more components have intermolecular interactions which are similar to a known pattern in other co-crystals (Wenger *et al.,* 2006). Another important aspect in co-crystallization is the combination of functional groups which are chosen. From the Cambridge Structural Database (CSD) it is evident that the most widely used synthons for the formation of co-crystals are species which contain a carboxylic acid on one component and a nitrogen group on the other. The presence of these groups allows for strong hydrogen bonding interactions and a preference of the different species to interact and bind heteromerically to each other (Aakeröy *et al.*, 2005).

A further attribute of co-crystallizing agents is the ability of the involved species to exhibit a degree of structural flexibility. A study performed by Aakröy *et al.* has indicated that polymorphic compounds are more likely to produce co-crystals than compounds which are not polymorphic. It has also been discovered that the co-crystals which do

form, all have the same primary hydrogen bonding motifs and can be described by a number of the same graph sets (Aakeröy *et al.*, 2005).

The pH of the solution also plays a role in the formation of co-crystals, particularly in the case of amino acids and carboxylic acids where the pH will determine the protonation of the amine and carboxyl groups (Wenger *et al.*, 2006). Therefore, it can be seen that the structural motifs and patterns related to hydrogen bonding, the functional groups present, the degree of flexibility of the individual species and the pH of the solution all play a vital role in determining whether co-crystals will form.

In this project, we focus on the neurotransmitter amino acids. In particular, we consider the structural analysis of the neurotransmitter, GABA, as well as the neurotransmitter analogue, gabapentin and co-crystals of these analogues with carboxylic acids.

1.7 Aims of this Project

In recent years, there has been intense interest in the structures of γ-aminobutyric acid (GABA) and the related drug compound gabapentin. The co-crystallization of amino acids has also been of interest. In light of this, the aims of this project can be summarized as follows:

- To make use of commercially available gabapentin in order to investigate the possibility of the existence of different polymorphs for this drug compound by attempting to grow crystals using various methods.
- To crystallize GABA under a variety of conditions, in order to explore the effect on crystal growth, habits and possible polymorphs.
- To attempt the co-crystallization of selected amino acids.
- To predict potential co-crystallization pairs and hence attempt the co-crystallization of amino acids, in particular neurotransmitter analogues with GRAS (generally regarded as safe) (www.cfsan.fda.gov/~rdb/opagras1.html, 9/01/2008) carboxylic acids.

- To fully characterise and compare the experimental methods, crystal structures, hydrogen bonding patterns, thermal behaviour and stability of the possible polymorphs of GABA and gabapentin.
- To fully characterise all co-crystals in terms of their crystal structures, hydrogen bonding patterns, thermal properties and possible phase transitions.

1.8 Chapter 1 References

Aakeröy, C. B., Salmon, D.J. (2005). Cryst.Eng.Comm., 7, 439–448.

Bernstein, J. (1993). J. Phys, D: Appl. Phys., 26, B66-B76.

Bernstein J., Polymorphism in molecular crystals, 2002, Oxford University Press, pg 55-57.

Brown, T.L., LeMay, H.E., Bursten, B.E. (2003). Chemistry, The Central Science, 9th edition, Prentice Hall, pg 1012.

Capes, J.S., Cameron, R.E. (2007). Crystal Growth & Design, Vol. 7, No. 1, 108-112.

Clugston, M., Flemming, R., Vogt, D., Chemistry, An introduction for Southern African student, 2002, Oxford University Press, First edition, pg 492 – 503.

Etter, M.C., MacDonald, J.C., Bernstein, J. (1990). Acta Cryst. B46, 256-262.

Görbitz, C.H. (2007). Chem. Eur. J., 13, 1022-1031.

Görbitz, C.H. (2005). Cryst.Eng.Comm.,7, 670-673.

Ibers, J. A. (2001). Acta Cryst. C57, 642-643.

Lapin, I. (2001). CNS Drug Rev., 7(4), 471-81.

Lin, C.H., Gabas, N., Canselier, J.P., Hiquily, N. (1996). Journal of Crystal Growth, 166, 104-108.

Mori, M., Gahwiler, B.H., Gerber, U. (2002). J. Physiol., 539, 191-200.

Mukhopadhyay, U., Bernal, I. (2004). Mendeleev Commun., 270-276.

Torbeev, V.Y., Shavit, E., Weissbuch, I., Leiserowitz, L., Lahav, M. (2005). Crystal Growth & Design, Vol.5, No.6, 2190-2196.

Venu, N., Vishweshwar, P., Ram, T, Suryaa, D., Apurbac, B. (2007). Acta Cryst. C63, 306-308.

Vishweshwar, P., McMahon, J.A., Bis, J.A., Zaworotko, M. J. (2006). Journal of Pharmaceutical Sciences. Vol. 95, 499-516.

Weissbuch, I., Lahav, M., Leiserowitz, L. (2003). Crystal Growth and Design, Vol 3. No. 2, 125-150.

Weissbuch, I., Torbeev, V.Y., Leiserowitz, L., Lahav, M. (2005). Angew.Chem. Int. Ed, 44, 3226-3229.

Wenger, M., Bernstein, J. (2006). Angew.Chem. Int. Ed, 45, 7966-7969.

www.britannica.com/eb/article-9007182/amino-acid, (15/06/2007).

www.cfsan.fda.gov/~rdb/opagras1.html, (9/01/2008).

www.cmt.dur.ac.uk/sjc/thesis_prt/node11.html, (15/06/2007).

www.encyclopedia.com/doc/1E1-neurotr.html, (06/11/2007).

www.ktf-split.hr/glossary/en_o.php?def=polymorphism, (05/11/2007).

www.micro.magnet.fsu.edu/aminoacids/index.html, (31/10/2007).

www.web.indstate.edu/thcme/mwking/nerves.html, (31/10/2007).

www.xtal.gws.uky.edu/info_polymorph.html, (05/11/2007).

Chapter 2
Experimental Techniques

2.1 Introduction

In this project, it was necessary to use various crystallization techniques. This is due to the fact that there is difficulty in producing single crystals of specific polymorphs. The quantities of crystals produced using the various techniques are also very small. X-ray powder and single crystal diffraction was used in the characterisation of the crystals and powders obtained. In addition to this, spectroscopic techniques were necessary to fully characterise certain compounds. In order to examine and compare the properties of the polymorphs obtained, different methods of thermal analysis were carried out.

2.2 Crystallization Techniques

The crystallization methods that were used involved open air evaporation and also a vapour diffusion method. Both methods involve dissolving a solid compound in the desired solvent. The main objective of this study, was to obtain polymorphs and co-crystals for various compounds, therefore, in the case of open air evaporation, the crystallization environment was varied extensively. The rate of solvent evaporation was changed by making use of different crystallization vessels. The temperatures of the solutions were varied and a number of the solutions were placed under reflux for different lengths of time. The solubility of the compounds in different solvents also had an effect on the type of solvent which was chosen.

The method of vapour diffusion involved placing the solution into a small vial and wrapping cotton wool around the vial. This small vial was then placed into a larger vial containing a small amount of solvent. The solvent used in the larger vial was one in which the compound is not soluble. The large vial was sealed and this allowed the vapour

from the outer solvent to move slowly through the cotton wool and settle on the inner solution, thus decreasing the rate at which the inner solvent evaporates (figure 2.1).

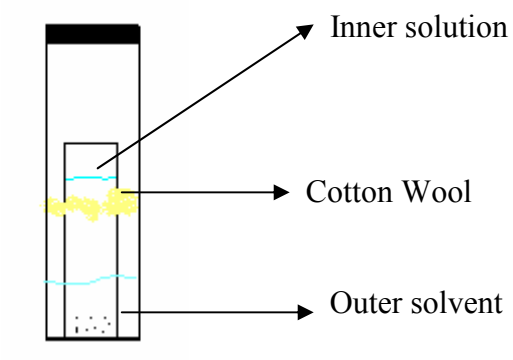


Figure 2.1 Vapour diffusion method set-up.

2.3 X-ray Diffraction

Since the discovery of X-rays in 1895, the development of X-ray diffraction techniques, has allowed for the examination of crystalline materials at the atomic level. There are two main uses of X-ray diffraction. Firstly, to find the unique characteristic X-ray powder pattern for a specific crystalline solid by making use of X-ray powder diffraction and secondly to determine the crystal structure of the material using X-ray single crystal diffraction (Atkins, 1998, ed. 6, www.materials.binghamton.edu.html).

2.3.1 X-ray Powder Diffraction

Historically, the greatest use for X-ray powder diffraction is to identify crystalline compounds by their unique diffraction patterns. The method was developed by Debye and Scherrer in 1916 and involves the use of monochromatic radiation and a powdered sample containing crystallites. The powdered sample is ground and then placed on a flat plate holder and leveled out. If there is only a very small amount of sample available, a zero background holder is used. Once placed on the holder, some of the crystallites in the sample will be orientated so as to satisfy Bragg's conditions. The sample can then be

placed onto a powder diffractometer where the diffraction pattern and the intensities of the reflections are electronically monitored (Atkins, 1998, ed. 6).

X-ray powder diffraction was particularly useful in this project as it allowed for the different polymorphs of the drug compounds to be clearly distinguished. Each polymorph has its own characteristic peaks due to possible differences in crystal systems, space groups and cell dimensions. It was also very useful when analyzing the samples in which crystals could not be grown, as in the case of a number of co-crystal attempts. The possible formation of new substances could be examined from the powder patterns.

Powder diffraction patterns were collected on a Bruker D8 AXS powder diffractometer employing copper radiation for the range 5 to 90° 2θ with a step size of 0.02° and a total run time of 10 minutes. A zero background holder was used due to the small amount of product obtained.

2.3.2 X-ray Single Crystal Diffraction

X-ray single crystal diffraction makes use of a monochromatic beam of X-rays in which a single crystal is rotated in the beam. The angles as well as intensities of the reflections for specific orientations are recorded. From the diffraction pattern obtained, all information about the atomic structure of a compound can be found including aspects such as bond lengths, angles, torsions, molecular conformation, unit cell dimensions, space group and the packing within the unit cell (Atkins, 1998, ed. 6).

This technique was used extensively in this project as it allowed for the structures of the polymorphs to be determined and hence compared in terms of conformation. It also allowed for the structures of the co-crystals to be determined. Phase transitions could also be examined, by determining the unit cell dimensions at increasing temperatures.

One disadvantage of this method is the need to obtain crystals which are sufficiently large, pure in composition and regular in structure. Large imperfections and cracks result

in difficulties in structural data collection. This method obviously cannot be used if good quality crystals are not obtained.

For this project, two different X-ray single crystal diffractometers were used in order to collect data. Room temperature collections were performed on a Bruker SMART 1K CCD area detector with graphite monochromated Mo K_α radiation (40kV, 40mA). The collection method involved ω-scans of width 0.3°. Data reduction was carried out using the program *SAINT+* (Bruker, 1999a) and face indexed absorption corrections were made using the program *XPREP* (Bruker, 1999a).

All low temperature and high temperature collections were performed on the Bruker APEX II CCD area detector diffractometer with graphite monochromated Mo K_α radiation (50kV, 30mA) using the APEX 2 (Bruker, 2005a) data collection software. The collection method involved ω-scans of width 0.5° and 512 x 512 bit data frames. Data reduction was carried out using the program *SAINT+* (Bruker, 2005b) and face indexed absorption corrections were made using the program *XPREP* (Bruker, 2005b).

The crystal structures were solved by direct methods using *SHELX97* (Sheldrick, 1997). Non-hydrogen atoms were first refined isotropically followed by anisotropic refinement by full matrix least-squares calculations based on F^2 using *SHELX97*. Hydrogen atoms were positioned geometrically and allowed to ride on their respective parent atoms. Diagrams and publication material were generated using WinGX (Farrugia, 1999), SHELX97 (Sheldrick, 1997), PLATON (Spek, 2003), ORTEP-3 (Farrugia, 1997) and Mercury (Macrae *et al.*, 2006).

2.4 Thermal Analysis

2.4.1 Hot Stage Microscopy

Hot stage microscopy makes use of a polarizing microscope which contains a stage that is temperature controlled. A recording device is attached to the microscope. The sample is placed on a microscope slide which is positioned so that a video camera can focus on the sample and capture the image on a computer screen. The sample can then be heated at an appropriate rate. This thermal analytical technique allows for the melting points of samples to be determined. It also allows for the possible visualization of phase transitions.

In this project, the melting points of the samples were determined by hot stage microscopy using a Micro Met Scientific microscope and Kohler hot stage. The melting points were then compared with the values obtained from differential scanning calorimetry. Attempts were also made to observe possible phase transitions.

2.4.2 Differential Scanning Calorimetry (DSC)

Differential scanning calorimetry is an analytical technique which measures the difference in the amount of heat required to increase the temperature of a sample and an inert reference material. The sample and reference are maintained at the same temperature throughout, but when the sample melts or undergoes a phase transition; either more heat or less heat is received by the sample, depending upon whether an exothermic or endothermic change takes place. The curve produced by the calorimeter is a measure of the heat flow (mW) as the temperature (°C) increases.

The differential scanning calorimeter which was used produces curves in which peaks pointing downwards are endothermic and peaks pointing upwards are exothermic. Integration over the area of a peak allows for the measurement of the enthalpy associated with the particular transition.

There are a number of factors which can affect the appearance of a DSC curve. The heating rate and mass of sample used can have a significant effect upon the resolution of the thermal change. They may result in changes in the peak temperature. Slower heating rates and smaller masses allow for better resolution of the peaks. When making comparisons between samples eg. polymorphs, the mass of the samples used should be similar (Giron, 1995).

The differential scanning calorimeter used for measurements in this project was a Mettler Toledo DSC 822 instrument. Aluminum, 40 µl sample pans were used in which a hole was punched into the lid of the pans prior to sealing. The reference pan was left empty and simply sealed with a punctured lid. For each scan, a heating rate of 5°C per minute was used and the temperatures ranged from 25°C to approximately forty degrees above the melting points determined by hot stage microscopy. The computer package used to analyze the DSC curve was the Star^{e} software.

Although it would have been informative to use thermo gravimetric analysis (TGA) and other spectroscopic techniques, such as infrared and Raman spectroscopy, this proved to be unfeasible due to the minute amounts of pure crystalline material available for most of the compounds, often only a few milligrams.

2.5 ^{1}H Nuclear Magnetic Resonance (NMR) Spectroscopy

Proton nuclear magnetic resonance involves the recording of spectra in which specific chemical shifts and spin-spin coupling between protons of a substance are recorded. This technique is useful in allowing for the structure of an unknown organic substance to be determined. It provides information regarding the number of different types of hydrogen atoms which are present in the molecule. It also indicates the number of hydrogen atoms on a neighboring group as well as the electronic environment of the different hydrogen atoms. An integration curve for each set of peaks can be plotted and this allows for the abundance of the individual protons to be determined.

The instrument used for ^{1}H Nuclear Magnetic Resonance (NMR) spectroscopy in this project was the Bruker Avance 300 which operated at a ^{1}H frequency of 300.1318534 MHz. ^{1}H NMR spectroscopy was used specifically in order to identify the solvent present in solvate crystals. The crystals were dissolved in deuterated water (D_2O).

2.6 Chapter 2 References

Atkins, P.W., Physical Chemistry,1998, Oxford University Press, 6th edition, pg 625-634.

Bruker (1999a). *SAINT+*. Version 6.02. (includes XPREP and SADABS) Bruker AXS Inc., Madison, Wisconsin, USA.

Bruker (2005a). APEX2. Version 2.0-1. Bruker AXS Inc., Madison, Wisconsin, USA.

Bruker (2005b). SAINT-NT. Version 6.0. (includes XPREP and SADABS) Bruker AXS Inc., Madison, Wisconsin, USA.

Farrugia, L. J. (1997). J. Appl. Cryst. 30, 565.

Farrugia, L. J. (1999). J. Appl. Cryst. 32, 837-838.

Giron, D. (1995). Thermochimica Acta, 248, 1-59.

Macrae, C.F., Edgington, P.R., McCabe, P., Pidcock, E., Shields, G.P., Taylor, R., Towler, M., van de Streek, J. (2006). *J. Appl. Cryst.*, 39, 453-457.

Sheldrick, G. M. (1997). SHELX97. Programs for Crystal Structure Analysis (Release 97-2). University of Gottingen, Germany.

Spek, A. L. (2003). *J. Appl. Cryst.* 36, 7-13.

www.materials.binghamton.edu/labs/xray/xray.html, (25/05/2008).

Chapter 3
γ- Aminobutyric acid

3.1 Introduction and related work

As discussed in chapter 1, γ-aminobutyric acid (GABA) is an inhibitory neurotransmitter. The structure of GABA has been widely studied for its significant inhibitory action in the central nervous system where it operates in the brain and allows for a decrease in the firing of neurons, resulting in minimized chances of seizures (www.health.enotes.com, 9/11/2007). In this chapter, the structures of GABA which have been previously reported will be discussed and compared with the results of this research project.

GABA appears as a white crystalline solid with the molecular formula $C_4H_9NO_2$ and molecular weight 103.12 g/mol. The structural formula for GABA in its zwitterionic form is shown in figure 3.1.

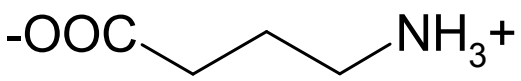


Figure 3.1 Structural formula of GABA.

Two structures as well as one chloride salt of GABA have been previously published. The first GABA structure has a monoclinic crystal system with the space group $P2_1/c$ (Tomita *et al.*, 1973), while the second structure has a tetragonal crystal system with a space group of $I4_1cd$ (Dobson *et al.*, 1996). These two structures are polymorphs. They exhibit distinct conformational differences and a number of intermolecular and hydrogen bonding variations, as will be discussed later in the chapter.

The chloride salt of GABA ($C_4\ H_{10}\ N\ O_2^{\ +}$, Cl^-) has a monoclinic crystal system and the space group $P2_1$ (Steward *et al.*, 1973). This is the only salt of GABA which has thus far been reported.

In this project we have obtained a new unpublished solvate crystal structure of GABA. The structure of this pseudo polymorph is related in terms of its crystal system, to a range of dipeptides such as L-valyl-L-alanine (Görbitz *et al.*, 1996) and L-leucyl-L-serine (Görbitz *et al*., 2005) which form structures with hexagonally symmetric pores. These dipeptide crystals contain channels which run along the hexagonal axes and these channels contain solvent molecules, for example acetonitrile. The acetonitrile can also be substituted by another substance such as iodine, by placing the crystals in an iodine saturated solution of toluene (Görbitz *et al*., 2005).

3.2 Hexagonal GABA and published polymorphs

3.2.1 Experimental

In attempts to co-crystallize GABA and the neurotransmitter analogue gabapentin, equimolar amounts of Sigma Aldrich GABA and gabapentin were dissolved in 96% ethanol at room temperature. The solution was then placed into a vial and set up under vapour diffusion. Hexane was used as the initial external solvent due to its relatively high vapour pressure. The setup was then placed into a water bath maintained at 18 ± 1°C. After approximately 2 weeks, long, thin needle shaped crystals formed accompanied by the formation of block shaped monoclinic α-gabapentin (Ibers, 2001) and tetragonal GABA (Dobson *et al.*, 1996) crystals within the same vial. The needle shaped crystals grew either upwards or downwards from the contact line of the solution. In subsequent crystallization attempts, gabapentin was removed and only GABA was dissolved in 96% ethanol under the same conditions. This resulted in the formation of two different thin needle shaped crystal types, where the slightly thicker needle shaped crystals were monoclinic GABA (Tomita *et al.*, 1973).

The solvents were also varied in terms of using water, absolute ethanol, varying percentages of water in absolute ethanol, methanol, 2-propanol and 2-butanol. The same conditions were adopted and it was found that the thin needle shaped crystals only formed when 96% ethanol or 2–butanol were used.

The external solvent was also varied by trying acetonitrile, 2-propanol and methanol while keeping the initial conditions. As was the case with the hexane, acetonitrile as the external solvent also allowed for the formation of the thin needle shaped crystals. The other external solvents did not have this effect.

3.2.2 Visual Comparison of GABA Forms

The different crystal forms of GABA could firstly be examined by taking snapshot images using a Micro Met Scientific microscope at a 45x magnification. This allows for the various forms to be examined in terms of visual differences, including differences in the crystal habit of the crystalline forms. Images of the two previously published forms and the newly formed pseudo polymorph were recorded (see figure 3.2).



(a) (b) (c)

Figure 3.2 Optical microscope (Micro Met Scientific, 45x magnification) images of different crystalline forms of GABA. (a) GABA Monoclinic (exists as blocks and needles) (b) GABA tetragonal (c) New thin needle shaped crystals (GABA solvate).

It was observed that there are significant differences in the morphologies of the three crystal types. However, different morphologies of crystals, does not imply different structural forms. Further characterisation was needed in order to fully characterise these different forms.

3.2.3 X-ray Powder Diffraction

A method which can be used to indicate the presence of different structures is X-ray powder diffraction, therefore, diffraction patterns were obtained for all three samples and superimposed using Winplotr (Roisnel *et al.*, 2000) in order to compare the patterns. The comparison is shown in figure 3.3.

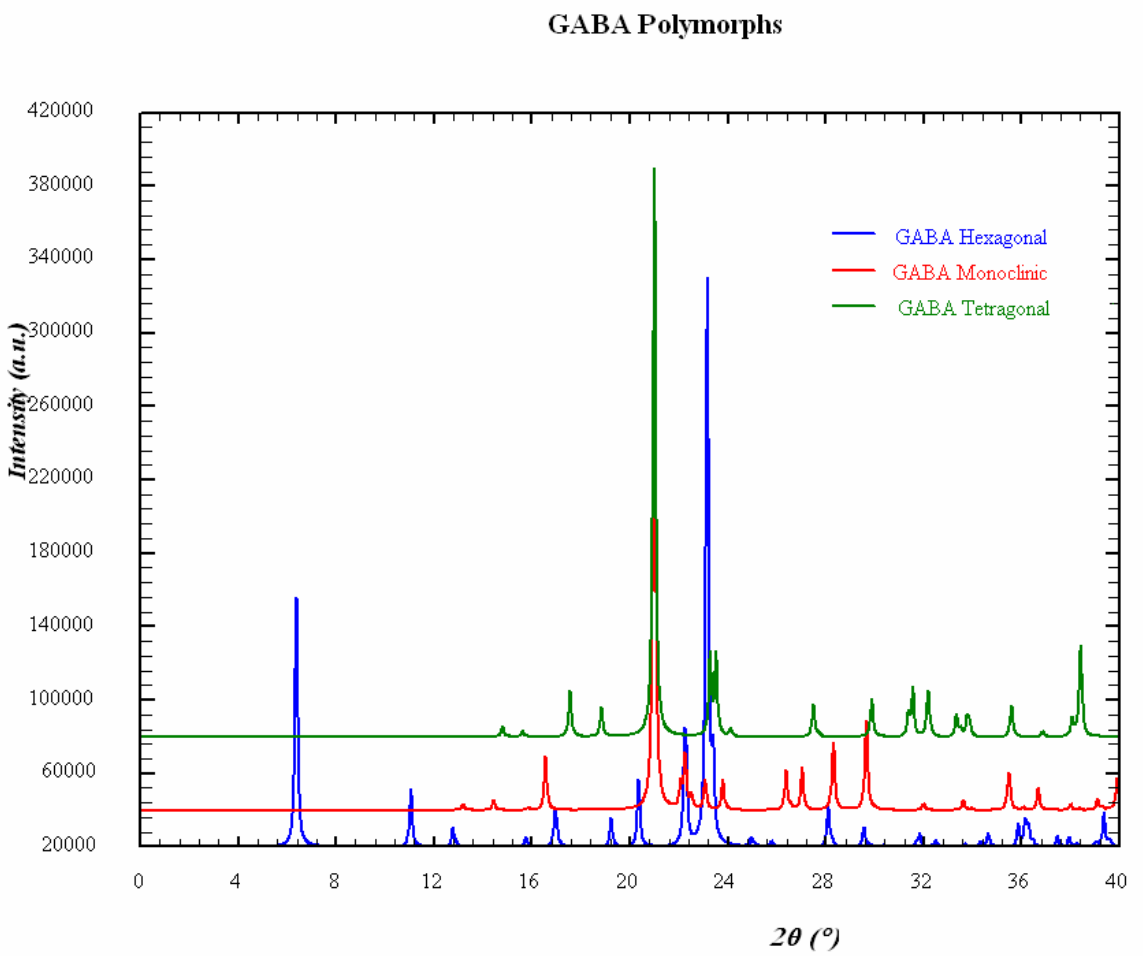


Figure 3.3 X-ray powder diffraction pattern comparison of the three forms of GABA.

Figure 3.3 clearly indicates that there is very little overlapping of the three diffraction patterns. The patterns are very different and this is proof that the crystalline phases are different. A full examination of the structures of these three crystalline GABA forms can only be done using X-ray single crystal diffraction.

3.2.4 X-ray Single Crystal Diffraction

Using X-ray single crystal diffraction, the two forms, (a) GABA monoclinic and (b) GABA tetragonal in figure 3.2 were identified as the previously reported monoclinic (Tomita *et al.*, 1973) and tetragonal (Dobson *et al.*, 1996) forms of GABA.

The thin needle shaped crystals of the third form, (c) in Figure 3.2 were examined by X-ray single crystal diffraction at -100°C on the Bruker, APEX II diffractometer and found to be a new hexagonal solvate of GABA. The data presented in table 3.1 below lists the parameters for this form and gives a comparison with the two previously reported GABA polymorphs.

Table 3.1: Crystallographic data of the new GABA solvate compared with data from two existing polymorphs.

	GABA Solvate	**GABA Monoclinic** (Tomita *et al.*, 1973)	**GABA Tetragonal** (Dobson *et al.*,1996)
Empirical Formula	$2(C_4 H_9 N O_2)$ Disordered solvent	$C_4 H_9 N O_2$	$C_4 H_9 N O_2$
Formula Weight	220.90g/mol	103.12g/mol	103.12g/mol
Temperature	173(2)K	138K	296K
Crystal System	Hexagonal	Monoclinic	Tetragonal
Space Group	$P6_2$	$P2_1/a$	$I4_1cd$
Description	Colourless, needles	Colourless, blocks	Colourless, blocks
Unit cell dimensions	a=15.9164 (4) Å	a=8.214(2) Å	a=11.963(1) Å
	b= 15.9164(4) Å	b= 10.000(2) Å	b= 11.963(1) Å
	c= 7.8769(4) Å	c= 7.208(2) Å	c= 15.282(2) Å
	α = 90°	α = 90°	α = 90°
	β = 90°	β = 110.59(2)°	β = 90°
	γ = 120°	γ = 90°	γ = 90°
Volume	$V=1728.13(1)A^3$	$V= 2187.0(6)A^3$	$V= 2187.0(6)A^3$
Z	12	4	16
Density	$1.29g/cm^{-3}$	$1.20g/cm^{-3}$	$1.25g/cm^{-3}$
Absorption coefficient	$0.101mm^{-1}$	$0.095mm^{-1}$	$0.093mm^{-1}$
Θ range for data col.	1.5-27.1°	2.5 -28.1°	3.4 -28.3°
Reflections collected	15552	2816	1440
Independent reflect.	1367	1686	767
Final R indices	0.0475	0.044	0.033

Note: Disordered solvent: 0.36(C1X), 0.12(C2X), 0.34(C3X), 0.28(C5X), 0.1(O) where the numbers represent the site occupancy factors for each atom.

The above crystallographic data indicates significant differences in all the parameters for the three structures. It is evident that the newly formed GABA structure is a pseudo polymorph of the two previously published forms. Further comparison of the three structures can be done by examining the molecular conformations which are obtained from x-ray single crystal diffraction.

The molecular conformation of the two molecules in the asymmetric unit of the hexagonal GABA polymorph is shown in figure 3.4.

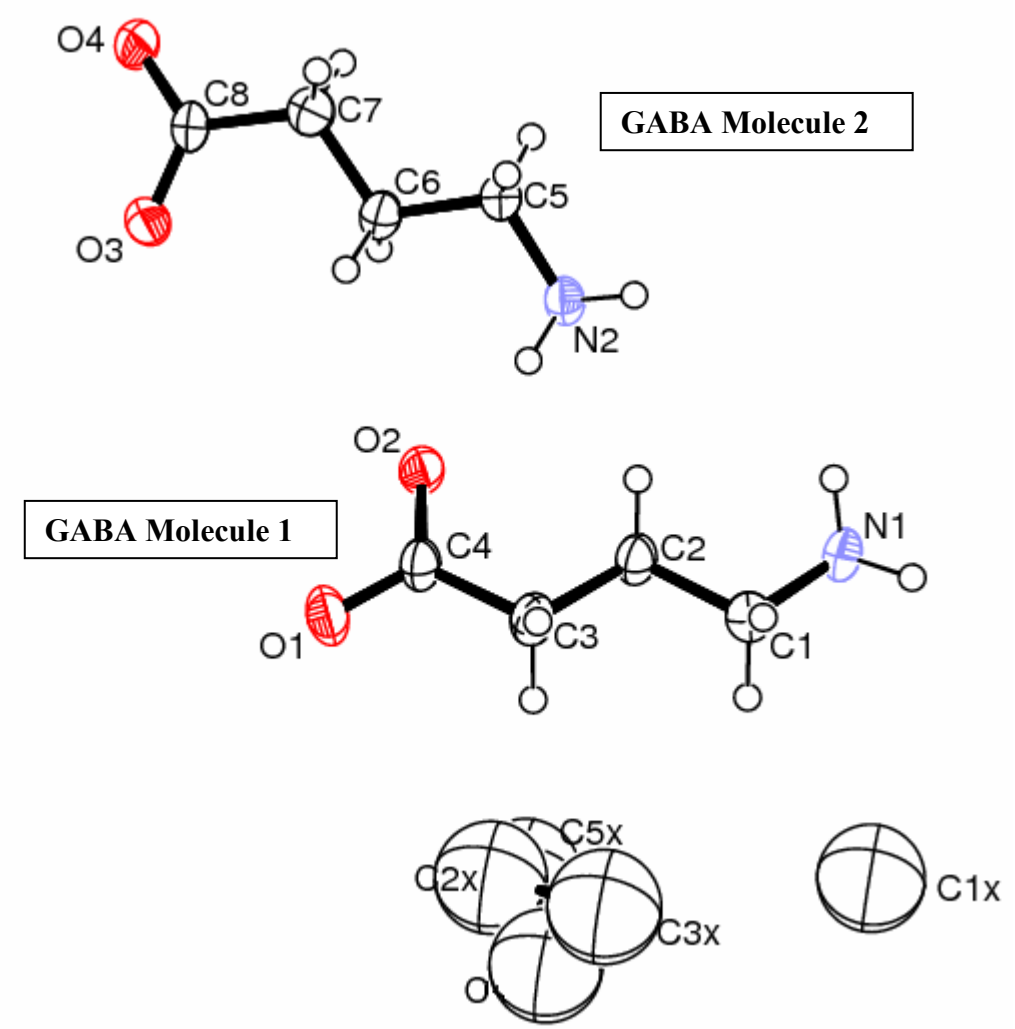


Figure 3.4 An Ortep diagram of the two independent GABA molecules in the asymmetric unit with disordered solvate molecules. The non-hydrogen atoms of the two GABA molecules have the displacement ellipsoids drawn at 50% probability.

This hexagonal GABA solvate has two GABA molecules and disordered solvent molecules in the asymmetric unit. The disordered solvent molecules could not be

resolved. As is shown in figure 3.4, the two GABA molecules are similarly orientated. However, there are slight conformational differences which can be seen by a comparison of the torsion angles.

Figure 3.5 below indicates three different torsion angles which can be compared in order to examine the differences between the two molecules.

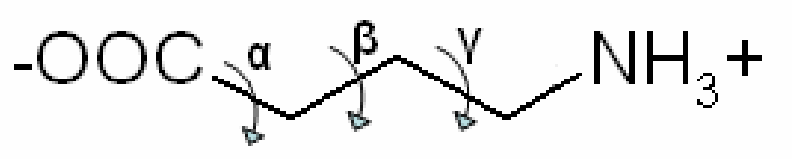


Figure 3.5 The three torsion angles to be compared on the GABA molecules where α = O1-C4-C3-C2 and O4-C8-C7-C6; β = C4-C3-C2-C1 and C8-C7-C6-C5; γ = C3-C2-C1-N1 and C7-C6-C5-N2 for GABA molecules 1 and 2 respectively.

Table 3.2 below gives an indication of the differences.

Table 3.2: Comparison of the torsion angles of the two GABA molecules within the hexagonal GABA asymmetric unit.

Torsion Angle	Molecule 1(°)	Molecule 2(°)
α	172.4(3)	162.5(3)
β	-178.7(3)	175.2(3)
γ	177.7(3)	171.1(3)

Table 3.2 shows that there are only minor differences between the two GABA molecules. The differences range between approximately 7- 10°. This shows that the two molecules in the same asymmetric unit for hexagonal GABA have similar conformations. The conformations however are not exactly the same; otherwise the space group in which they exist would have been different. A higher symmetry space group such as $P6_1$ would have been present. In this structure, the lowering of the symmetry can also be as a result of the presence of the solvent molecules.

The molecular conformation of the hexagonal GABA molecules can also be compared to the conformations of the monoclinic and tetragonal GABA polymorphs together with the GABA molecule in the chloride GABA salt.

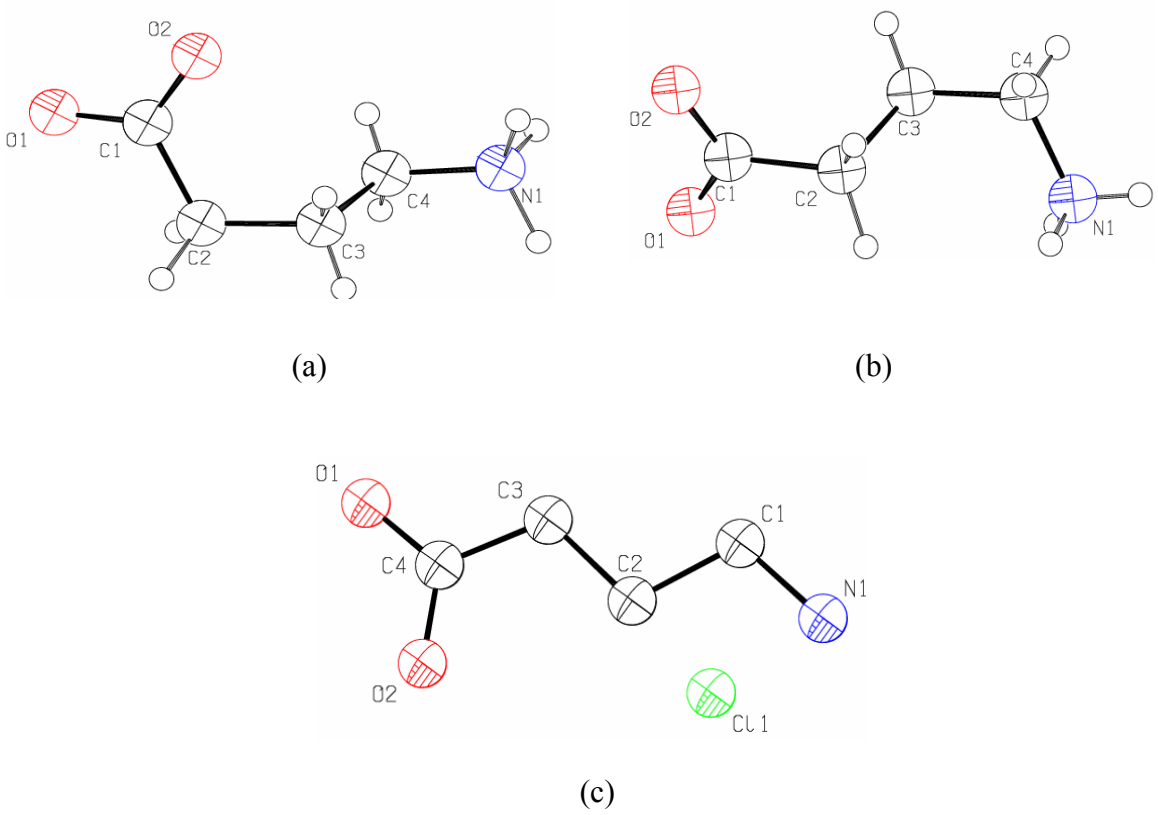


Figure 3.6 Molecular conformations of GABA in (a) Monoclinic GABA, (b) Tetragonal GABA and (c) GABA chloride salt where the formula is $HOOCCH_2CH_2CH_2NH_3^+$, Cl^-.

The three conformations in figure 3.6 are significantly different. A comparison of the hexagonal GABA molecular conformations with the monoclinic and tetragonal GABA conformations indicates that they are significantly different. There are however, similarities between the hexagonal GABA molecular conformations and the conformation of the GABA molecule in the chloride salt compound. Table 3.3 gives a comparison of the torsion angles for these structures.

Table 3.3: Comparison of the torsion angles of the hexagonal GABA molecules with the GABA molecule in the chloride salt compound.

Torsion Angle	Hexagonal GABA		GABA Chloride Salt(°)
	Molecule 1(°)	Molecule 2(°)	
α	172.4(3)	162.5(3)	180.00(3)
β	-178.7(3)	175.2(3)	180.00(3)
γ	177.7(3)	171.1(3)	180.00(3)

The values in table 3.3 indicate that the torsion angles of the two hexagonal GABA molecules are similar to the torsion angles for the GABA molecule in the chloride salt compound. GABA adopts the '*trans-trans'* conformation in both the chloride salt and hexagonal GABA compounds.

3.2.5 Hydrogen Bonding

As mentioned in chapter 1, the possible hydrogen bonding for zwitterionic amino acids is extensive due to the presence of the COO^- and NH_3^+ groups. The hydrogen bonding network for hexagonal GABA as viewed down the c-axis is shown in figure 3.7.

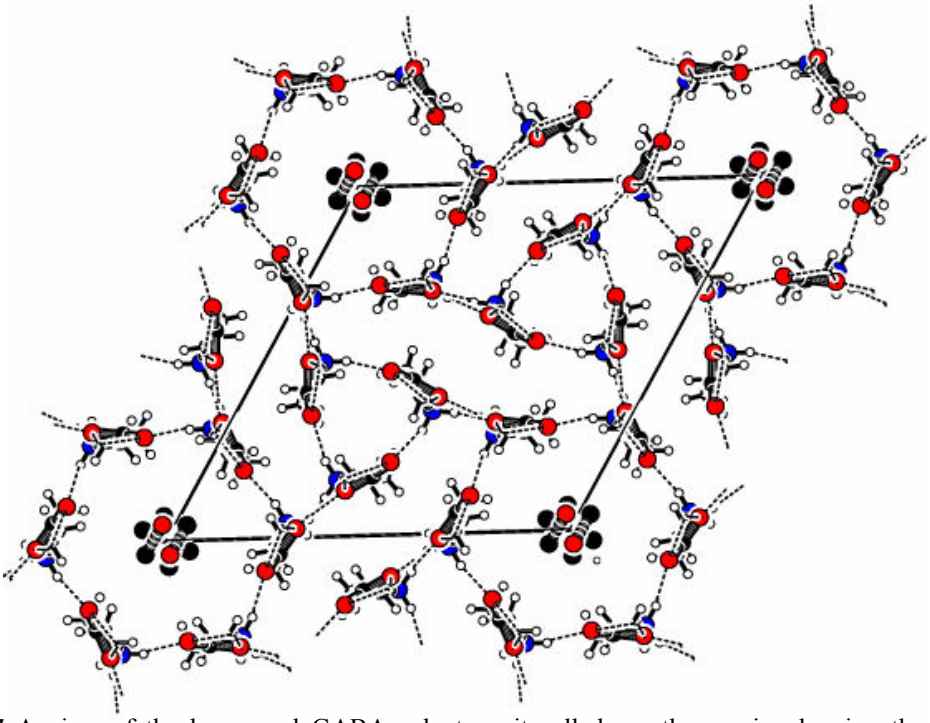


Figure 3.7 A view of the hexagonal GABA solvate unit cell down the c-axis, showing the hydrogen bonding network.

The hydrogen bonding network in figure 3.7 indicates the presence of a 6_2 axis, three fold screw axis and a two fold rotation axis. This is in line with the symmetry operators within the $P6_2$ space group. The disordered solvent molecules lie along the c-axis of the unit cell. The GABA molecules are arranged around the disordered solvent molecules to form a channel which would contain the solvent molecules. Apart from the hydrogen bonding indicated in figure 3.7, there also exists short contact interactions between the GABA molecules and the solvent within the channels, which are smaller than the sum of the Van der Waals radii. The lengths of these contacts are approximately 3.1Å. No distances compatible with hydrogen bonding interactions could be found between the GABA and disordered solvent molecules, although the disorder could not be resolved as stated above.

The space-filled model shown in figure 3.8 gives a better indication of the arrangement of the solvent molecules within a channel of GABA molecules, where the GABA molecules are all orientated in the same direction. When the c-axis is viewed from the one end, the NH_3^+ groups are visible as indicated in figure 3.8, but when viewed from the opposite end, the COO^- groups will be visible. This is a consequence of the fact that $P6_2$ is a polar space group. The diameter of each channel is approximately 4.8Å and therefore, only solvent molecules of diameter smaller than this can be included in the channel. The solvent molecules occur in two different sites in the asymmetric unit. The site occupancy factor is 10.2 % for the four atoms which are attached and 0.17% for the other single atom. This indicates that within the channel, the disordered solvent molecules occupy approximately 10% of the space and the remainder of the channel is empty.

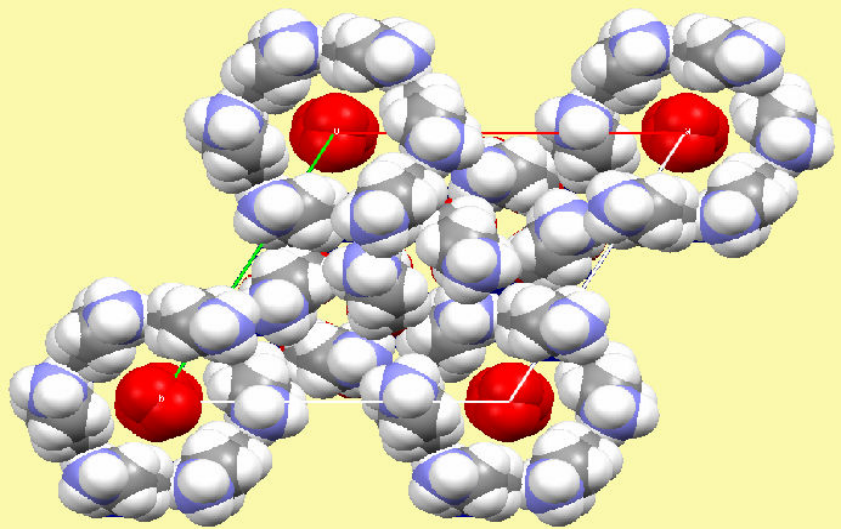


Figure 3.8 Space-filling model of the unit cell of the hexagonal GABA solvate viewed down the c-axis.

A closer look at the hydrogen bonding between the GABA molecules, as presented in figure 3.9, indicates that one of the hydrogen atoms from the NH_3^+ group on a molecule 1 GABA acts as a bifurcated hydrogen bond donor and forms hydrogen bonds with the two oxygen atoms of a neighbouring molecule 1 GABA. This results in a chain of molecule 1 GABA being formed in the c-direction. The N-H---O bond lengths are 3.091(4)Å and 2.878(3) Å for N1-H3---O1 and N1-H3---O2 respectively. A chain of molecule 2 GABA is also formed in the c-direction in a similar manner, with the hydrogen bond lengths being 2.840(4)Å and 3.197(4)Å for the bonds N2-H10---O3 and N2-H10---O4 respectively. Therefore, the average N-H---O lengths of the hydrogen bonds forming the two different GABA chains within the network are 2.985 and 3.019Å for the chains made up of molecule 1 and molecule 2 GABA respectively. The three dimensional hydrogen bonding network is then formed by the cross-linking of the two different chain types. Each chain type contains hydrogen bonding which links it to a chain of both molecule 1 and molecule 2 GABA in the a-direction. Within the hydrogen bonding network, molecule 1 GABA forms the six membered ring channels and molecule 2 GABA forms the 3-fold axis chains which coincide with the 3-fold screw axis.

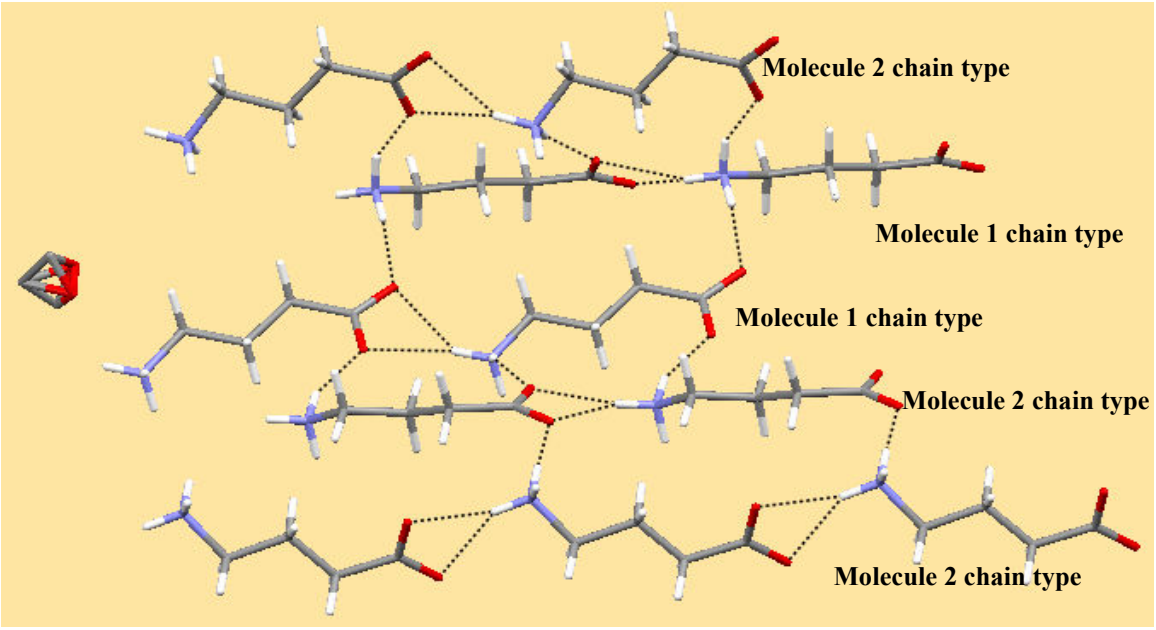


Figure 3.9 View of the linking of the two different types of GABA chains present in the hydrogen bonding network.

A comparison of this hydrogen bonding network with those presented in the papers by Tomita *et al.*, (1973) and Dobson *et al.*, (1996) for each GABA polymorph, indicates that due to the differences in the molecular conformations and crystal systems of these GABA polymorphs, there exist very different hydrogen bonding networks for the three structures.

3.2.6 Thermal Analysis

In order to determine the melting point of hexagonal GABA, hot stage microscopy was used and the value was verified by means of differential scanning calorimetry (DSC). Through hot stage microscopy, the melting point was found to be approximately 206°C. The DSC curve of hexagonal GABA was then obtained. The curve is presented in figure 3.10.

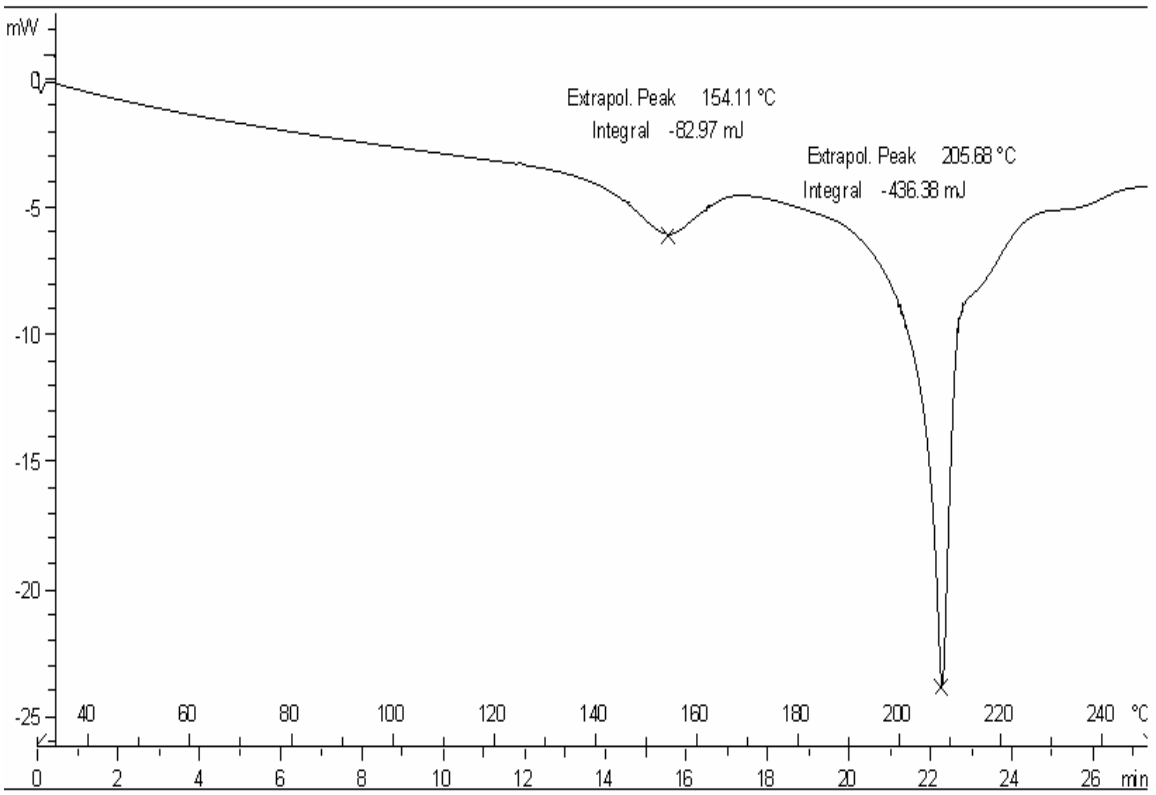


Figure 3.10 DSC curve of heat flow (mW) vs. temperature (°C) for the hexagonal GABA solvate grown in the presence of gabapentin.

The first peak obtained at 154.1°C corresponds to the melting point of gabapentin, which could not be separated from the hexagonal GABA crystals. The second peak corresponds to the melting of the hexagonal GABA crystals. This shows that the melting point is 205.9°C which is close to the melting point obtained using hot stage microscopy. The DSC plot further allows for the enthalpy of fusion to be determined.

Integral = 436.38mJ

Number of moles of GABA: n = m/M = 2.05mg/ 103.12
$= 1.988 \times 10^{-5}$ mol

Enthalpy = 436.38mJ/1.988×10^{-5} mol
Enthalpy = 21.95kJ/mol

This value is positive, indicating that it is endothermic as expected.

The melting points of the monoclinic and tetragonal GABA forms, which were also determined from DSC plots, were found to be 207.3°C and 203.9°C respectively (see Appendix 1.1.1 and 1.1.2). The enthalpy values for these two polymorphs are 65.56kJ/mol and 65.88kJ/mol. These enthalpy values are much greater than the enthalpy of hexagonal GABA (21.95kJ/mol), thus indicating that the monoclinic and tetragonal forms are thermodynamically more stable. The greater stability of the monoclinic and tetragonal GABA polymorphs can also be seen by the fact that crystals of these polymorphs are more easily grown. In the case of the hexagonal GABA solvate, very specific conditions are required in order to produce crystals.

3.3 Further characterisation of the GABA solvate

3.3.1 Hot Stage Microscopy

X-ray single crystal diffraction allowed for the structure of hexagonal GABA to be determined and indicated that there are two GABA molecules and a disordered solvent molecule within the asymmetric unit. Hot stage microscopy was used in order to examine the presence of the solvent within the crystal. The crystals were placed on a microscope slide and covered with paraffin oil. They were then mounted on a modified Kohler hot stage and heated.

At approximately 190°C, the solvate bubbles started to be emitted from the needle-like crystal, down the centre channel of the needle. Figure 3.11 indicates the release of solvate bubbles and other gases as the temperature increases from 190°C to the melting point at 206°C.

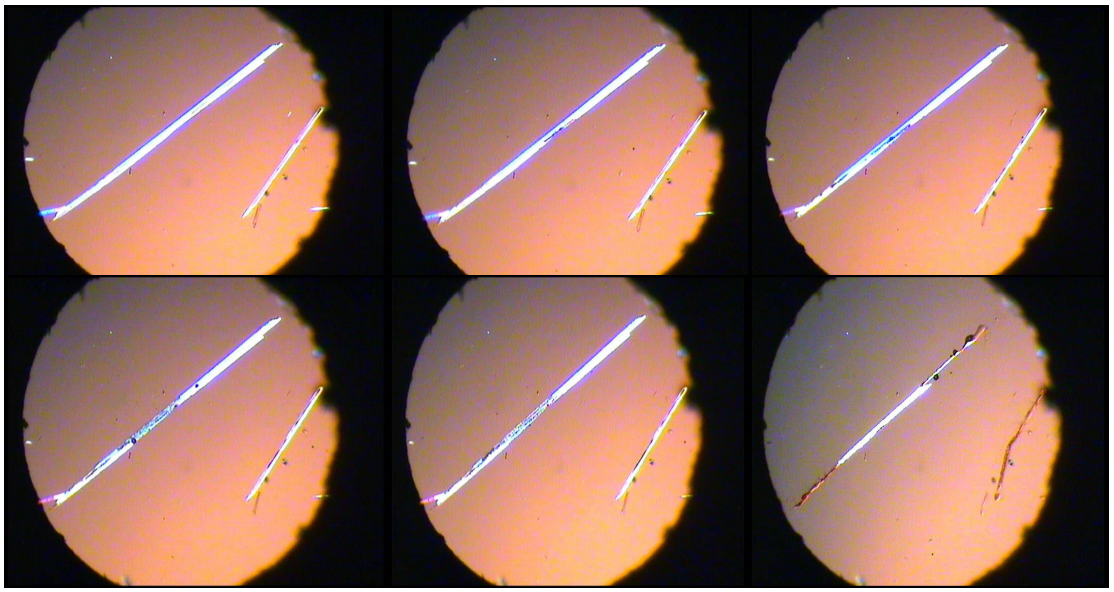


Figure 3.11 Optical microscope images of the release of solvate bubbles from the hexagonal GABA solvate crystals as the temperature is increased from 190 to 206°C.

3.3.2 Nuclear Magnetic Resonance (^{1}H NMR) Spectroscopy

Due to the disorder of the solvent molecules, it was not possible to determine what solvent is present in the crystals from the crystal structure alone. A thermo gravimetric analysis was carried out; however, the curve produced could not be interpreted. Therefore, ^{1}H nuclear magnetic resonance was used in order to determine the nature of the solvent. It could not be assumed that the solvent present in the crystals was ethanol due to the fact that 96% ethanol was used. In addition to this, experiments that were carried out using absolute ethanol did not produce hexagonal GABA crystals. Therefore there was the possibility of H_2O, ethanol or some impurity being present within the crystals. In order to examine the nature of the solvent, the hexagonal GABA crystals were dried by placing them in an oven at 120°C in order to remove the external ethanol solvent. The crystals were then dissolved in deuterated water (D_2O) and a proton NMR was run. The ^{1}H NMR spectrum is shown in figure 3.12 with the assigned functional groups given in table 3.4.

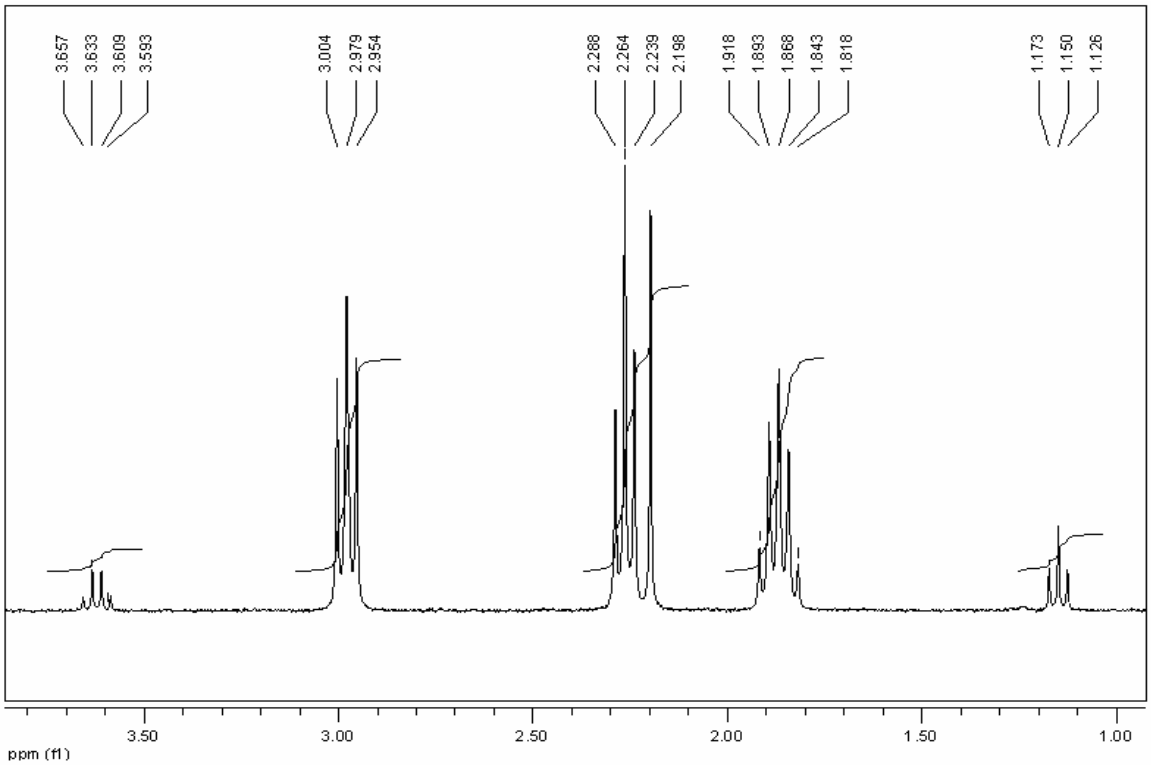


Figure 3.12 ^{1}H NMR spectrum of the hexagonal GABA solvate (excluding D_2O solvent peak at 4.780ppm).

Table 3.4: ^{1}H NMR chemical shifts and assigned functional groups.

Chemical Shift(ppm)	Multiplicity	Functional Group
1.1258 1.1495 1.1731	Triplet	CH_3(ethanol)
1.8181 1.8429 1.8678 1.8928 1.9176	Pentet	OOC-**CH_2**(GABA)
2.1978	Singlet	Acetone
2.2392 2.2637 2.2881	Triplet	Central **CH_2** group (GABA)
2.9533 2.9790 3.0036	Triplet	N-**CH_2**(GABA)
3.5856 3.6092 3.6329 3.6564	Quartet	HO-CH_2(ethanol)
4.7800	Singlet	D_2O(solvent)

From table 3.4, it is evident that the solvent present within the GABA channels is ethanol. Due to proton exchange, the amine and carboxyl groups form ND_3 and COOD when the crystals are dissolved in deuterated water, therefore, only the three CH_2 groups of the GABA molecule are represented in the NMR spectrum. The relative intensities of the peaks allow for the determination of the ratio of GABA molecules to ethanol molecules present within the crystal.

When the heights of the integration curves are measured for the ethanol peaks, it is found that the ratio of the number of ethanol solvent molecules to the number of GABA molecules present is 1:10. The refined site occupancy factors for ethanol (as indicated in section 3.2.5) agree with the NMR results. Therefore, within the channels there are large vacancies and only about 10% of the space is occupied.

3.4 Further Experimentation

Further experimentation was done in order to test whether the ethanol within the crystals could be replaced by a different substance, as was carried out by Görbitz *et al.*, (2005) in the replacement of acetonitrile by iodine in dipeptide crystals. The crystal system of the dipeptides is closely related to this hexagonal GABA solvate and the diameter of the channels are also comparable. Therefore, a similar method was used to that of Görbitz *et al.* (2005), where a saturated solution of iodine in toluene was made and this was then placed drop wise onto single hexagonal GABA solvate crystals under a microscope. Figure 3.13, gives an indication of the effect that the solvent had on the GABA crystals.

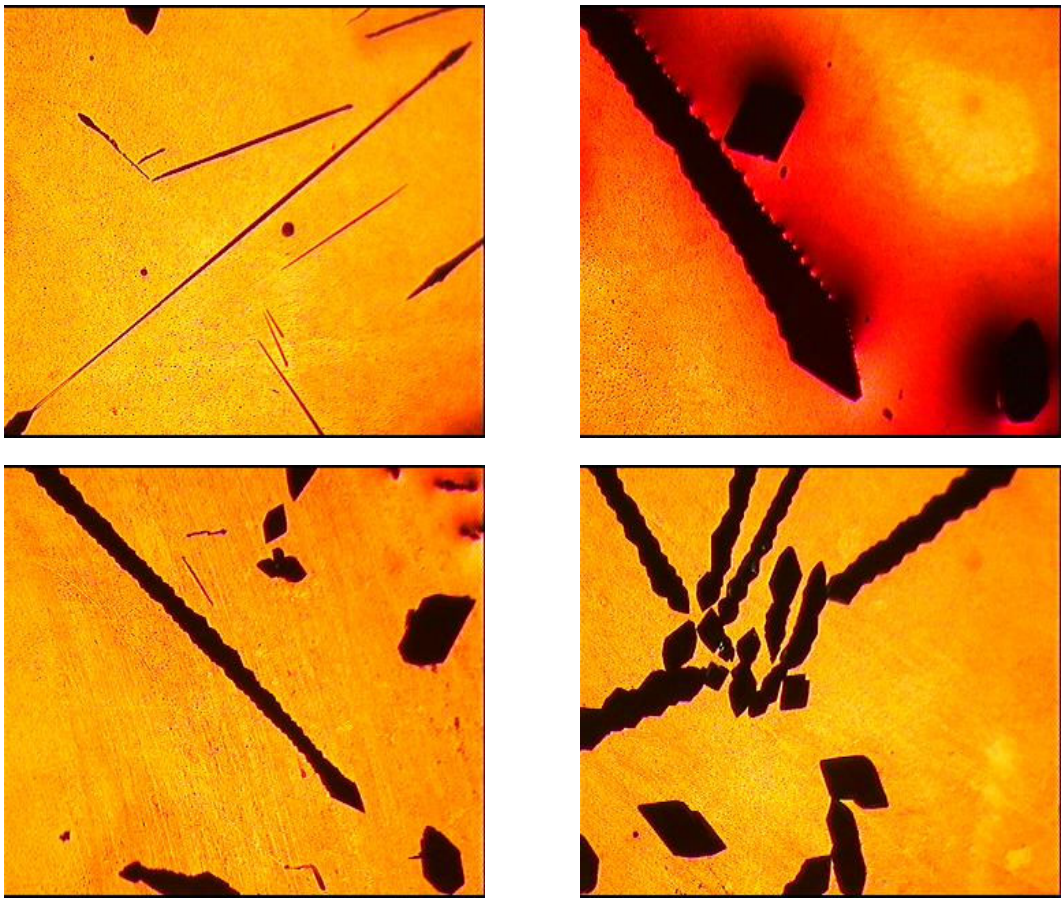


Figure 3.13 Visual indication of the effect of iodine saturated toluene on the hexagonal GABA solvate crystals.

The images in figure 3.13 indicate that the hexagonal GABA solvate crystals start to react with the solution and initially form diamond shapes at the end of the thin, needle shaped crystals. As the reaction proceeds, the entire crystal reacts and the diamond shaped fragments start to break away from the rest of the crystal. Some smaller crystals did remain needle shaped and changed to a brown colour, however, these were not suitable for X-ray single crystal diffraction. Although it appears that iodine is absorbed by the hexagonal GABA crystals, it is evident that this method is not suitable to exchange ethanol with iodine while still maintaining the structure of these crystals. Alternate methods need to be examined in order to test whether solvent exchange is possible for these hexagonal GABA solvate crystals.

3.5 Discussion and Conclusion

It is evident from the above X-ray diffraction as well as thermal and spectroscopic techniques, that a new, unpublished GABA solvate structure has been obtained. This structure is a pseudo polymorph of the previously published GABA structures. The conditions under which the new hexagonal GABA crystals form are by the diffusion of either hexane or acetonitrile into a saturated ethanol or 2-butanol solution maintained at 18±1°C. The inability of these crystals to grow in the presence of 2-propanol and 2-butanol could be due to the fact that GABA is more readily soluble in the alcohols when compared to the hexane and acetonitrile external solvents. The purpose of using the vapour diffusion method was in order for the external solvent to decrease the rate of evaporation of the ethanol. This method would therefore not be as effective with the alcohol solvents as they could become miscible with the ethanol and affect the crystal growth. The hexane and acetonitrile would simply form a thin layer on top of the ethanol and slow down the evaporation rate, thus allowing for the hexagonal GABA solvate crystals to form.

Hexagonal GABA solvate crystals were also formed by using 2-butanol as the internal solvent, however this was not the case when methanol, 2-propanol and absolute ethanol were used. In these solvents, the more stable polymorphs were formed. This could be due to the fact that the crystal growth depends on the initial solubility of GABA in the solvents. GABA dissolves in methanol and 2-propanol more readily than in ethanol and 2-butanol, therefore the increased solubility in these solvents could have the effect of causing the more stable polymorphs to form and not allowing the hexagonal GABA polymorph to grow.

As was the case with paracetamol (Capes *et al.*, 2007), mentioned in the introduction, the hexagonal GABA solvate crystals also grew from the contact line of the solution. However, in this case, the nucleation occurred at the contact line of the meniscus and then grew either upwards or downwards as evaporation occurred. As was the case with the paracetamol example, this hexagonal GABA polymorph is also the least stable of the polymorphs.

For GABA, the visual differences between the three crystal types were an indication, in this case of the presence of three different structures. The technique of x-ray single crystal diffraction was effective in allowing for the crystal structure to be obtained. The two GABA molecules within the hexagonal GABA asymmetric unit had minor differences, but their conformations were significantly different from the conformations of the other polymorphs. Therefore, each GABA polymorph, salt and solvate has distinct thermal properties, morphologies, conformations and hydrogen bonding networks.

A factor which is significant for the GABA hexagonal structure is the presence of the short Van der Waals interactions between the GABA molecules which form the channel and the disordered ethanol molecules within the channel. There is no indication of any hydrogen bonds present. Nevertheless, the ethanol molecules remain in the channels until the crystals are heated to a temperature of 190°C. This temperature is approximately 112°C higher than the regular boiling point of ethanol. This could be due to a high stability of the hexagonal channels, where the ethanol and other gases are only released when the hexagonal channels collapse, close to the melting point.

The new hexagonal GABA structure is also unique in that it is the first single amino acid to be crystallized in this form, where it has hexagonal channels which contain solvent molecules. Further studies will need to be done in the future in order to examine the potential of these crystals as microporous organic crystals where the ethanol can be removed from the crystals and replaced by another appropriate solvent.

3.6 Chapter 3 References

Capes, J.S., Cameron, R.E. (2007). Crystal Growth & Design, Vol. 7, No. 1, 108-112.

Dobson, A.J., Gerkin, R.E. (1996). Acta Cryst., C52, 3075.

Görbitz, C.H., Gundersen, E. (1996). Acta Cryst., C52, 1764-1767.

Görbitz, C.H., Nilsen, M., Szeto, K., Tangen, L.W. (2005). Chem. Commun., 4288–4290.

Ibers, J. A. (2001). Acta Cryst., C57, 642-643.

Roisnel, T., Rodrigues, J., (2000). Materials Science Forum, Proceeding of the seventh European powder diffraction conference, ed. R. Delhez and E.J. Mittenmeijer, 118-123.

Steward, E.G., Player, R.B., Warner, D. (1973). Acta Cryst., B29, 2825-2826.

Tomita, K.I., Higashi, H., Fujiwara, T. (1973). Bull.Chem.Soc.Jpn., 46, 2199.

www.health.enotes.com/cancer-encyclopedia/gabapentin, (19/11/2007).

Chapter 4

Gabapentin

4.1 Introduction and related work

As discussed in chapter 1, gabapentin (1-(aminomethyl)cyclohexaneacetic acid) is a neurotransmitter analogue and amino acid drug compound. It was first developed in 1994 by the pharmaceutical company Pfizer under the commercial name Neurontin® and was originally approved as an antiepileptic drug. Its applications have recently been extended to the treatment of neuropathic pain (Magnus, 1999).

Gabapentin was originally synthesized to mimic the structure of the neurotransmitter γ-aminobutyric acid (GABA). It is structurally similar to GABA and simply contains an additional cyclohexane ring attached to the GABA fragment. As is the case with GABA, gabapentin also operates within the central nervous system; however it does not act on the same brain receptors (www.health.enotes.com, 10/10/2006).

Gabapentin has the molecular formula $C_9H_{17}NO_2$ and a molecular weight of 171.24g/mol. It is a white crystalline solid which is extremely soluble in water and mildly soluble in a number of acidic and basic aqueous solutions. The structural formula is shown in figure 4.1.

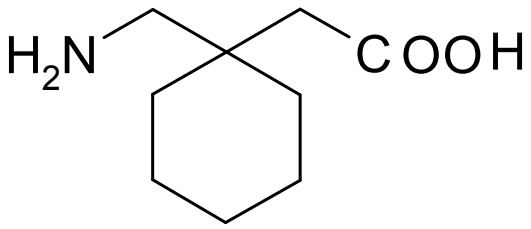


Figure 4.1 Structural formula of gabapentin.

In recent years, there has been intense interest in the polymorphs of gabapentin and the synthesis of gabapentin analogues. One form of anhydrous gabapentin has been published (α-gabapentin). It exists as a zwitterion and crystallizes with a monoclinic crystal system

in the space group $P2_1/c$ (Ibers, 2001). This form corresponds to Form II in US Patent 6521787 (Lladó *et al.*, 2003) and to the form of gabapentin found in the commercially available Pfizer pharmaceutical, Neurontin®. It contains an extensive hydrogen bonding network due to the presence of the NH_3^+ and COO^- groups.

The structure of a gabapentin monohydrate has also been published and, as is the case with the anhydrous structure, it crystallizes in a monoclinic crystal system with a $P2_1/c$ space group. The molecules in this crystal form are involved in additional hydrogen bonding due to the presence of the water molecule (Ibers, 2001).

Several gabapentin derivatives have also been synthesized including gabapentin HCl, gabapentin lactam, t-butyloxycarbonyl-gabapentin-OH, pivaloyl-gabapentin-OH, tosyl-gabapentin-OH, t-butyloxycarbonyl-gabapentin-N-hydroxysuccinimide ester and t-butyloxycarbonyl-gabapentin-NHMe. In some of the structures, the aminomethyl group lies in an axial position while others have the carboxymethyl group lying axially. The paper published by Ananda *et al.*, (2003) discusses these different structures, their orientations and their individual crystal and diffraction parameters.

Structures of peptides incorporating gabapentin have also been studied where the conformation of gabapentin is stereochemically constrained in order to adopt folded conformations, resulting in the formation of intramolecular hydrogen bonded structures. A paper published by Vasudev *et al*., (2007) discusses examples of 7, 9, 12 and 13 atom hydrogen bonded rings which form in these peptide structures containing the gabapentin residue.

In addition to these derivatives, a 1-(aminomethyl)- drug compound, pregabalin, has also been reported. This compound is both structurally and functionally related to gabapentin and has been designed to be more medicinally potent than gabapentin in the treatment of seizures and neuropathic pain (Venu, 2007).

In this chapter, the structure of α-gabapentin which has previously been reported will be compared with the results obtained in this research project, namely, the structures of two unreported gabapentin polymorphs, β-gabapentin and γ-gabapentin.

4.2 Gabapentin polymorphs

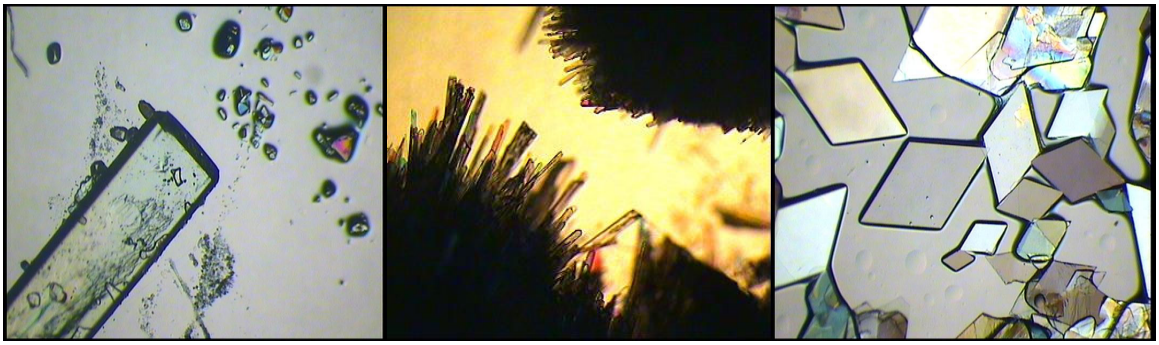
4.2.1 Experimental

Using x-ray powder diffraction, it was found that the gabapentin available from Sigma Aldrich corresponds to α-gabapentin. The gabapentin found in Neurontin® capsules also corresponds to α-gabapentin. This gabapentin was extracted from the Neurontin® capsules by dissolving the contents of 300mg capsules in 96% ethanol and then filtering the solution using 0.45μm hydrophilic microporous filters in order to remove the inactive materials in the capsule. The filtered solution was then left under open-air evaporation in order to crystallize. β-gabapentin was prepared by dissolving commercially available gabapentin (Sigma Aldrich) in 96% ethanol at ambient temperature until the solution was saturated. The solution was then placed into a vial and heated in an oil bath at 60°C for 48 hours. Needle-like crystals of β-gabapentin were grown from the solution.

In the preparation of γ-gabapentin, commercially available gabapentin (Sigma Aldrich) was dissolved in 96% ethanol at 60°C. The solution was then cooled to room temperature. Plate-like diamond shaped crystals of γ-gabapentin formed after 3 days of slow open-air evaporation.

4.2.2 Visual comparison of gabapentin structures

As was the case with GABA, an initial comparison could be done by examining the visual differences and crystal habit of the three different crystal types. Again, images were taken using a Micro Met Scientific microscope at a 45x magnification (see figure 4.2).



(a) (b) (c)

Figure 4.2 Optical microscope (Micro Met Scientific, 45x magnification) images of three different crystalline forms of gabapentin, (a) α-gabapentin, (b) β-gabapentin, (c) γ-gabapentin.

Therefore, it can be observed from figure 4.2 that there exist significant differences in the morphologies of the three gabapentin forms. However, further characterisation needed to be performed in order to verify that these crystals are in fact different polymorphs.

4.2.3 X-ray Powder Diffraction

The X-ray powder diffraction patterns of β-gabapentin and γ-gabapentin were recorded and compared with the diffraction pattern of α-gabapentin. The patterns were superimposed using Winplotr (Roisnel *et al.*, 2000). Figure 4.3 shows the comparison.

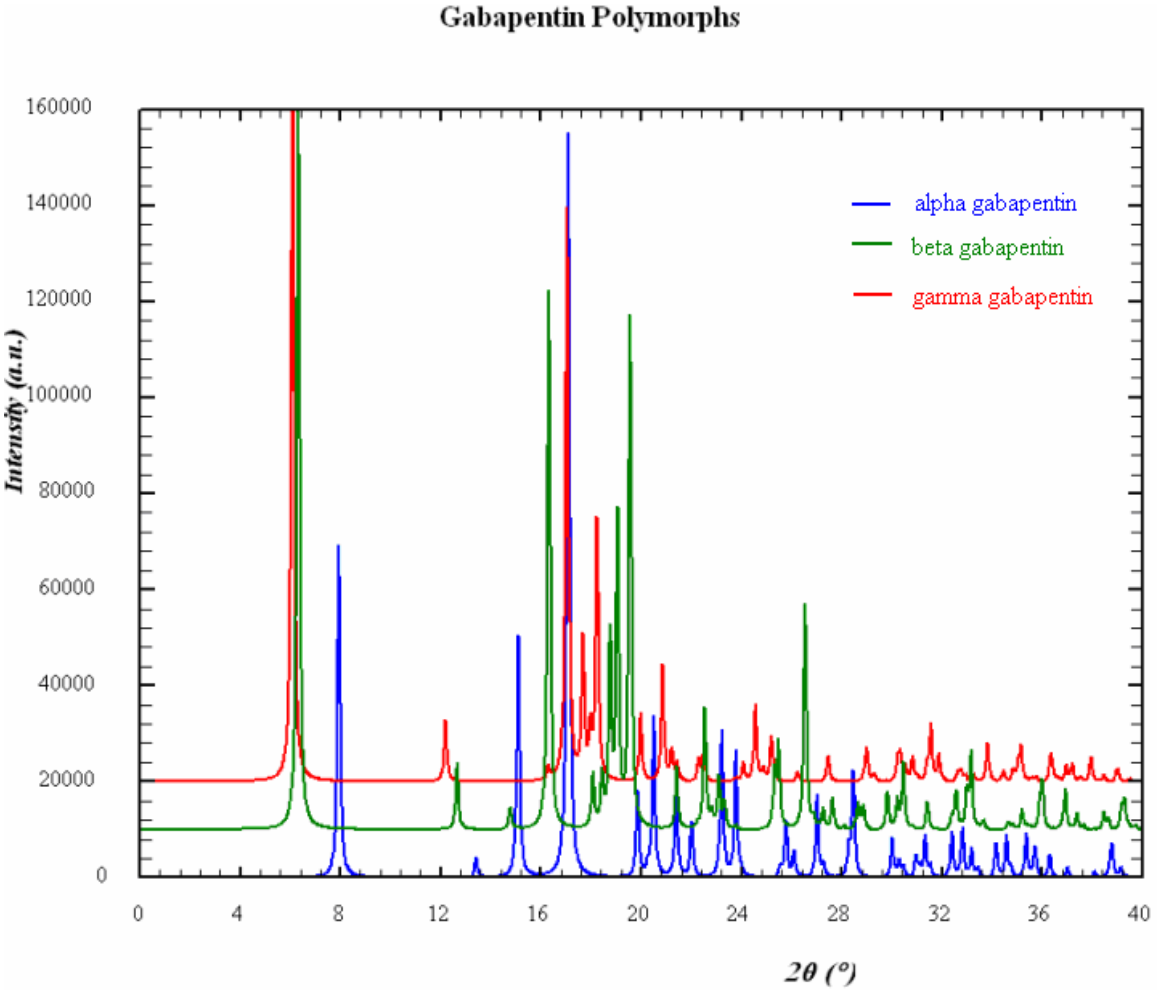


Figure 4.3 X-ray powder diffraction pattern comparison of α-, β- and γ-gabapentin.

It is clear from figure 4.3, that the diffraction pattern of α-gabapentin is very different from the patterns of the other two forms, as there is very little peak overlapping. In the case of the β- and γ-gabapentin diffraction patterns, the first peak for each pattern appears to be overlapping. However, there is a slight difference, where the 2θ values are 6.08° and 6.30° for β- and γ-gabapentin respectively. The second peak in each of these patterns also shows a difference of approximately 0.5°. A comparison of the remainder of the peaks for these two forms indicates very little peak overlap. Therefore, it is evident that the powder diffraction patterns of the three structures are different, proving that different crystalline phases are present.

The X-ray powder diffraction pattern of β-gabapentin was also compared with the pattern found in US Patent 6255526 (Pesachovich *et al.*, 2001) and it was found that β-gabapentin corresponds to Form III in this US patent. The X-ray powder diffraction pattern of γ-gabapentin was compared with the pattern found in patent WO/2004/110342 and it was found that γ-gabapentin corresponds to Form IV in this patent (Satyanarayana *et al.*, 2004). The crystal structures of these forms have not been reported.

4.2.4 X-ray Single Crystal Diffraction

X-ray single crystal diffraction was used in order to examine the molecular conformations and fully characterise β- and γ-gabapentin. A crystal was mounted and examined at -100°C on the Bruker, APEX II diffractometer. The data presented in table 4.1 below gives an indication of the parameters of β- and γ-gabapentin as well as a comparison between the three structures.

Table 4.1: Crystallographic data of the gabapentin crystalline forms.

	α-gabapentin	β-gabapentin	γ-gabapentin
Empirical Formula	$C_9H_{17}NO_2$	$C_9H_{17}NO_2$	$C_9H_{17}NO_2$
Formula Weight	171.24g/mol	171.24g/mol	171.24g/mol
Temperature	153(2)K	173(2)K	173(2)K
Crystal System	Monoclinic	Monoclinic	Monoclinic
Space Group	$P2_1/c$	$P2_1/c$	C2/c
Description	Block, colourless	Needle, colourless	Plate, colourless
Unit cell dimensions	a = 5.8759 (6) Å	a=14.5376(16) Å	a=30.5452(11) Å
	b = 6.9198 (7) Å	b= 6.6329(6)Å	b= 5.9268(2)Å
	c = 22.262 (2) Å	c= 9.8343(9)Å	c= 10.8841(4)Å
	α = 90°	α = 90°	α = 90°
	β = 90.08°	β = 105.922(5)°	β = 108.316(2)°
	γ = 90°	γ = 90°	γ = 90°
Volume	V = 905.18 (16) $Å^3$	V=911.91(15) $Å^3$	V=1870.58(12) $Å^3$
Z	4	4	8
Packing efficiency	71.3%	70.5%	68.7%
Density(calculated)	1.26g/cm^{-3}	1.25g.cm^{-3}	1.22g.cm^{-3}
Absorption coefficient	0.088mm^{-1}	0.087mm^{-1}	0.085mm^{-1}
Θ range for data collection	1.83 - 28.40°	1.46 - 27.99°	1.40 - 26.99°
Reflections collected	7951	5118	7746
Independent reflections	2147	2195	2042
Final R indices	0.042	0.046	0.046

The above crystallographic data indicates clear differences for the three structures. The α- and β-gabapentin both have the same crystal system and space group; however, the unit cell parameters are very different. γ-gabapentin has a space group of C2/c which is also different from the other two forms. A comparison of the densities and packing efficiencies for the three structures shows that the molecules are most efficiently packed in α-gabapentin and this could indicate that it is the most thermodynamically stable form.

The structures can be further compared and characterised by examining the molecular conformations obtained by X-ray single crystal diffraction. The conformations are presented in figure 4.4.

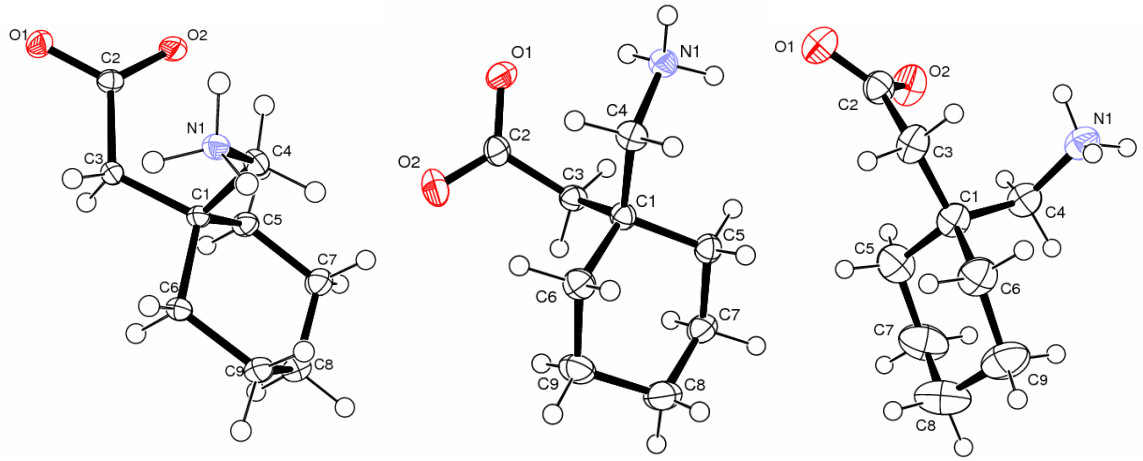
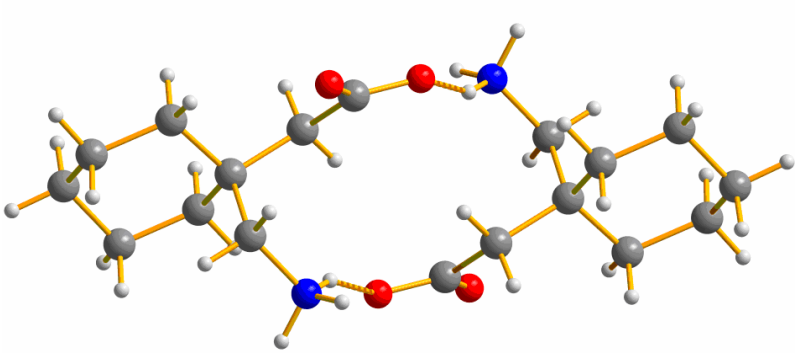


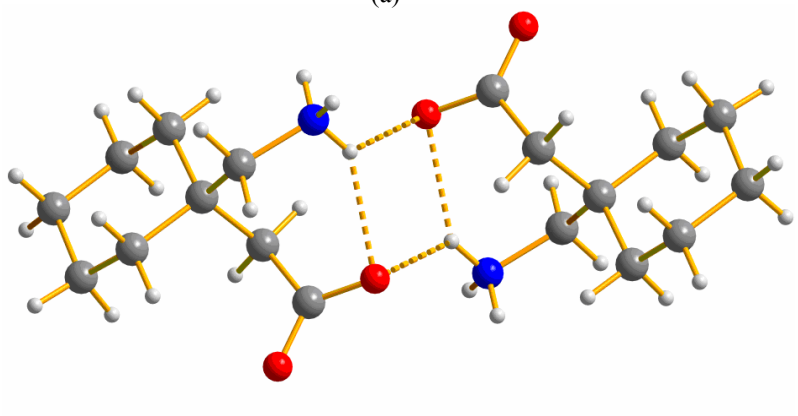
Figure 4.4 Ortep diagrams of (a) α-gabapentin, (b) β-gabapentin and (c) γ-gabapentin with the displacement ellipsoids drawn at the 50% probability level.

The conformational diagrams in figure 4.4 clearly indicate differences in the structures in terms of the positioning of the NH_3^+ and COO^- groups. β-gabapentin contains the NH_3^+ group in an equatorial position and the COO^- group in an axial position, however, in α- and γ-gabapentin these groups are in the opposite positions. This difference is further indicated by the torsion C3-C1-C5-C7 = -166.22°, -65.44°, -168.7° for α, β- and γ-gabapentin respectively, where the β-gabapentin value is significantly different from the other forms.

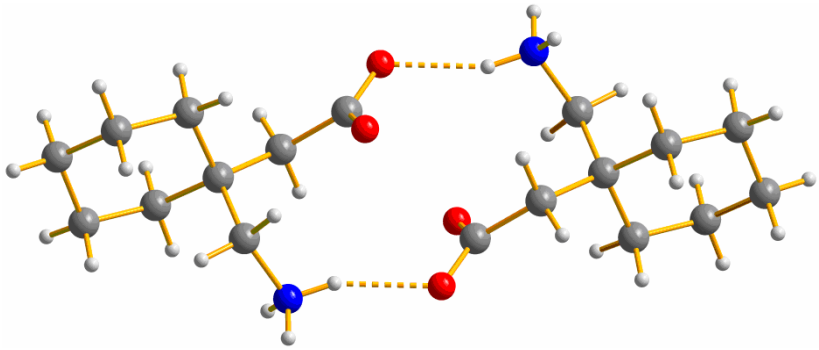
The differences in the torsion angles O1-C2-C3-C1= -161.36°, 95.97°, 151.56°, C2-C3-C1-C4 = 51.21°, -46.4°, 63.47° and C3-C1-C4-N1= 60.07°, -52.5°, 47.74° for the α-, β- and γ-gabapentin respectively, indicate the different angles and directions at which the NH_3^+ and COO^- groups are twisted. The above torsion angles indicate that the largest conformational difference which occurs is due to the twisting of the COO^- group. The centrosymmetric hydrogen bonded dimers of the three structures are presented in figure 4.5 and further indicate these differences.



(a)



(b)



(c)

Figure 4.5 Centrosymmetric dimers of (a) α-gabapentin, (b) β-gabapentin and (c) γ-gabapentin indicating the $C_2^2(14)$ graph set in each case.

Further torsion angles which indicate the differences in the three gabapentin polymorphs are listed in table 4.2.

Table 4.2: Selected torsion angle parameters of the gabapentin polymorphs (°).

Torsion Angle	α	β	γ
C2-C3-C1-C5	-68.63(14)	-168.37(14)	-56.38(18)
C2-C3-C1-C6	172.52(11)	71.87(18)	-174.14(14)
N1-C4-C1-C6	-58.28(14)	-173.57(14)	-72.56(17)
N1-C4-C1-C5	-178.71(10)	69.42(18)	168.72(13)

Comparing the polymorphs, it is seen that the cyclohexane rings all have the chair configuration, however, the aminomethyl and carboxyl groups are oriented in different positions. Therefore, the above torsion angles and diagrams clearly show that the three gabapentin polymorphs are structurally very different.

4.2.5 Hydrogen bonding

In all three polymorphs there exists extensive hydrogen bonding due to the presence of the NH_3^+ and COO^- groups. In each case, the NH_3^+ group on the gabapentin molecules, hydrogen bonds to three COO^- groups, each from a different neighbouring molecule. Table 4.3 gives an indication of the differences in the hydrogen bonding in each of the polymorphs.

Table 4.3: Hydrogen bonding parameters of the gabapentin polymorphs (Å,°).

D-H---A	D-H	H---A	D---A	D-H---A
α-gabapentin (Ibers, 2001)				
N1-H15—O1^{i,a,}	0.92	1.91	2.7827 (16)	158
N1-H16—O2^{ii,a}	0.92	1.85	2.7525 (16)	165
N1-H17—O1^{iii,a}	0.96	1.81	2.7547 (18)	166
β-gabapentin				
N1-H15—O1	0.91	2.19	2.9398 (19)	139
N1-H15—O1^{i,b}	0.91	2.42	3.0242 (18)	124
N1-H16—O2^{ii,b}	0.91	1.86	2.7230 (2)	157
N1-H17—O1^{iii,b}	0.91	1.81	2.7174 (19)	176
γ-gabapentin				
N1-H15—O1^{i,c}	0.91	1.93	2.7980 (16)	159
N1-H16—O2^{ii,c}	0.91	1.85	2.7324 (17)	161
N1-H17—O1^{iii,c}	0.91	1.91	2.7851 (18)	161

Symmetry Codes:

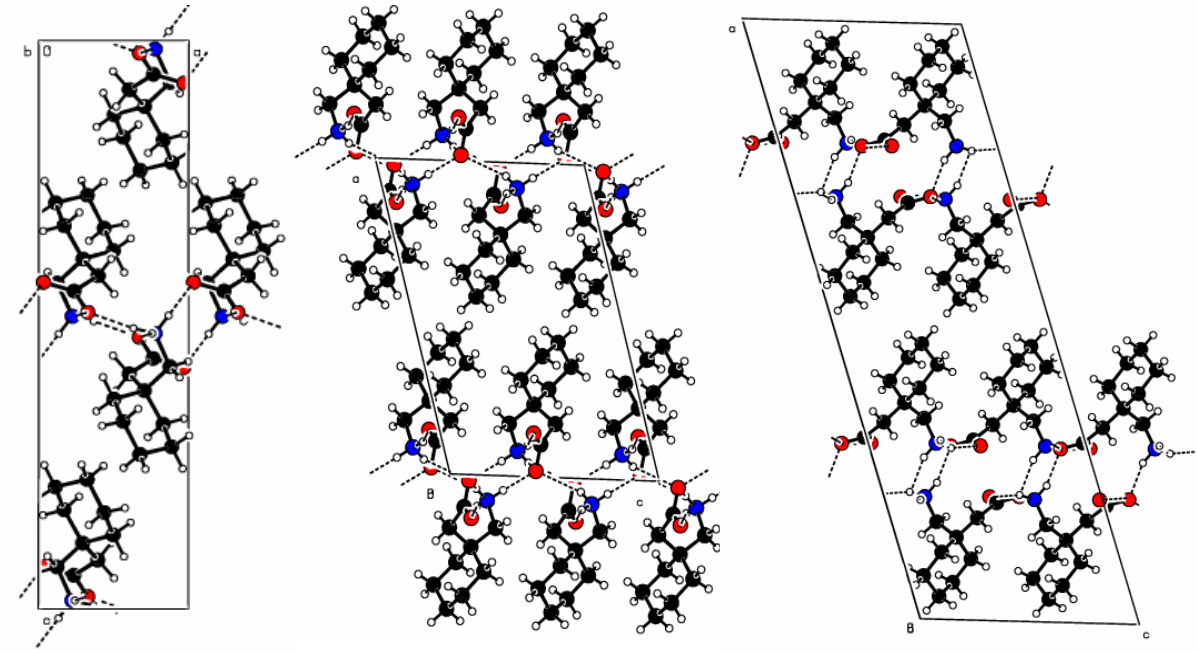
a. (i) -x+1, -y+1, -z+1; (ii) -x, -y+1, -z+1; (iii) x, y+1, z;

b. (i) -x, -y, -z+1; (ii) x, y-1, z; (iii) -x, y-1/2, -z+1/2;

c. (i) -x+1/2, -y+1/2, -z+1; (ii) x, -y+1, z+1/2; (iii) x, -y, z+1/2.

There is a significant difference in the hydrogen bonding networks of α- and β-gabapentin which is primarily due to the presence of an intramolecular hydrogen bond in β-gabapentin [N1-H15---O1 = 2.940(19)Å]. Atom O1 acts as a trifurcated hydrogen bond acceptor in β-gabapentin compared to the bifurcated acceptor in α-gabapentin. This results in the lengthening of the N1-H15---O1 bond between two neighbouring molecules, i.e. N1-H15---O1 = 2.783(16)Å and 3.024(18)Å for α- and β-gabapentin respectively.

As is the case with α-gabapentin, there is no intramolecular hydrogen bond in γ-gabapentin. The N-H---O hydrogen bond distances are very similar to those in α-gabapentin [average N1-H-O = 2.763Å and 2.771Å for α- and γ-gabapentin respectively]. The α- and γ-gabapentin polymorphs also both have the O1 atom acting as a bifurcated hydrogen bond acceptor. Figure 4.6 indicates the differences in the hydrogen bonding networks for the three structures.



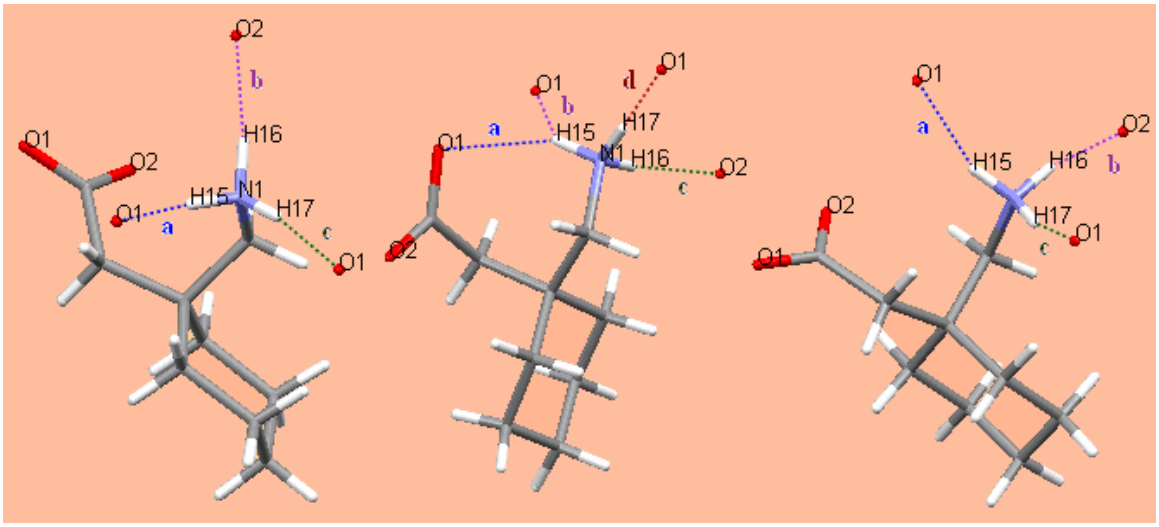
(a) (b) (c)

Figure 4.6 Hydrogen bonding networks of (a) α-gabapentin, (b) β-gabapentin and (c) γ-gabapentin where the α-form is viewed down the a-axis and the β- and γ-forms are viewed down the b-axis.

There are clear differences in the packing of gabapentin in the three polymorphs. The hydrogen bonding networks can further be compared by the use of graph sets. Some first and second level hydrogen bond motifs which are present for the hydrogen bonding networks of the three structures were determined by RPLUTO (Motherwell *et al.*, 1999). A summary of the main graph sets is shown in matrix form in table 4.4 which corresponds to figure 4.7.

Table 4.4: Matrix of selected graph sets for the hydrogen bonding of the gabapentin polymorphs.

α-gabapentin				
	a	**b**	**c**	
a	$C_2^2(6)$	-	-	
b	$C_2^2(14)$	$R_2^2(14)$	-	
c	$R_4^4(28)$	$R_4^4(28)$	$C_1^1(7)$	
β-gabapentin				
	a	**b**	**c**	**d**
a	$S_1^1(7)$	-	-	-
b	$C_2^2(14)$	$R_2^2(14)$	-	-
c	-	$R_4^4(28)$	$C_2^2(6)$	-
d	-	-	$C_2^2(14)$	$C_1^1(7)$
γ -gabapentin				
	a	**b**	**c**	
a	$R_2^2(14)$	-	-	
b	$C_2^2(6)$	$C_1^1(7)$	-	
c	$C_2^2(14)$	$C_2^2(14)$	$C_1^1(7)$	



(a) (b) (c)

Figure 4.7 Diagram representing the possible hydrogen bonds present for each structure (a) α-gabapentin, (b) β-gabapentin and (c) γ-gabapentin where the bold letters each represent a different individual hydrogen bond in each structure. Some of the first and second level graph set motifs, resulting from these bonds, are indicated in table 4.4 for α-gabapentin, β-gabapentin and γ-gabapentin. The single red dots refer to the oxygen atoms where the remainder of the molecule has been deleted for visual clarity.

There are four graph sets common to each polymorph including the unitary level $C_1^1(7)$ and $R_2^2(14)$, and secondary level $C_2^2(14)$ and $C_2^2(6)$ sets. The common $R_2^2(14)$ graph set was shown in the centrosymmetric dimers presented in figure 4.5. The β polymorph is the only form which contains the unitary level $S_1^1(7)$ graph set for the intramolecular interaction.

4.3 Thermal Analysis

The melting points of the gabapentin polymorphs were initially determined by hot stage microscopy and again these values were verified using differential scanning calorimetry. The melting point of α-gabapentin was measured to be 160°C. A DSC scan was run and the melting point was found to be over the range 155-166°C with the peak position at 160.9°C (please see Appendix 1.2.1). The enthalpy, as calculated by the standard method shown in section 3.2.6, was found to be 40.52 kJ/mol.

The melting point of β-gabapentin was measured to be 166°C. The DSC scan is shown in figure 4.8.

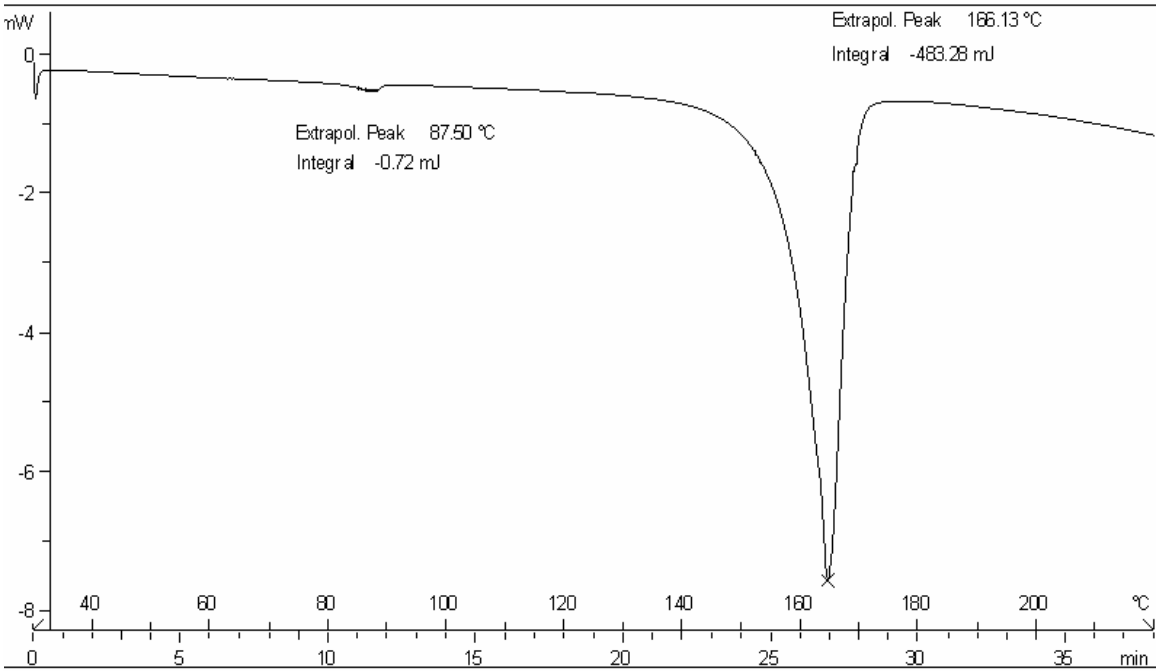


Figure 4.8 DSC curve of heat flow (mW) vs. temperature (°C) for β-gabapentin over the range 25- 220°C.

The DSC curve indicates that the melting point occurs over the range 155 – 168°C with the peak position at 166.1°C. This is close to the value obtained using hot stage microscopy. From the integral, the enthalpy was calculated to be 35.99 kJ/mol. The curve also indicates that there is a small endothermic peak present at approximately 87.5°C with an enthalpy of approximately 0.054 kJ/mol. This peak could relate to a possible phase transition. In order to examine this possible transition, parameters of a single crystal of β-gabapentin were measured at increasing temperatures in order to test whether a change occurs. Table 4.5 and figure 4.9 below indicate the changes in the unit cell parameters.

Table 4.5: Changes in the unit cell parameters of β-gabapentin with temperature.

Temperature(°C)	a(Å)	b(Å)	c(Å)	α(°)	β(°)	γ(°)	Volume(Å^3)
25	9.89	6.66	14.71	90	106.37	90	929
50	9.93	6.66	14.77	90	106.49	90	937
70	9.97	6.67	14.86	90	106.65	90	946
75	9.90	6.64	14.77	90	106.68	90	930
80	9.97	6.69	14.87	90	106.68	90	950
85	9.91	6.65	14.78	90	106.77	90	932
90	9.86	6.63	14.78	90	106.54	90	926
95	9.91	6.63	14.80	90	106.95	90	930
100	9.91	6.62	14.77	90	106.99	90	927
105	9.86	6.54	14.77	90	107.10	90	910
110	9.89	6.54	14.82	90	106.92	90	924

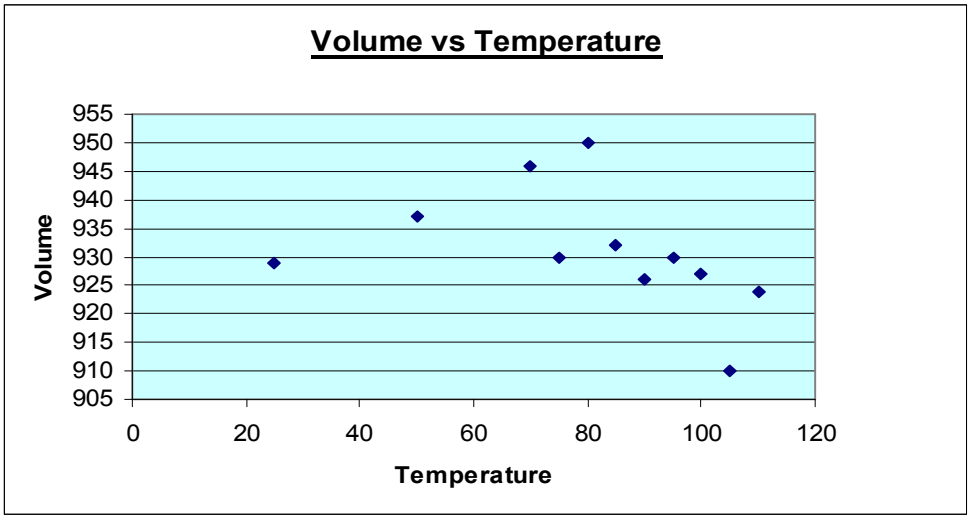


Figure 4.9 Plot of points obtained for the change in volume (Å^3) against the change in temperature (°C) for β-gabapentin.

This plot indicates that there is a drop in volume after 80°C. This could correspond with the change observed on the DSC curve. The other unit cell parameters remained fairly similar, with only slight increases in the unit cell lengths due to heating. Data collections were carried out at 70°C and at 100°C in order to examine possible differences. A comparison of the corresponding hydrogen bonding and selected geometric parameters is presented in tables 4.6 and 4.7.

Table 4.6: Comparison of the hydrogen bonding parameters of β-gabapentin at different temperatures (Å, °).

D-H---A	D-H	H---A	D---A	D-H--A
β-gabapentin(-100°C)				
N1-H15---O1(intra)	0.91	2.19	2.940(19)	139
N1-H15---O1	0.91	2.42	3.024(18)	124
N1-H16---O2	0.91	1.86	2.7230(2)	157
N1-H17---O1	0.91	1.81	2.717(19)	176
β-gabapentin(70°C)				
N1-H15---O1(intra)	0.89	2.21	2.936(2)	139
N1-H15---O1	0.89	2.48	3.065(2)	124
N1-H16---O2	0.89	1.88	2.713(2)	156
N1-H17---O1	0.89	1.84	2.722(2)	174
β-gabapentin(100°C)				
N1-H15---O1(intra)	0.89	2.21	2.933(3)	139
N1-H15---O1	0.89	2.49	3.084(3)	124
N1-H16---O2	0.89	1.88	2.718(3)	156
N1-H17---O1	0.89	1.83	2.720(3)	175

The above table indicates that there are only minor differences in the hydrogen bonding parameters of the three structures.

Table 4.7: Comparison of the torsion angles of β-gabapentin at different temperatures (°).

Torsion	β-gabapentin(-100°C)	β-gabapentin(70°C)	β-gabapentin(100°C)
C3-C1-C5-C7	-65.44(18)	-67.10(2)	-66.50(3)
O1-C2-C3-C1	95.97(18)	94.50(2)	93.70(3)
C2-C3-C1-C4	-46.40(2)	-46.90(2)	-46.10(3)
C3-C1-C4-N1	-52.50(2)	-52.20(2)	-52.90(3)
C2-C3-C1-C5	-168.37(14)	-168.54(17)	-168.6(2)
C2-C3-C1-C6	71.87(18)	71.4(2)	71.90(3)
N1-C4-C1-C6	-173.57(14)	-173.38(16)	-173.4(2)
N1-C4-C1-C5	69.42(18)	69.10(2)	69.60(3)

The comparison of the torsion angles indicates only very small differences. Therefore, the endothermic peak which appears at approximately 87.5°C is not as a result of a significant change in the structure or a change in the hydrogen bonding of β-gabapentin. It is possible that the structure could change at that specific temperature and then revert back to the original structure during the data collection. The packing for the structures at the three temperatures is very similar.

The melting point of the γ-gabapentin was found to be 164°C. The DSC scan was recorded and figure 4.10 shows the curve obtained.

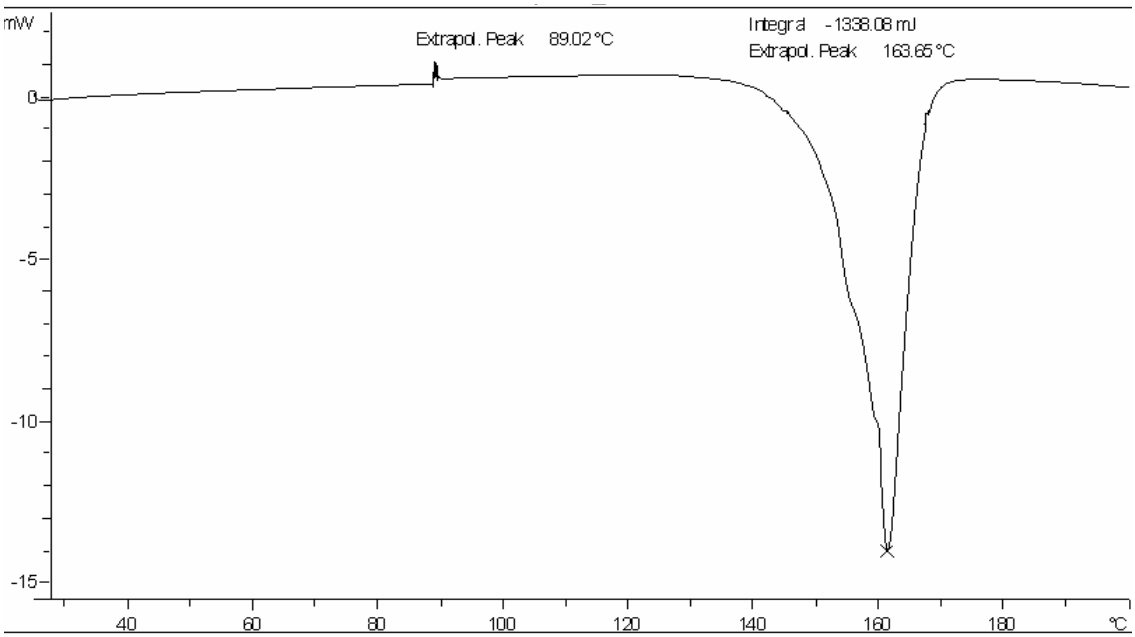


Figure 4.10 DSC curve of heat flow (mW) vs. temperature (°C) for γ-gabapentin over the range 25- 200°C.

The scan in figure 4.10 shows the melting point to be over the range 150 – 168°C and the peak position at 163.4°C which is very close to the value obtained using hot stage microscopy. The enthalpy value for this melting point is 43.97 kJ/mol. For this curve, there is also a small exothermic peak present at approximately 89°C with an enthalpy of approximately 1.5 kJ/mol. This could also indicate the presence of a phase change at this point. As was the case with β-gabapentin, the unit cell parameters were measured at various temperatures. In this case however, a plot of Volume ($Å^3$) vs. Temperature (°C) did not show a clear trend. Again, data was collected at 70°C and 100°C in order to examine whether any structural changes occur.

A comparison of the corresponding hydrogen bonding is given in table 4.8.

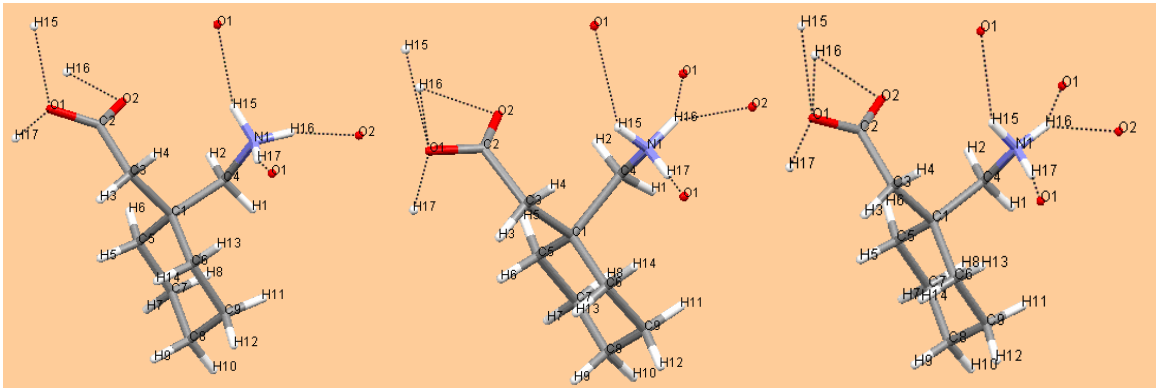
Table 4.8: Comparison of the hydrogen bonding parameters of γ-gabapentin at different temperatures(Å,°).

D-H---A	D-H	H---A	D---A	D-H--A
γ-gabapentin(-100°C)				
N1-H15---O1	0.91	1.929	2.798(16)	159
N1-H16---O2	0.91	1.854	2.732(17)	162
N1-H17---O1	0.91	1.908	2.785(18)	161
γ-gabapentin(70°C)				
N1-H15---O1	0.89	2.056	2.795(18)	140
N1-H16---O2	0.89	1.961	2.734(19)	144
N1-H17---O1	0.89	1.995	2.785(19)	147
N1-H16---O1	0.89	2.680	3.344(19)	132
γ-gabapentin(100°C)				
N1-H15---O1	0.89	2.090	2.830(15)	140
N1-H16---O2	0.89	1.962	2.759(19)	147
N1-H17---O1	0.89	2.041	2.815(15)	151
N1-H16---O1	0.89	2.686	3.343(19)	132

This comparison indicates that there are differences between the hydrogen bonding distances in the -100°C structure when compared to the 70°C and 100°C structures. The hydrogen bond lengths are shorter and hence stronger in the -100°C structure than the

other structures. There are also smaller differences between the 70°C and 100°C structures. In the two high temperature structures, there is also the presence of an additional weak hydrogen bonding interaction which results in H16 acting as a bifurcated hydrogen bond donor.

This can be seen in figure 4.11 below, which shows the hydrogen bonding contacts for each molecule.



(a) (b) (c)

Figure 4.11 Hydrogen bonding contacts for γ-gabapentin at (a) -100°C, (b) 70°C and (c) 100°C respectively.

A comparison of selected torsion angles is presented in table 4.9.

Table 4.9: Comparison of the torsion angles of γ-gabapentin at different temperatures(°).

Torsion	γ -gabapentin(-100°C)	γ -gabapentin(70°C)	γ -gabapentin(100°C)
C3-C1-C5-C7	-168.79(15)	-168.7(15)	-168.4(15)
O1-C2-C3-C1	151.56(14)	151.7(15)	142.6(14)
C2-C3-C1-C4	63.47(18)	63.30(19)	63.00(18)
C3-C1-C4-N1	47.74(17)	48.21(19)	55.40(19)
C2-C3-C1-C5	-56.38(18)	-56.31(19)	-55.01(18)
C2-C3-C1-C6	-174.14(14)	-173.99(15)	-179.8(14)
N1-C4-C1-C6	-72.56(17)	-72.22(18)	-70.70(17)
N1-C4-C1-C5	168.72(13)	168.94(14)	172.4(14)

The above table (Table 4.9) indicates that the three structures only have small differences in their torsion angles. The small exotherm could be an indication of energy given off, when the conformation of the structure is slightly altered. The packing for the structures at the three temperatures is very similar.

4.4 Molecular Modeling

Attempts were made at modeling the possible lowest energy conformations of isolated molecules of gabapentin, in order to determine whether the modeled structures would match those of the three gabapentin polymorphs. In Hyperchem Professional, a geometry optimisation was carried out with the charges set to zero. This file was then exported as a PDB file and opened in Gaussian. In order to assign accurate charges, a single point calculation was carried out using density functional theory with the BZLYP hybrid functional and the 3-21G* basis set. Density functional theory is an approach which makes use of electronic density as the basic quantity. It is a simple quantity to use when compared with other electronic wavefunction approaches as it is a function of only three variables. Charges were fitted to the electrostatic potential at points selected according to the Merz-Singh-Kollman scheme in which atomic charges are fitted to reproduce the molecular electrostatic potential at various points around the molecule. (Besler *et al.*, 1990; Singh *et al.*, 1984; www.physics.ohio-state.edu.html).

The charged gabapentin structure was then opened in Hyperchem and conformational searches with different constraints were carried out. The Generalised AMBER force field was used. The AMBER forcefield has often been used in the modeling of proteins and nucleic acids, however, it has limited parameters for organic molecules. The Generalised AMBER forcefield has been developed to accommodate most pharmaceutical molecules and was therefore chosen for this project (www.amber.scripps.edu.html). The lowest energy conformations which were found did not resemble the conformations of the three gabapentin polymorphs described above. Subsequent correspondence with Professor Graeme Day from the Cambridge Pfizer institute revealed that work is being done on the molecular modeling of gabapentin and thus far the crystal structures of α- and β-

gabapentin have been modeled. The complications in the modeling of this compound lie in the choice of force field to be used.

4.5 Discussion and Conclusion

Through an initial visual comparison and the analysis of the X-ray powder diffraction patterns of the three gabapentin forms, it was evident that different crystalline phases had been obtained. Further characterisation of the crystals through X-ray single crystal diffraction and the examination of the parameters, molecular conformations and hydrogen bonding networks, clearly indicated the presence of three different gabapentin polymorphs.

α-gabapentin has been published (Ibers, 2001), and this could be compared with the two unreported crystal structures of gabapentin. All three of the structures are monoclinic. However, the α-gabapentin and β-gabapentin have $P2_1/c$ space groups while γ-gabapentin has a C2/c space group. The molecular conformations of the three structures are also clearly different in terms of having the NH_3^+ and COO^- groups positioned very differently relative to the cyclohexane ring. All three structures have extensive hydrogen bonding due to the presence of the NH_3^+ and COO^- groups. Significant differences can be seen in the hydrogen bonding networks and a comparison can be made by examining the graph sets present. The three structures have two unitary and two secondary level graph sets in common, however the remainder are all different. β-gabapentin is the only structure which contains an additional intramoleular hydrogen bond.

The thermal analysis of the three structures indicates that the melting points differ by approximately 2-4°C. The DSC scans for the β-and γ-gabapentin indicate the presence of possible phase transitions. For β-gabapentin, only small changes occur in the structure and hydrogen bonding distances at the higher temperatures of 70°C and 100°C. In the case of γ-gabapentin, at the higher temperatures of 70°C and 100°C, an additional hydrogen bonding interaction is formed. However, the structures at the three different temperatures only have small differences. The small endothermic and exothermic peaks

which are present for β-and γ-gabapentin respectively, may be due to slight changes in the structures as the temperature increases. It is also possible that the structures change at the peak positions and then revert back to the original structures after that point. The possible phase transitions could indicate that the melting point measured in each case refers only to the melting point of one thermodynamically stable polymorph.

The relative stabilities of the polymorphs are also seen from the degree of ease with which crystals are formed. α-gabapentin is the polymorph which can most easily be obtained at room temperature while γ-gabapentin is much less stable and more difficult to obtain. Crystals of β-gabapentin can only be obtained at higher temperatures and have a lower enthalpy value than the other two forms.

Therefore, it is evident that the structures of two unreported gabapentin polymorphs have been obtained. A fourth polymorph has been reported in patent literature as Form I (US Patent 6521787, Lladó *et al.*, 2003). However, single crystals of this polymorph have not yet been isolated.

4.6 Chapter 4 References

Ananda, K., Aravinda, S., Vasudev, P.G., Raja, K.M.P., Sivaramakrishnan, H., Nagarajan, K., Shamala, N., Balaram, P. (2003). Current Science, Vol. 85, No.7, 1002-101.

Besler, B.H., Merz, K.M. Jr., Kollman, P.A. (1990). J. Comp. Chem., 11, 431.

Ibers, J.A. (2001). Acta Cryst. C57, 642-643.

Lladó, J.B., Cruz, R.G., Grau, E.M., del Carmen, M., Miguel, O. (2003). PCT Int. Appl. US 6521787.

Magnus, L. (1999). Epilepsia. 40 (s6), s66-s72.

Motherwell, W.D.S, Shields, G.P., Allen, F.H. (1999). Acta Cryst., B55, 1044-1056.

Pesachovich, M., Singer, C., Pilarski, G. (2001). PCT Int. Appl. US 6255526.

Satyanarayana, C., Ramanjaneyulu, G.S., Kumar, I. V. S. (2004). PCT Int. Appl. WO 2004110342.

Roisnel, T., Rodrigues, J. (2000). Materials Science Forum, Proceeding of the seventh European powder diffraction conference, ed. R. Delhez and E.J. Mittenmeijer, 118-123.

Singh, U.C., Kollman, P.A. (1984). J. Comp. Chem. 5, 129 - 145.

Vasudev, P.G., Ananda, K., Chatterjee, S., Aravinda, S., Shamala, N., Balaram, P. (2007). J. AM. Chem. Soc., Vol. 129, 4039-4048.

Venu, N., Vishweshwar, P., Ram, T, Suryaa, D., Apurbac, B. (2007). Acta Cryst. C63, 306-308.

www.amber.scripps.edu/antechamber/gaff.html, (24/10/2008).

www.health.enotes.com/cancer-encyclopedia/gabapentin, (10/10/2006).

www.physics.ohio-state.edu/~aulbur/dft.html, (24/05/2008).

Chapter 5
Co-crystals

5.1 Introduction and related work

As discussed in chapter 1, the study of co-crystals has become very significant in the pharmaceutical industry as there is a continuous search for drug compounds which exhibit the best possible properties for therapeutic use and manufacturability. Factors which affect the value of these compounds include the stability, hygroscopicity, dissolution rate, solubility and bioavailability.

The possibility of forming co-crystals is often considered when the properties of the most thermodynamically stable form of a substance are not acceptable. In the past, the development of co-crystal forms for drug compounds had not been extensively researched, however, in recent years there has been growing interest in co-crystals as a means of improving the properties of drugs, while leaving the active pharmaceutical ingredients unaltered (Thayer, 2007).

There has been much debate regarding the definition of a co-crystal. Some suggestions in terms of designating co-crystals have been to define co-crystals according to the state of their components under standard conditions, for example the suggestion by Aakeröy *et al*., (2005) that co-crystals should only be composed of components that are solids at ambient temperature as opposed to suggestions by Dunitz, (2003) that co-crystals encompass molecular compounds, molecular complexes, solvates, inclusion compounds, channel compounds and clathrates. It has thus been suggested that the components must individually be solids under ambient conditions, but it is not essential that they retain their individual identity within the co-crystal (Bond, 2007).The generally accepted definition of a co-crystal, is a crystalline solid containing multiple components, where the two or more components are associated through intermolecular interactions.

A method which has been used as a means to distinguish between co-crystals and salts has been based upon whether a proton transfer occurs from an acid to a base. This is largely dependant upon the strengths of the acids and bases as well as the crystalline environment (Childs *et al.*, 2007).

It has been found that in general, a reaction of an acid with a base is expected to produce a salt when the ΔpK_a value is greater than 2 or 3. It has also been found that for ΔpK_a values less than 0, co-crystal formation is the most likely. These rules however, do not apply in every situation and it has been difficult to predict the formation of either co-crystals or salts in the region of ΔpK_a 1 to 3 (Childs *et al.*, 2007).

It has been found through the examination of proton transfer, that when a solution contains an organic acid and organic base, if the proton is present on the base, then proton transfer has occurred and the crystalline acid-base complex would be classed as a salt. However, if the proton remains on the acid, then proton transfer has not occurred and the crystalline complex would be a co-crystal. The relation of the pK_a values for the acid and base in solution as well as the difference between these values allows for the extent of proton transfer to be determined in a solution. When examining the crystalline structures ie. the solid state, the extent of proton transfer can be determined by making use of various techniques such as X-ray single crystal diffraction, neutron diffraction or infrared spectroscopy in order to locate the protons or determine the bond lengths and angles. There are however cases in which there is disorder that can lead to multiple protonation states with partial occupancy. In such cases, it is not possible to distinguish between co-crystals and salts (Childs *et al.*, 2007). Therefore, co-crystals and salts can be considered as species which exist at either end of a continuum of multicomponent crystal structures (Stahly, 2007).

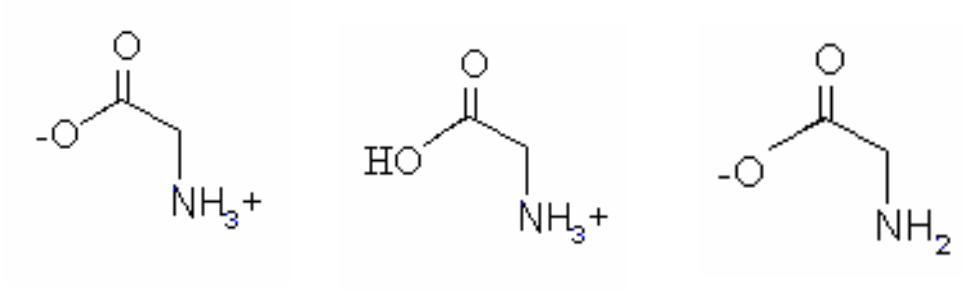
An area of research which has found particular interest, has been the co-crystallization of amino acid compounds with carboxylic acids, where drug company researchers have made use of carboxylic acids which are on the FDA's Generally Recognized as Safe(GRAS) list (www.cfsan.fda.gov/~rdb/opagras1.html, 9/01/2008). Some examples of

acids which have been used include oxalic acid, benzoic acid, tartaric acid, formic acid, acetic acid and maleic acid. In the case of the amino acids L- and DL-arganine, lysine and histidine, these have been co-crystallized with a number of carboxylic acids including tartaric acid (Selvaraj *et al.*, 2007), formic acid (Suresh *et al.*, 1995), dicarboxylic oxalic acid (Chandra *et al.*, 1998) and malonic acid (Saraswathi *et al.*, 2002). Other examples include the co-crystallization of L-leucine (Rajagopal *et al.*, 2003) and bis-(DL-aspartic acid) (Alagar *et al.*, 2003) with oxalic acid.

From the research done on the above co-crystallization examples, it is evident that significant features in the co-crystallization of amino-carboxylic acid complexes include the ionization states of the individual amino and carboxylic acid compounds, the aggregation patterns and the stoichiometry.

When examining the possibility of co-crystallization, it is necessary to examine the ionization states which exist at various pH values. In order to do this, the pK_a values need to be examined, where pKa = -log Ka and Ka is the acid dissociation constant. The pKa value is also related to the pH value by pKa = pH – log $[A^-]/[AH]$ where AH could represent a group of atoms in a molecule (www.web-books.com/moBio/Free/Ch2A4.html, 09/01/2008).

In the case of amino acids, they can exist in three possible forms as indicated in figure 5.1.1.

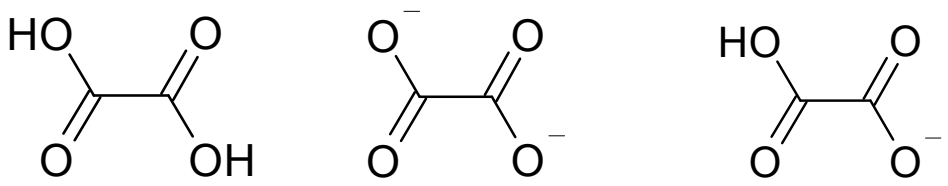


(a) (b) (c)

Figure 5.1.1 Three possible ionization states of an amino acid, (a) zwitterionic form, (b) cationic form, (c) anionic form.

Figure 5.1.1 indicates the presence of the amino acid in a zwitterionic form, in a cationic form with the carboxyl group being neutral and the amino group positively charged as well as in an anionic form where the amino group is neutral and the carboxyl group is negatively charged. Each type of amino acid has pKa values which have been determined and are specific to that acid.

In the case of carboxylic acids, they can also exist in various forms as shown in figure 5.1.2.



(a) (b) (c)

Figure 5.1.2 Three possible forms of a carboxylic acid, (a) neutral form, (b) carboxylate dianion, (c) semi-carboxylate anion.

Figure 5.1.2 indicates that the carboxylic acid can be neutral or exist as a carboxylate dianion or semi-carboxylate anion.

The various forms of the amino acids and carboxylic acids are obtained by adjusting the pH of the solution in which the acids are dissolved. It is therefore possible to obtain a range of different combinations of the above forms.

In this project, the possible co-crystallization of the neurotransmitter and neurotransmitter analogues, GABA, Gabapentin, glycine and β-alanine with oxalic acid (HO_2CCO_2H) were studied by varying the pH of equimolar, aqueous solutions of the amino acids and oxalic acid. Oxalic acid was chosen due to the success with which it has been co-crystallized with amino acids as discussed above.

5.2 Co-crystals of Glycine and Oxalic acid

5.2.1 Introduction

Glycine is an amino acid which operates as an inhibitory neurotransmitter in the central nervous system. It functions particularly in the spinal cord, retina and brainstem. When the glycine receptors are activated, they cause chloride to enter the neurons via receptors, which causes an inhibitory postsynaptic potential (www.britannica.com, 15/06/2007). Three different polymorphs of glycine have been reported, namely the α form (Jonsson *et al.,* 1972), β form (Drebushchak *et al.*, 2002) and γ form (Iitaka, 1958). The protonation constants of glycine are approximately 2.34 and 9.6 (www.research.chem.psu.edu/brpgroup/pka_compilation.pdf, 07/10/2007) and it can therefore exist in three different ionization states. A plot of the calculated molar fractions of glycine (determined from the protonation constants) against the pH, gives an indication of the regions in which each different ionization state occurs (figure 5.2.1).

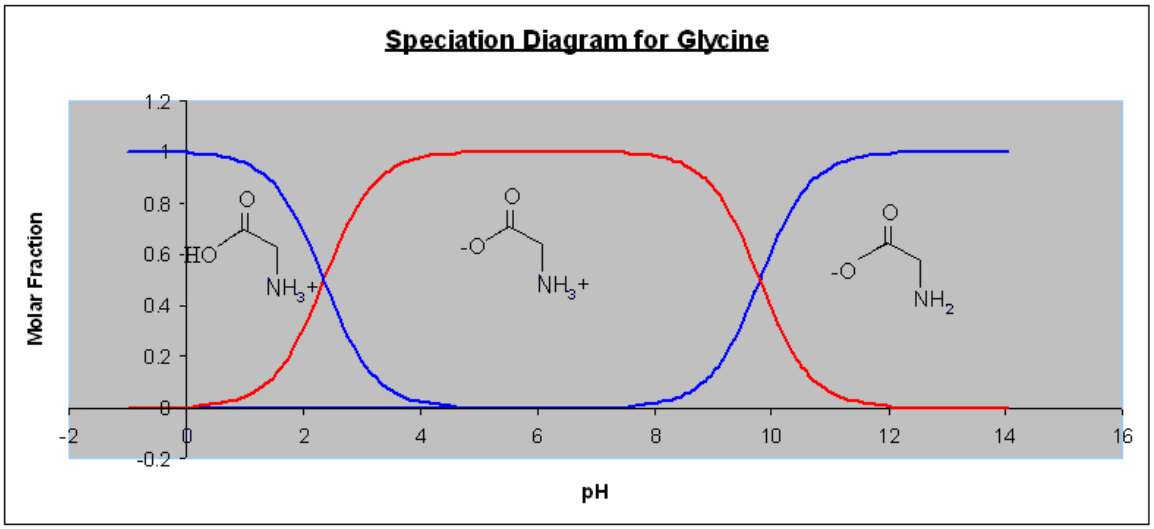


Figure 5.2.1 Speciation diagram of glycine.

Oxalic acid has pKa values of approximately 1.25 and 4.14 (www.research.chem.psu.edu/brpgroup/pka_compilation.pdf, 07/10/2007) and it can also exist in three different ionization states. Again, a plot of the calculated molar fraction

against pH indicates the regions in which the different forms of oxalic acid exist (figure 5.2.2).

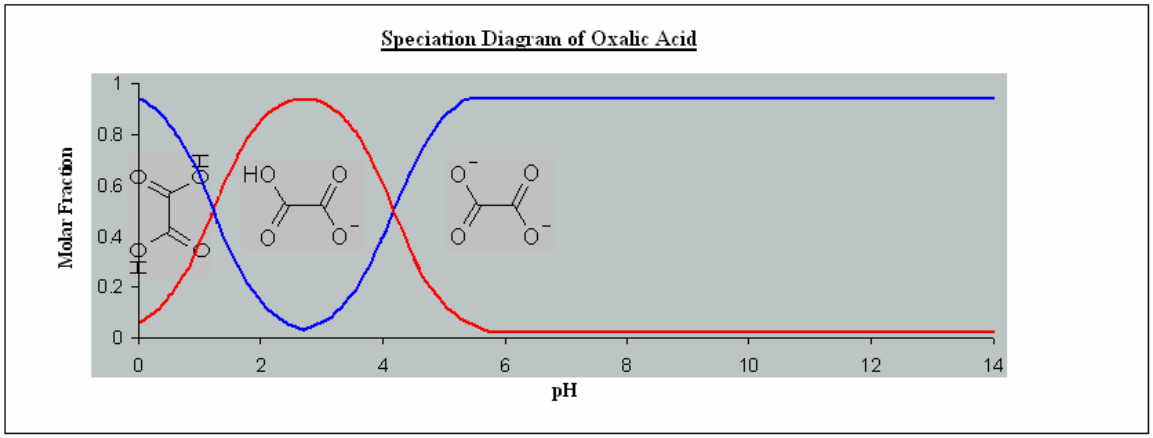


Figure 5.2.2 Speciation diagram of oxalic acid.

The curve in figure 5.2.2 indicates that oxalic acid is primarily found in its neutral state below a pH of 1.25, its semi-carboxylate state between 1.25 and 4.14 and as a carboxylate dianion above 4.14.

Therefore, in the different pH ranges, different combinations of the two compounds would be present. At a pH of approximately 3, glycine can exist as a mixture of the zwitterionic and protonated forms and oxalic acid exists as the semi-carboxylate anion. For a pH of 6, glycine is still in the zwitterionic form; however oxalic acid exists as the carboxylate dianion. Finally, at a pH of 12, glycine exists as an anion and oxalic acid exists as the carboxylate dianion.

5.2.2 Experimental

Equimolar amounts of glycine (Sigma Aldrich) and oxalic acid were dissolved in deionised water at room temperature. The solution was then adjusted to the desired pH using 1M hydrochloric acid and 2M sodium hydroxide solutions. Solutions of the compounds were adjusted to pH 3, 6 and 12. The pH values were estimated using indicator paper. The solutions were then placed into vials and left in a fume hood in order for open-air evaporation to take place.

5.2.3 X-ray Powder Diffraction

The products which formed from open-air evaporation were ground up and tested using X-ray powder diffraction. The powder diffraction patterns obtained for pH 3, 6 and 12 were compared with diffraction patterns of the original glycine and oxalic acid materials (figure 5.2.3).

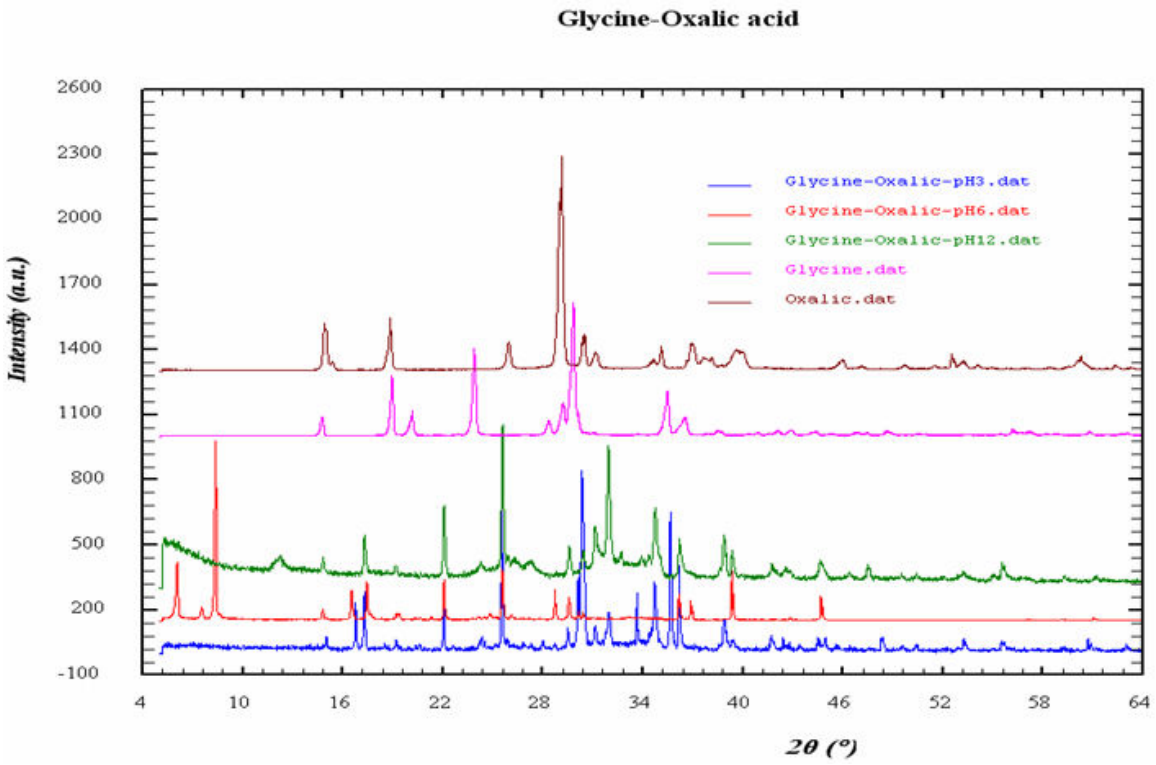


Figure 5.2.3 X-ray powder diffraction patterns of glycine-oxalic acid at pH 3, 6 and 12 compared with patterns of the starting materials.

The above comparison indicates that there are differences between the glycine-oxalic acid patterns and the patterns of the starting materials. This indicates that the substances formed at the various pH values have different crystalline phases, however, they cannot be fully characterised as only pH 6 yielded single crystals. Therefore, they could be polymorphs, solvates, salts, co-crystals or hydrates. Through a comparison of the reduced unit cell parameters, the single crystals obtained at pH 6 were found to be sodium oxalate crystals.

5.2.4 Discussion and Conclusion

Although single crystals could not be obtained, it was evident from a comparison of the powder diffraction patterns, that different crystalline phases were formed. The structures of glycinium oxalate (Nandhini *et al.*, 2001) and bis-glycinium oxalate (Chitra *et al.*, 2007) co-crystals have been reported. The reported method used for the formation of the glycinium oxalate crystals is very similar to the method attempted; however a comparison of the patterns obtained for pH 3, 6 and 12 with the calculated patterns for the reported structures, showed a number of differences. Therefore, the forms obtained are most likely not the co-crystal, but rather other possible forms of glycine or oxalic acid.

5.3 Co-crystals of GABA and Oxalic acid

5.3.1 Introduction

The protonation constants of the inhibitory neurotransmitter GABA are 4.23 and 10.43 (www.research.chem.psu.edu/brpgroup/pka_compilation.pdf, 07/10/2007) and it can therefore also exist in three different ionization states. A plot of the calculated molar fractions versus the pH for GABA gives an indication of the pH regions in which the different forms exist (figure 5.3.1).

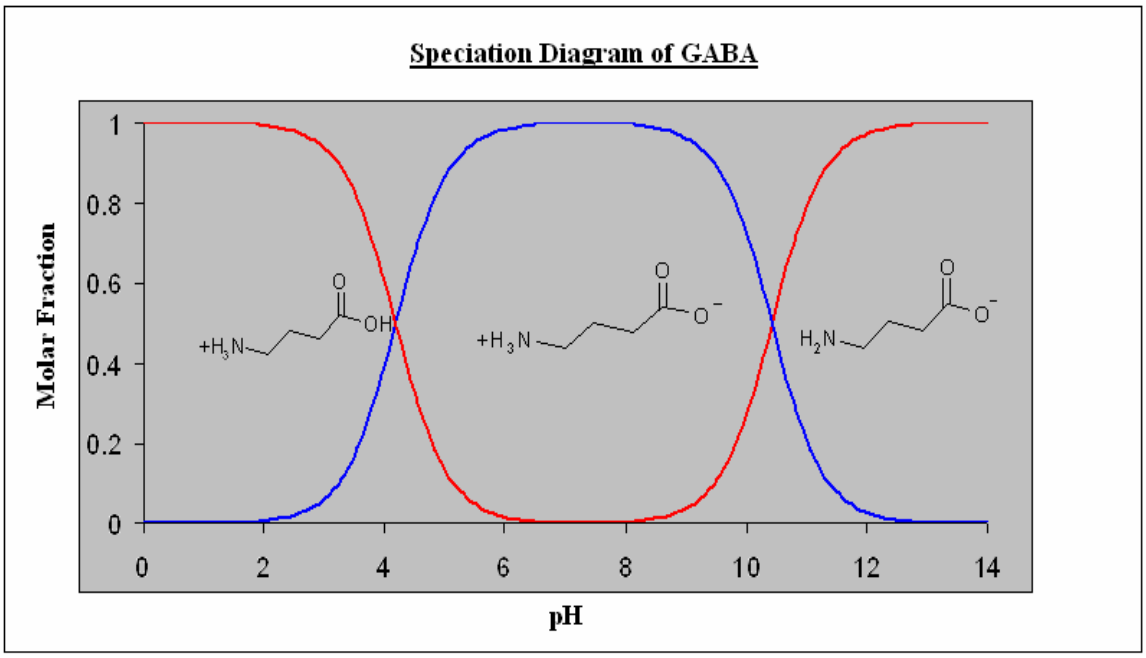


Figure 5.3.1 Speciation diagram of GABA.

At a pH of approximately 4, GABA exists as a mixture of the zwitterionic and protonated forms, while oxalic acid exists in the semi-carboxylate anion form. For a pH of 6, GABA is in the zwitterionic form and oxalic acid exists as the carboxylate dianion. Finally, at a pH of 10 GABA exists as a mixture of zwitterions and anions, while oxalic acid exists as the carboxylate dianion.

5.3.2 Experimental

Equimolar amounts of GABA (Sigma Aldrich) and oxalic acid were dissolved in deionised water at room temperature. The solution was then adjusted to the desired pH using 1M hydrochloric acid and 2M sodium hydroxide solutions. Solutions of the compounds were adjusted to pH values of approximately 4, 6 and 10. The pH values were estimated using indicator paper. The solutions were then placed into vials and left in a fume hood in order for open-air evaporation to take place. For the solutions of pH 4 and 10, no suitable crystals were formed. In the pH 6 solution, large crystals of oxalic acid were initially produced, however, when these crystals were removed, crystals of a different morphology began to form in the vial.

5.3.3 Microscopic analysis of crystals formed

The crystals which formed after the removal of the large oxalic acid crystals were examined and images were taken using an optical Micro Met Scientific microscope with a magnification of 45x. This allowed for the morphology of the crystals to be examined. Figure 5.3.2 shows the images of the crystals.

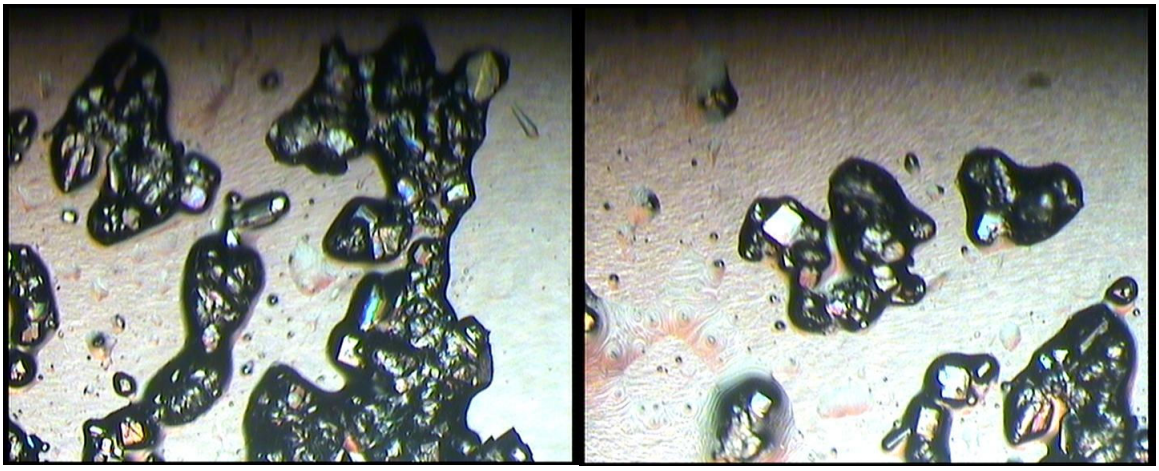


Figure 5.3.2 Optical microscope images of crystals formed from a pH 6 solution at 45x magnification.

As indicated from the images in figure 5.3.2, the crystals are very small (0.30 x 0.24 x 0.20mm), however, suitable crystals could be isolated for analysis.

5.3.4 X-ray Powder diffraction

X-ray powder diffraction patterns were recorded for the substances obtained at pH 4, 6 and 10. These were compared with the patterns of the original starting materials as well as an additional pattern of a tetragonal GABA polymorph (Dobson *et al.*, 1996). Figure 5.3.3 shows the overlapping of the patterns.

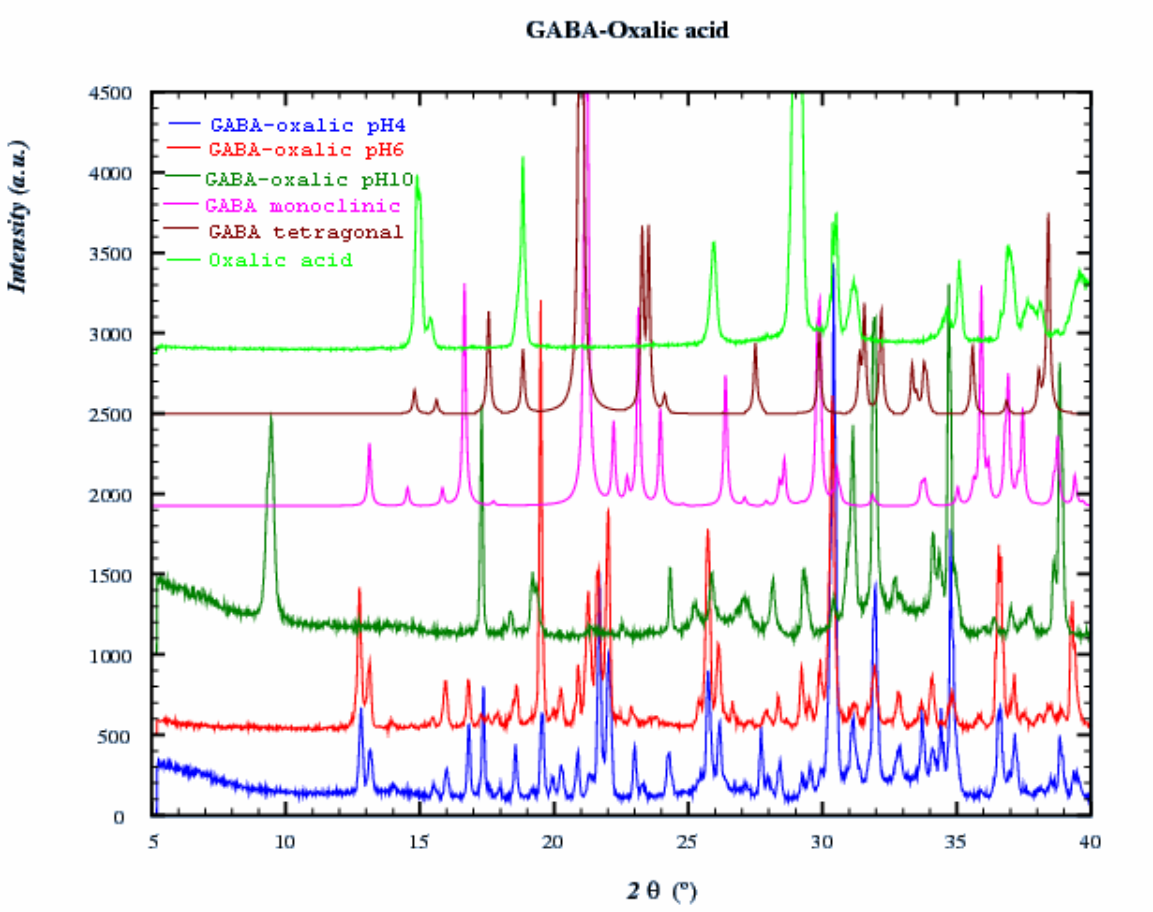


Figure 5.3.3 X-ray powder diffraction patterns of the products obtained at pH 4, 6 and 10, compared with the patterns of the starting materials and an additional known GABA polymorph.

The above comparison indicates that the powder patterns of crystals grown at pH 4 and 6 are very similar; however they do not correspond to any of the patterns for the pure starting materials. The pattern for pH 10 appears to be very different from the other patterns. Therefore, it is evident that different crystalline forms have been produced. At pH 6, single crystals were obtained and could be further characterised.

5.3.5 X-ray Single Crystal Diffraction

The block shaped crystals which were formed at pH 6, were examined by X-ray single crystal diffraction at 25°C on the Bruker, SMART 1K CCD area detector diffractometer. The crystallographic data is presented in table 5.3.1 below.

Table 5.3.1: Crystallographic data for GABA-oxalic acid crystals.

Formula	$(C_4 H_{10} N O_2), (C_2 O_4)$
Formula Weight	200.14g/mol
Temperature	298(2)K
Crystal System	Monoclinic
Space Group	$P2_1/C$
Description	Colourless, blocks
Unit cell dimensions	a = 7.4755(9)Å
	b = 10.2973(13)Å
	c = 9.8115(12)Å
	α = 90°
	β =108.477(3)°
	γ = 90°
Volume	$V = 716.33(15)Å^3$
Z	4
Density	$1.374g/cm^{-3}$
Absorption coefficient	$0.119mm^{-1}$
Θ range for data col.	2.9-28.0°
Reflections collected	4705
Independent reflect.	1722
Final R indices	0.0388

The molecular conformational diagram obtained through X-ray single crystal diffraction and the numbering scheme for the GABA-oxalic acid conformation is shown in figure 5.3.4.

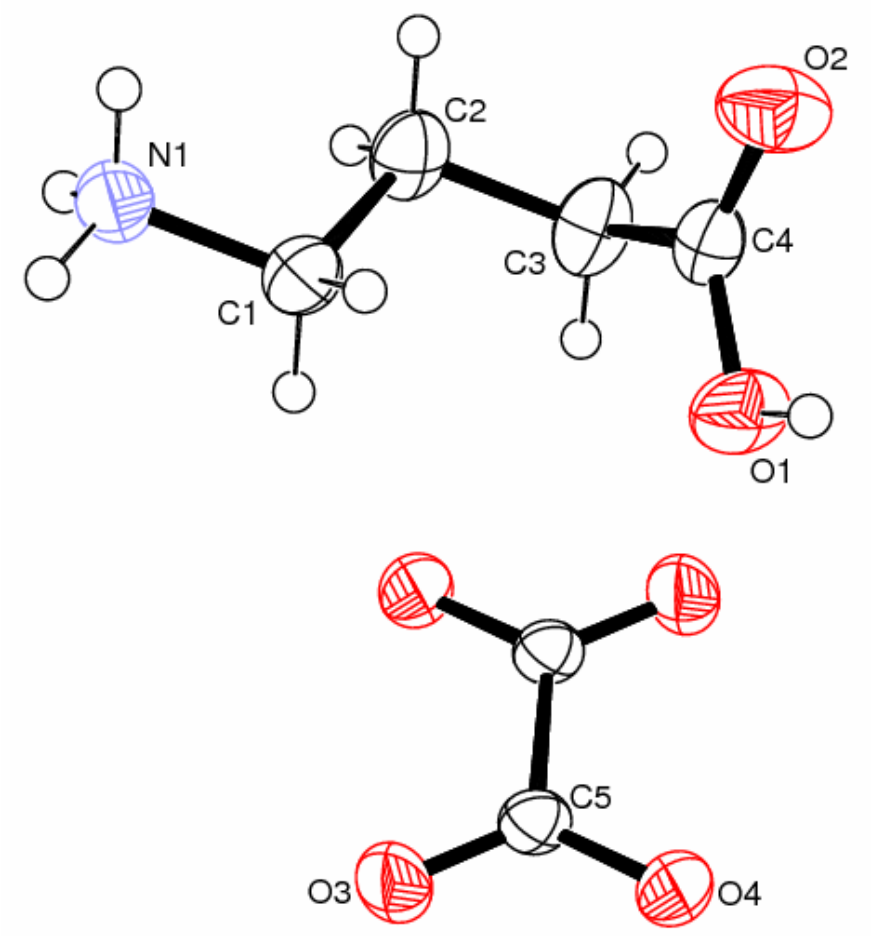


Figure 5.3.4 Ortep diagram of the molecular conformation of the GABA-oxalic acid co-crystal, with the displacement ellipsoids at a 50% probability level.

The single crystal structure analysis shows that the crystals obtained at a pH of 6 are in fact the co-crystal of GABA and oxalic acid. A visual comparison of the molecular conformation of the GABA molecule within this co-crystal and the GABA molecules discussed in chapter 3, shows that there are significant differences. Structurally, the most closely related GABA molecule is the monoclinic GABA; however, the presence of the oxalic acid molecule has a large effect on altering the conformation of the GABA molecule within the co-crystal. The GABA molecule in this case is also protonated as opposed to being a zwitterion or anion. The oxalic acid appears as a dianion species and has a slightly elongated C-C bond length of 1.56Å.

The unit cell of this co-crystal is shown in figure 5.3.5.

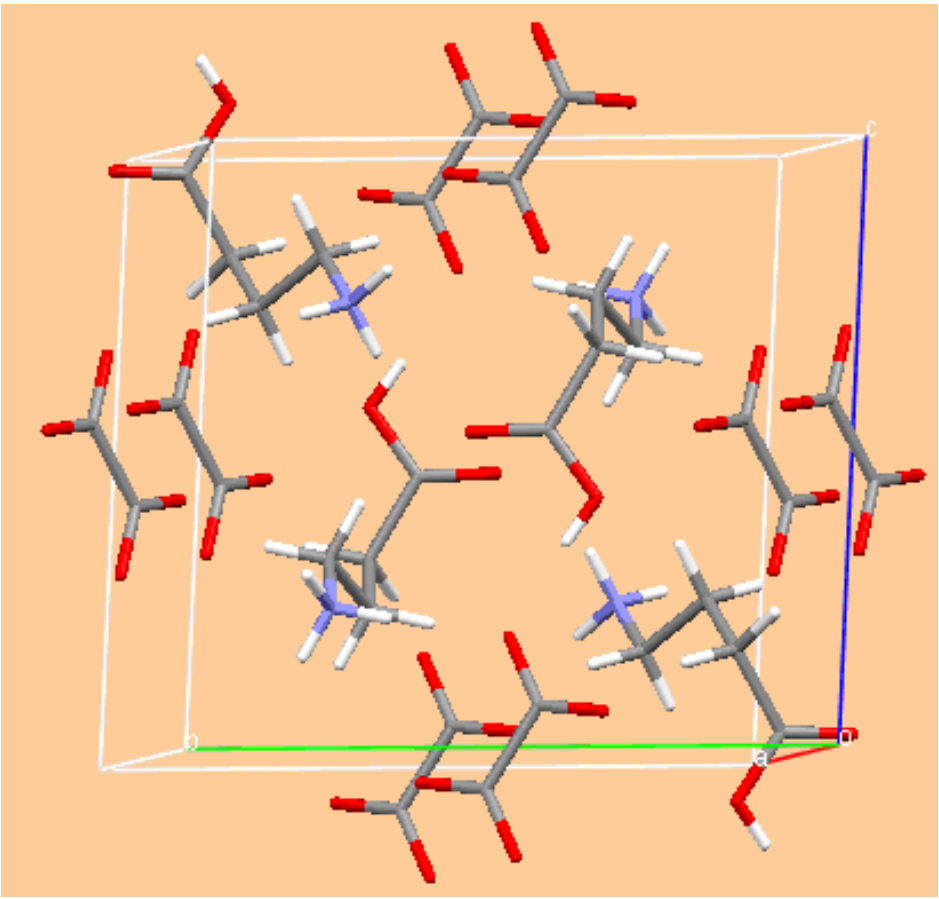


Figure 5.3.5 Unit cell of the GABA-oxalic acid co-crystal.

There are 4 GABA molecules and 0.25 x 8 = 2 oxalate dianions within the unit cell. Therefore this is a 2:1 GABA-oxalic acid co-crystal with the formula $2(C_4\ H_{10}\ N\ O_2)$, $(C_2\ O_4)$.

5.3.6 Hydrogen bonding

The co-crystal of GABA-oxalic acid has an extensive hydrogen bonding network due to the presence of the NH_3^+ and COOH groups on the GABA molecules and the COO^- groups of the oxalate dianion. The numbering scheme of the hydrogen atoms present on the GABA molecule is given in figure 5.3.6.

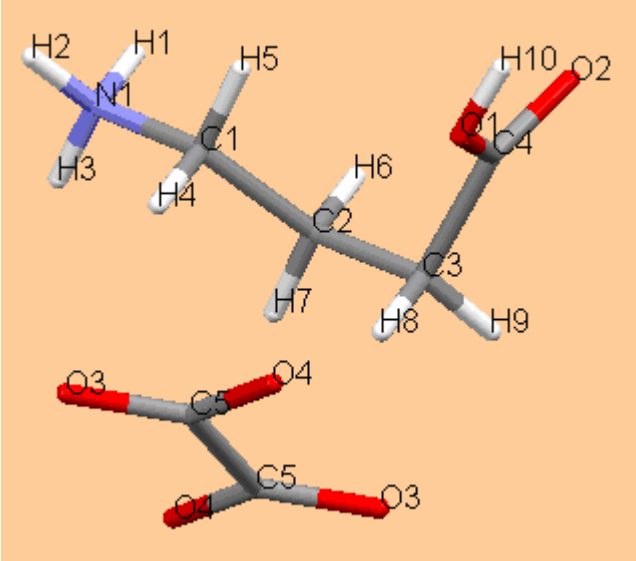


Figure 5.3.6 Diagram indicating the numbering scheme of the hydrogen atoms present on the GABA molecule.

Each NH_3^+ group is involved in five hydrogen bonding interactions, where four of the interactions are with neighbouring oxalate dianion molecules and one of the interactions is with a neighbouring GABA molecule. Atom H1 acts as a bifurcated hydrogen bond donor and interacts with both the O3 and O4 atoms on a single neighbouring oxalate dianion ie. H1---O4 = 1.94Å and H1---O3 = 2.63Å. These lengths show that the H1---O4 interaction is a relatively strong interaction, whereas the H1---O3 bond would be a very weak hydrogen bonding interaction. Atom H2 acts as a single hydrogen bond donor and interacts with an O3 atom on a different neighbouring oxalate dianion to the one with which H1 interacted. The hydrogen bond length for the interaction is H2---O3 = 1.94Å. Atom H3 also acts as a bifurcated hydrogen bond donor and interacts with O3 on the same oxalate dianion as mentioned for the H1 interactions. It also interacts with O2 on a neighbouring GABA molecule. The hydrogen bond lengths are H3---O2 = 2.05Å and H3---O3 = 2.68Å. Again, there is a strong interaction with O2 on a neighbouring GABA molecule, but the interaction with O3 on the oxalate dianion molecule is very weak.

Atom H10 which is part of the OH group of the GABA molecule is a single hydrogen bond donor which also interacts with an O4 atom on a different oxalate dianion. The

hydrogen bond length is H10---O4 = 1.73Å. When compared with the other hydrogen bonding interactions, this is a very strong interaction.

A summary of the hydrogen bonding is presented in table 5.3.2.

Table 5.3.2: Hydrogen bonding parameters for the GABA-oxalic acid co-crystal(Å, °).

D-H---A	D-H	H---A	D---A	D-H---A
N1-H1---O4	0.89	1.94	2.8250(17)	171
N1-H1---O3	0.89	2.63	3.0592(16)	111
N1-H2---O3	0.89	1.94	2.8096(16	164
N1-H3---O2	0.89	2.05	2.8961(17)	158
O1-H10---O4	0.89	1.73	2.5474(14)	175
N1-H3---O3	0.89	2.68	3.0592(16)	107

Note: The bond length H3---O3 = 2.68Å from N1-H3---O3 is regarded as being too long to be a hydrogen bond. It can only be classed as a weak hydrogen interaction.

Each GABA molecule interacts with three different oxalate dianion molecules and two different neighbouring GABA molecules as shown in figure 5.3.7.

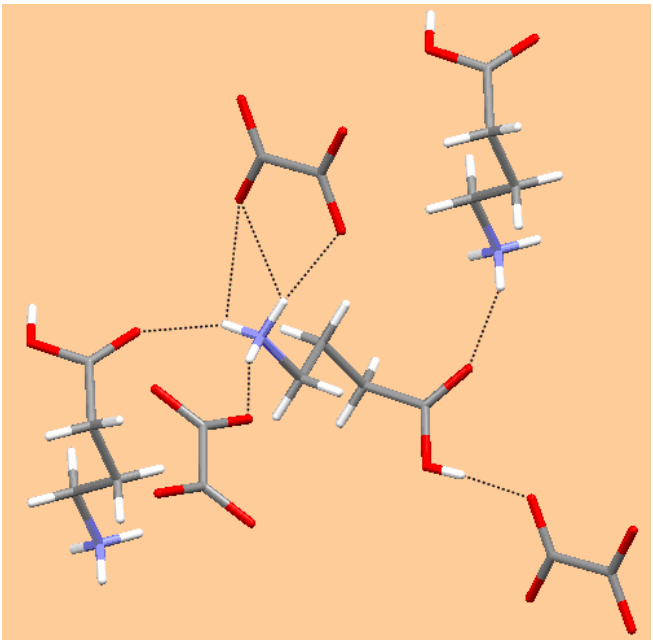


Figure 5.3.7 Hydrogen bonding interactions between GABA and oxalic acid.

In the hydrogen bonding network, the GABA molecules interact with each other to form a chain along the b-axis, as indicated in figure 5.3.8.

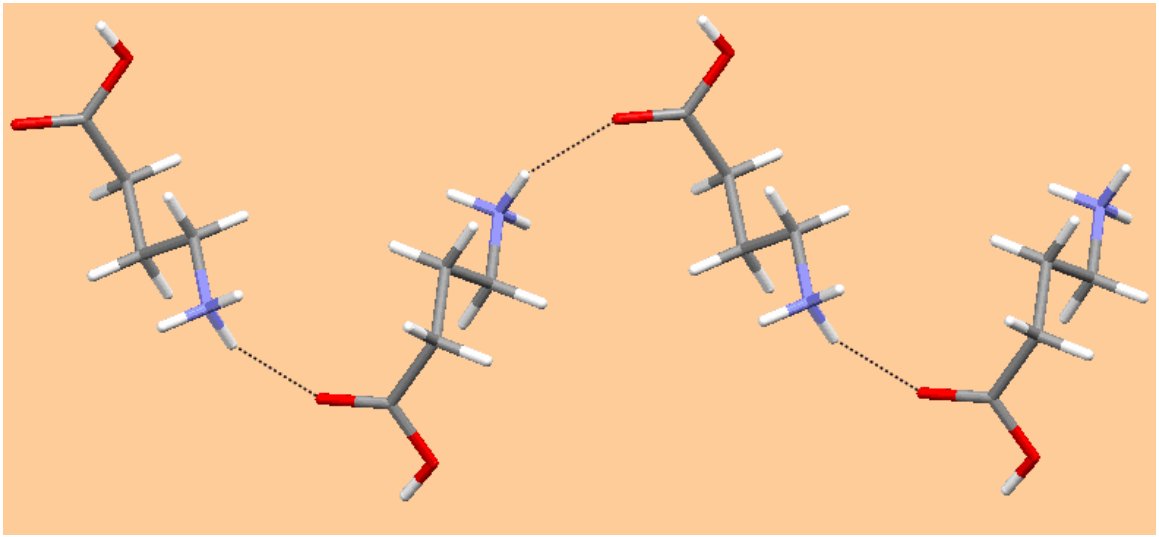


Figure 5.3.8 Hydrogen bonds linking the GABA molecules along the b-axis in the hydrogen bonding network.

These chains are then linked through various hydrogen bonding interactions with the oxalate dianion molecules.

The hydrogen bonding network can be further characterised by examining the graph sets present in the network. The first and second level hydrogen bond motifs which are present for the four strong hydrogen bonds were determined by RPLUTO (Motherwell *et al.*, 1999). A summary of the main graph sets is shown in matrix form in table 5.3.3 which corresponds to figure 5.3.9.

Table 5.3.3: Matrix of selected graph sets for the hydrogen bonding of the GABA-oxalic acid co-crystal.

	a	b	c	d
a	$D_2^2(6)$	-	-	-
b	$C_2^2(12)$	$D_2^2(6)$	-	-
c	$R_4^2(18)$	$C_2^2(7)$	$D_2^2(6)$	-
d	$C_3^3(16)$	$C_3^3(14)$	$C_3^3(14)$	$C_1^1(7)$

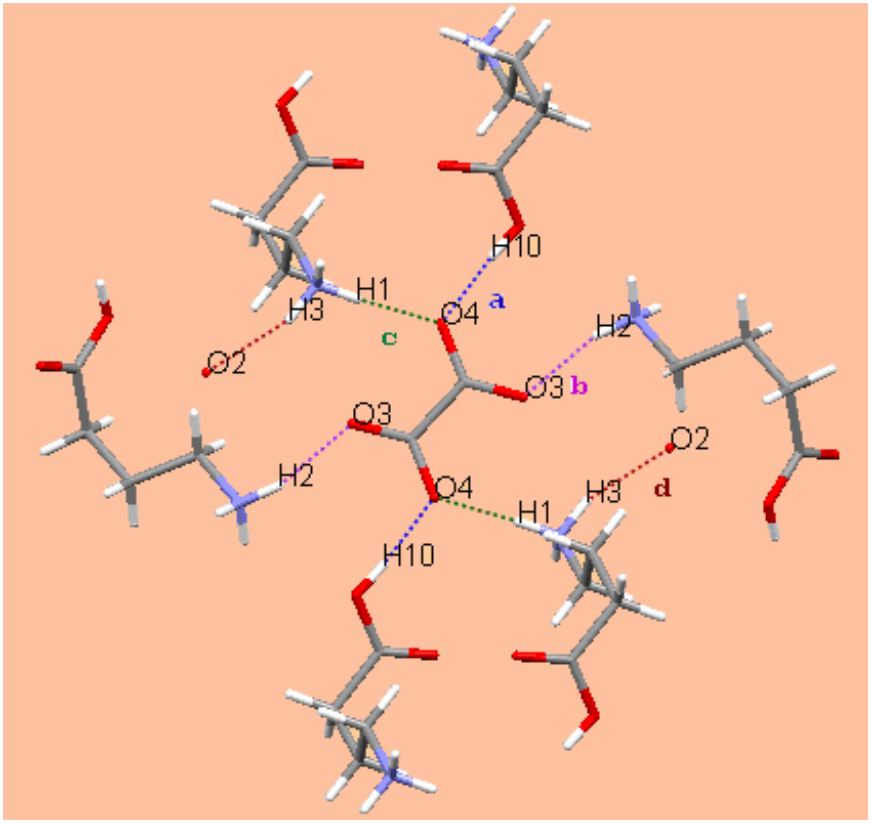


Figure 5.3.9 The letters **a** - **d** refer to the four strongest individual hydrogen bonds which are present, where some of the first and second level graph set motifs resulting from these bonds are indicated in table 5.3.3 above. The single red dots refer to the oxygen atoms where the remainder of the molecule has been deleted for visual clarity.

Figure 5.3.9 shows the strongest hydrogen bonds present for the GABA-oxalic acid structure. The figure also shows the different ways in which the GABA molecules are linked to each other and to the oxalic acid molecules. There are two weaker hydrogen bonding interactions (N1-H3-O3 and N1-H1-O3) which do not appear in figure 5.3.9, but are listed in table 5.3.2. These additional hydrogen bonds would cause the hydrogen bonding network to be more extensive and therefore, the large number and variety of graph sets for this 2:1 GABA-oxalic acid co-crystal would have the effect of greatly increasing the stability of the compound.

5.3.7 Thermal Analysis

The melting point of the GABA-oxalic acid co-crystal was initially determined by hot stage microscopy and this value was verified by running a DSC scan on a ground up sample of the co-crystal formed at pH 6. From microscopy, the melting point was determined to be approximately 159ºC. The DSC curve of the 2:1 GABA-oxalic acid co-crystals is shown in figure 5.3.10.

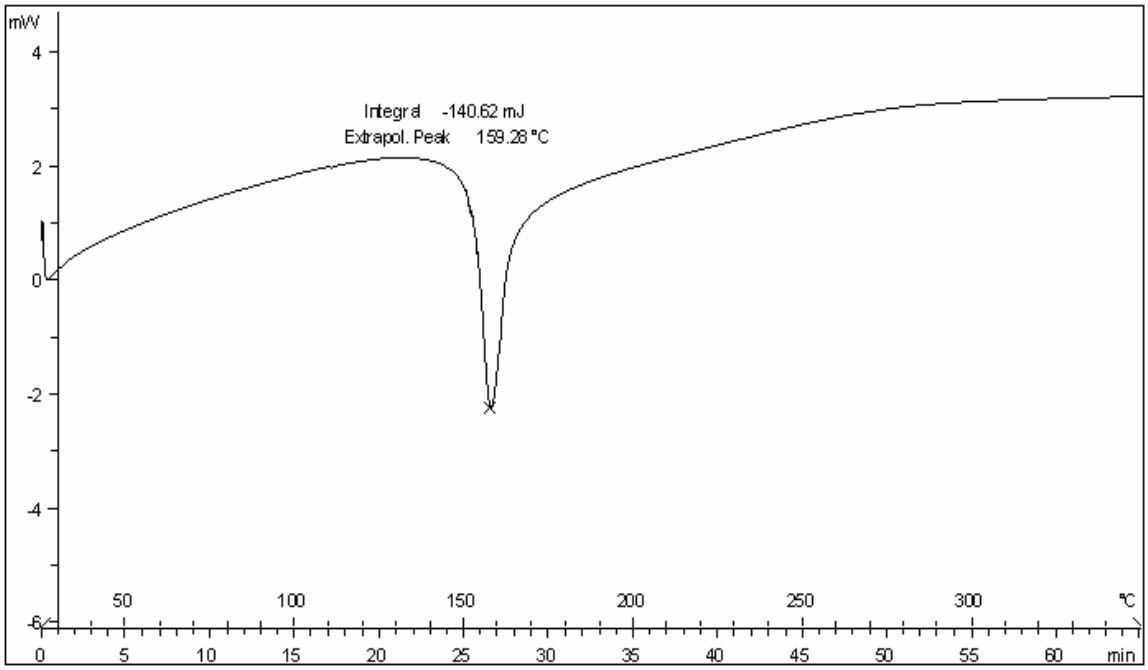


Figure 5.3.10 DSC plot of heat flow (mW) vs. temperature (°C) for the 2:1 GABA-oxalic acid co-crystals over the range of 25 - 350°C.

This curve indicates that the 2:1 co-crystal of GABA-oxalic acid melts at 159.3°C. This value is very close to the melting point obtained by hot stage microscopy. The melting points of the starting materials, GABA and oxalic acid are approximately 206°C and 101°C respectively. Therefore, the melting point of this co-crystal is significantly different from that of the starting materials, indicating that it is a completely different crystalline phase. The DSC plot also indicates that no additional phase changes take place for these crystals.

5.3.8 Discussion and Conclusion

The X-ray powder and single crystal diffraction as well as thermal analysis, clearly indicate that a co-crystal of GABA and oxalic acid has been formed. The co-crystals were formed at a pH of approximately 6. The conformational diagram shows that within the co-crystal, GABA is protonated and oxalic acid exists as a carboxylate dianion. The morphology, powder pattern, melting point and the molecular conformation show that this crystalline material is significantly different from the starting materials.

The unit cell representation indicates the presence of four GABA molecules and two oxalic acid dianion molecules and therefore, a 2:1 co-crystal of GABA-oxalic acid has formed. The presence of the oxalate dianion clearly has an effect on the conformation of the GABA molecule as it is oriented differently from all other GABA polymorphs and salts. The hydrogen bonding network for this structure is extensive and is made up of GABA chains linked together in different ways by the oxalic acid molecules.

An extensive search of the Cambridge Structural Database was carried out by using the fragments present in this structure, in order to determine whether the structure has been reported. It was found that it is not present in the database. The structure has however, been reported in the Angewandte Chemie International journal by M. Wenger and J. Bernstein (Wenger *et al.*, 2006). A comparison of the structure presented here and the reported structure (CIF file was received directly from the authors) indicates that the structures have very similar unit cell parameters, molecular conformations and hydrogen

bonding networks. Therefore, this structure is the same as the published structure for this 2:1 co-crystal of GABA-oxalic acid.

Chapter 5.4 Co-crystals of Gabapentin and Oxalic Acid

5.4.1 Introduction

The neurotransmitter analogue and drug compound, gabapentin has protonation constants of 3.7 and 10.7 (www.drugs.com/mmx/gabapentin.html, 07/10/2007) and it can therefore exist in three different ionization states. A plot of the calculated molar fractions versus the pH for gabapentin, gives an indication of the pH regions in which the different forms exist (figure 5.4.1).

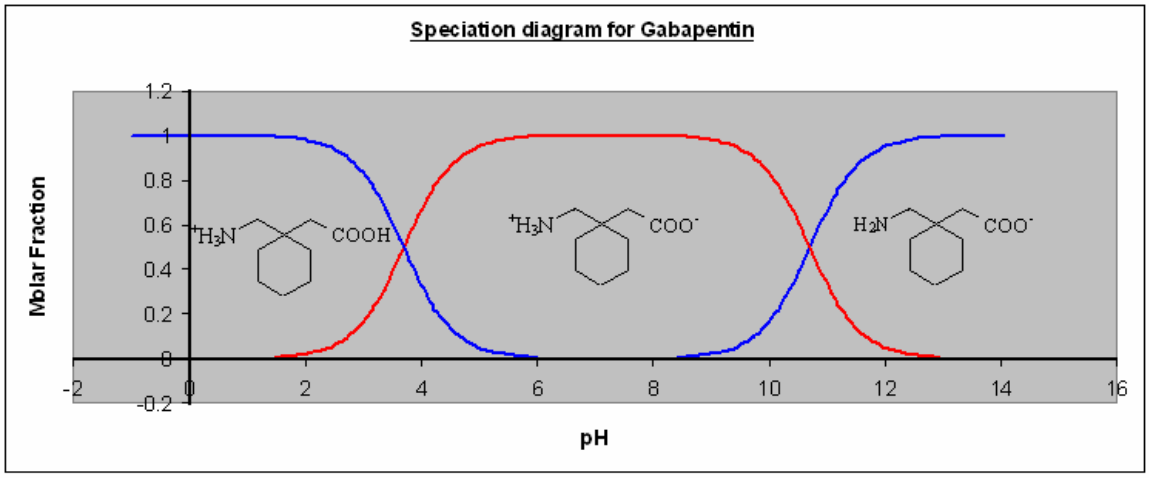


Figure 5.4.1 Speciation diagram for gabapentin.

At a pH of 4, gabapentin exists as a mixture of zwitterionic and protonated species, while oxalic acid exists in the semi-carboxylate anion form. At a pH of 6 it exists in the zwitterionic form and oxalic acid exists as the carboxylate dianion. Finally, at pH 12 gabapentin is found as an anion and oxalic acid exists as a carboxylate dianion.

5.4.2 Experimental

Equimolar amounts of gabapentin (Sigma Aldrich) and oxalic acid were dissolved in deionised water at room temperature. The solution was then adjusted to the desired pH using 1M hydrochloric acid and 2M sodium hydroxide solutions. Solutions of the compounds were adjusted to pH values of approximately 4, 6 and 12. The pH values were estimated using indicator paper. The solutions were then placed into vials and left in a fume hood in order for open-air evaporation to take place. For the solutions of pH 6 and

12, no suitable crystals were formed and a tacky, colourless layer was produced in each case. In the pH 4 solution, block shaped crystals were obtained.

5.4.3 Microscopic analysis of the crystals formed

The crystals which were formed at pH 4 were visually analyzed by capturing images using an optical Micro Met Scientific microscope at a 45x magnification. The images are shown in figure 5.4.2.

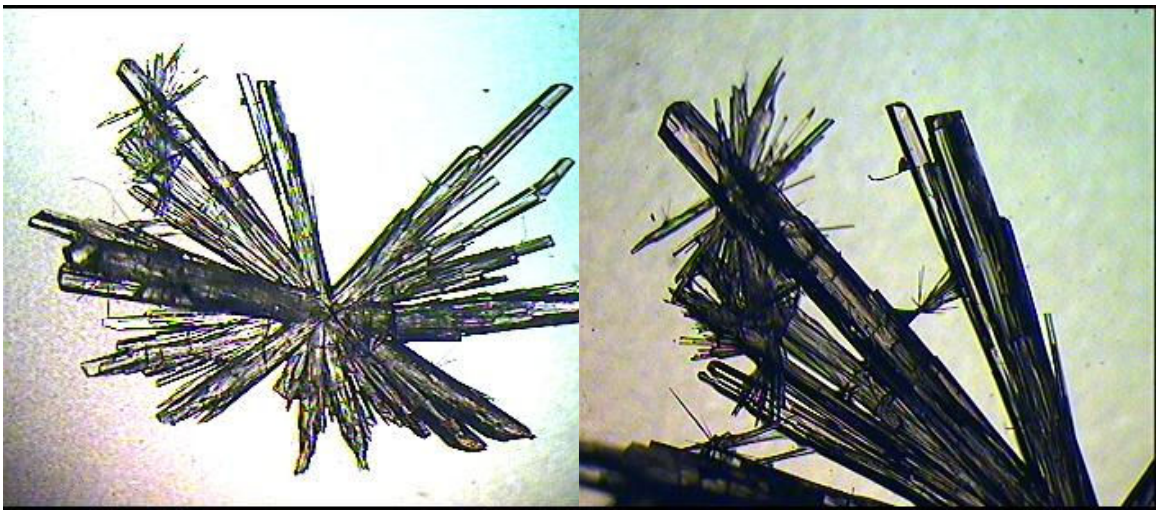


Figure 5.4.2 Optical microscope images of the crystals formed at pH4 using a 45x magnification.

These images indicate that the crystals grow outwards from a central point. Individual crystals, suitable for further analysis could be separated.

5.4.4 X-ray Powder Diffraction

Powder diffraction patterns could not be obtained for the products formed at pH 6 and 10, as these formed tacky substances which could not be dried out. An X-ray powder diffraction pattern was run on the substance formed at pH 4 as an initial test to determine whether a new crystalline phase had been produced. A comparison of the substance formed at pH 4, with the three gabapentin polymorphs mentioned in chapter 4(α-gabapentin was the starting material) as well as oxalic acid was made. Figure 5.4.3 shows that overlapping of the patterns.

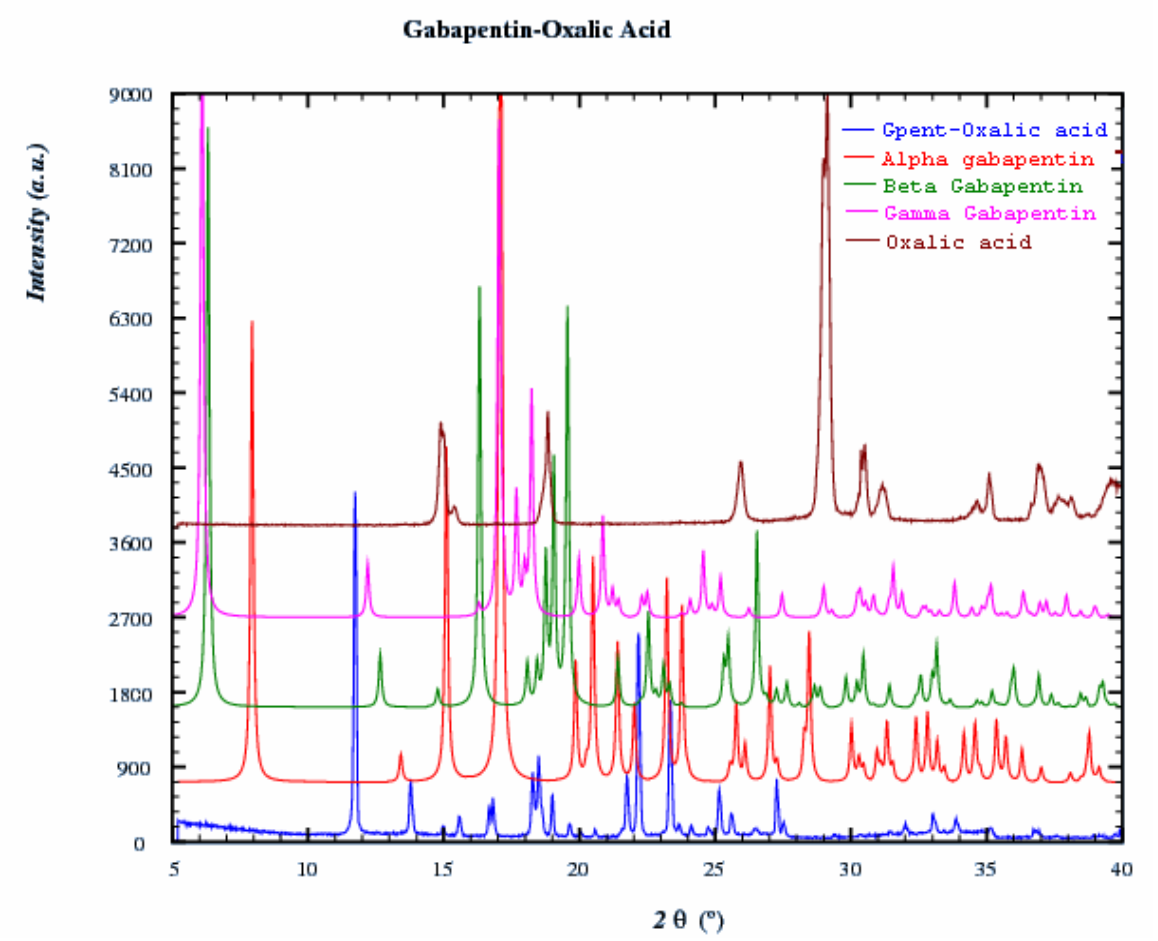


Figure 5.4.3 X-ray powder diffraction pattern comparison of the crystals obtained at pH 4 with the patterns of known polymorphs of gabapentin and the oxalic acid starting material.

It is evident from this powder diffraction pattern comparison that the pattern for the substance formed at pH 4 is very different from the powder patterns of the starting materials and other possible polymorphs. Due to the presence of suitable crystals, further characterisation could be done.

5.4.5 X-ray Single Crystal Diffraction

The block shaped crystals formed at pH 4, were examined by X-ray single crystal diffraction at -100°C on the Bruker, APEX II diffractometer. The crystallographic data is presented in table 5.4.1.

Table 5.4.1: Crystallographic data for gabapentin-oxalic acid crystals.

Formula	$(C_9 H_{18} N O_2), (C_2 O_4)$
Formula Weight	260.25g/mol
Temperature	173(2)K
Crystal System	Monoclinic
Space Group	$P2_1/n$
Description	Colourless, blocks
Unit cell dimensions	a= 6.0941(4)
	b = 8.1995(6)
	c = 21.3933(15)
	$\alpha = 90$
	β =94.2940(10)
	$\gamma = 90$
Volume	$V = 1065.99(13)A^3$
Z	4
Density	$1.347g/cm^{-3}$
Absorption coefficient	$0.104mm^{-1}$
Θ range for data col.	1.9-28.3°
Reflections collected	8942
Independent reflect.	2643
Final R indices	0.039

The molecular conformational diagram obtained through X-ray single crystal diffraction as well as the numbering scheme of the structure, is presented in figure 5.4.4.

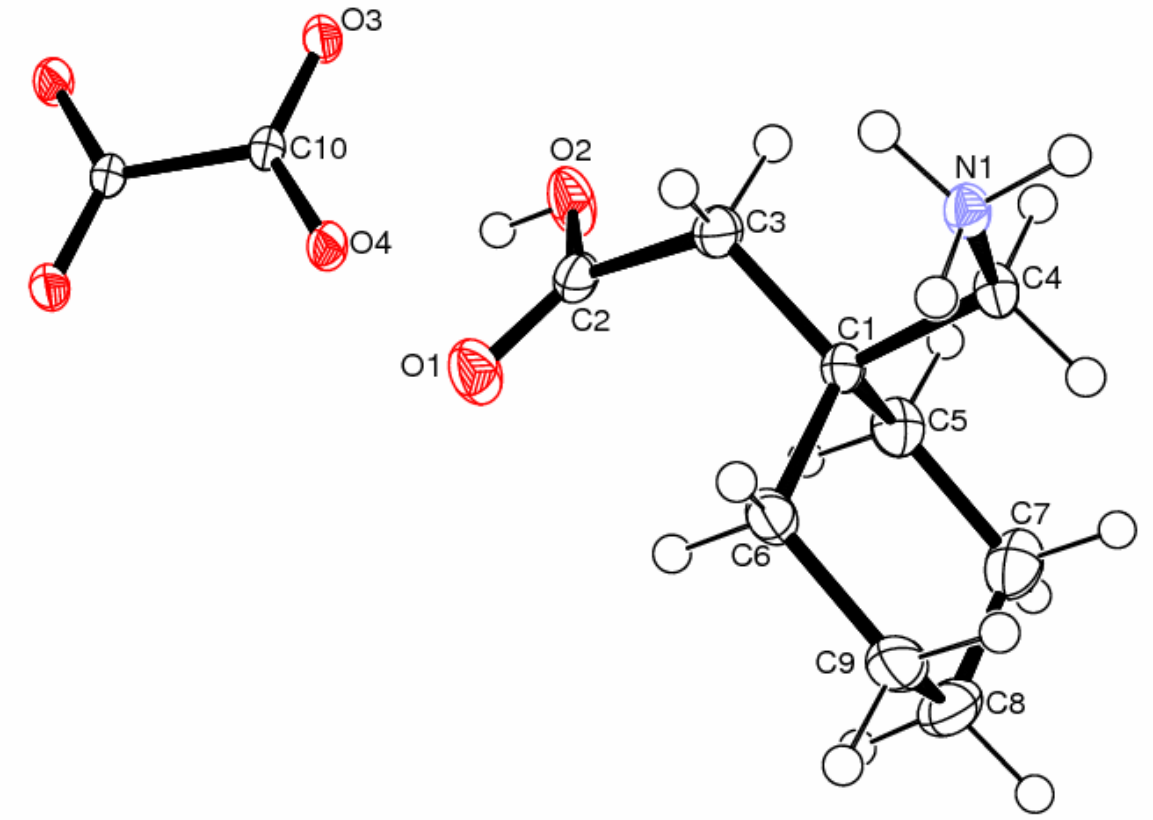


Figure 5.4.4 Ortep diagram of the molecular conformation of the gabapentin-oxalic acid structure with displacement ellipsoids at a 50% probability level.

The above molecular conformational diagram indicates that the crystals obtained at a pH of 4 are co-crystals of gabapentin and oxalic acid.

A comparison of the molecular conformation of the gabapentin molecule within this co-crystal and the gabapentin molecules discussed in chapter 4 show that there are significant torsion angle differences. Table 5.4.2 indicates the differences in selected torsion angles.

Table 5.4.2: Selected torsion angles of gabapentin from the co-crystal compared with other gabapentin polymorphs.

Torsion	Gabapentin-oxalic acid co-crystal	α[a] -gabapentin(°)	β-gabapentin(°)	γ-gabapentin(°)
C3-C1-C5-C7	-177.67(8)	-166.22(11)	-65.44(18)	-168.79(15)
O1-C2-C3-C1	65.25(14)	-161.36(11)	95.97(18)	151.56(14)
C2-C3-C1-C4	174.41(8)	51.21(15)	-46.40(2)	63.47(18)
C3-C1-C4-N1	61.25(10)	60.07(14)	-52.50(2)	47.74(17)
C2-C3-C1-C5	58.24(11)	-68.63(14)	-168.37(14)	-56.38(18)
C2-C3-C1-C6	-62.50(12)	172.52(11)	71.87(18)	-174.14(14)
N1-C4-C1-C6	-62.02(10)	-58.28(14)	-173.57(14)	-72.56(17)
N1-C4-C1-C5	178.88(8)	-178.71(10)	69.42(18)	168.72(13)

Note: a.) Parameters taken from Ibers, (2001).

Table 5.4.2 indicates that the conformation of the gabapentin molecule within this co-crystal is different from its conformation for the three polymorphs discussed in chapter 4, particularly the torsions related to the positions of the NH_3^+ and COOH groups. The differences would be largely due to the presence of the oxalate dianion as a result of the interactions between these molecules. The cyclohexane ring is oriented in the chair conformation with the GABA fragment of the gabapentin, oriented in a trans-like configuration. The gabapentin molecule is also protonated in this co-crystal with the oxalic acid being in a dianion form. The oxalic acid in this co-crystal also has a slightly elongated C-C bond length of 1.56Å.

The unit cell of the gabapentin-oxalic acid co-crystal is shown in figure 5.4.5.

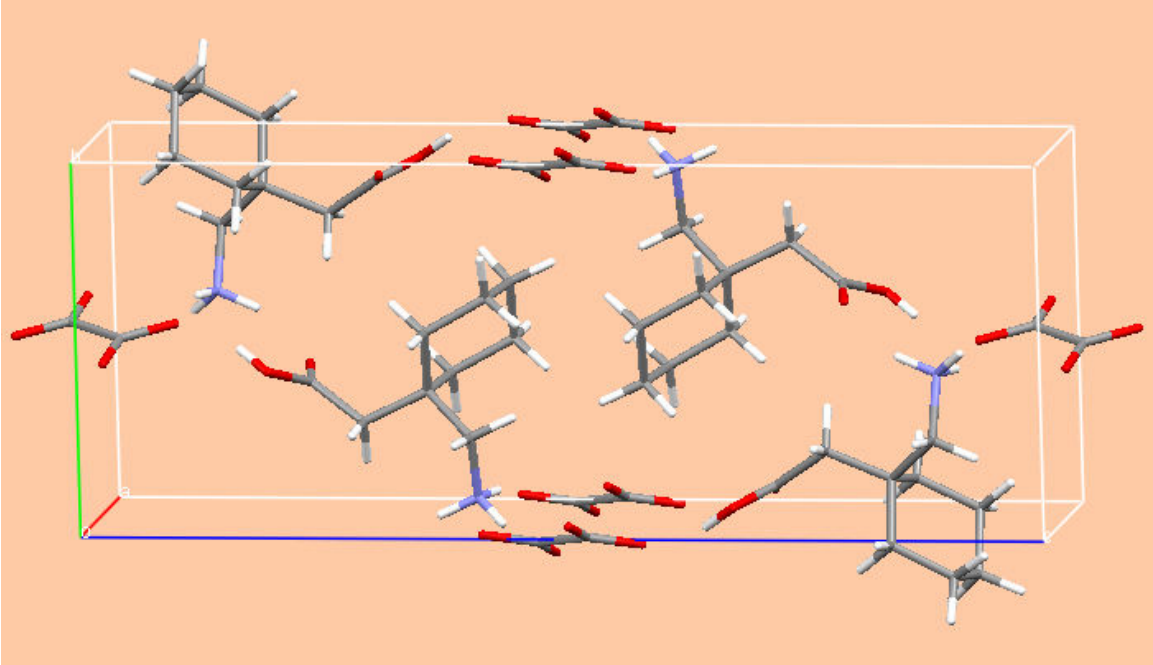


Figure 5.4.5 Unit cell of the gabapentin-oxalic acid co-crystal.

There are 4 gabapentin molecules and ((0.25 x 4) + (0.5 x 2)) = 2 oxalate dianion molecules. Therefore, this is a 2:1 gabapentin-oxalic acid co-crystal with the formula $2(C_9\ H_{18}\ N\ O_2)$, $(C_2\ O_4)$.

5.4.6 Hydrogen Bonding

The co-crystal of gabapentin-oxalic acid has an extensive hydrogen bonding network again due to the presence of the NH_3^+ and COOH groups on the GABA molecules and the COO^- groups of the oxalate dianion. The numbering scheme of the hydrogen atoms present on the gabapentin molecule is given in figure 5.4.6.

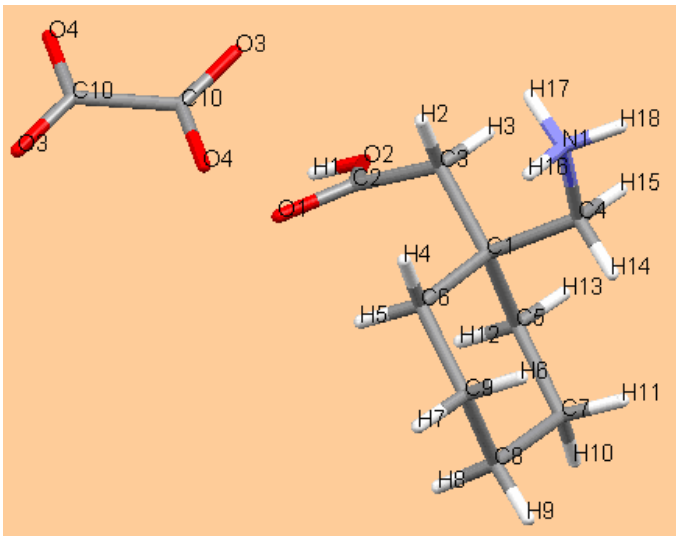


Figure 5.4.6 Numbering scheme for the hydrogen atoms present on the gabapentin molecule.

Each NH_3^+ group on the gabapentin molecule has six hydrogen bonding interactions where four interactions are with neighbouring oxalate dianion molecules and the other two are with neighbouring gabapentin molecules. Atom H16 acts as a bifurcated hydrogen donor and interacts with both the O3 and O4 atoms on a single neighbouring oxalate dianion ie. H16---O3 = 2.40Å and H16---O4 = 1.88Å. Therefore, the H16---O4 interaction is the stronger of the interactions. Atom H17 interacts with an O1 and O2 atom on different gabapentin molecules. The interaction of H17 with O1 has a hydrogen bond length of H17---O1= 2.34Å. The other interaction that the H17 atom has is with the O2 atom of the OH group. This is a very weak interaction and has the hydrogen bond length H17---O2 = 2.63Å. Atom H18 also acts as a bifurcated hydrogen bond donor and interacts with two different O3 atoms on different oxalate dianion molecules. The one hydrogen bonding interaction H18---O3 = 1.90Å is a strong hydrogen bond, however, the interaction of H18 with the other O3 atom (the same atom with which H16 interacts) is very weak and the hydrogen bond length of H18---O3 = 2.690Å is too long to be classified as a typical hydrogen bond. It is rather a weak hydrogen interaction.

Atom H1 which is part of the OH group of gabapentin is a single hydrogen bond donor. It forms a hydrogen bond with an O4 atom on a neighbouring oxalate dianion. The

hydrogen bond length is H1---O4 = 1.74Å. This is the strongest hydrogen bonding interaction present within the network.

A summary of the hydrogen bonding is presented in table 5.4.3.

Table 5.4.3: Hydrogen bonding parameters of the gabapentin-oxalic acid co-crystal (Å, °).

D-H---A	D-H	H---A	D---A	D-H---A
N1-H16-O4	0.91	1.88	2.767(11)	164
N1-H16-O3	0.91	2.40	2.890(11)	114
N1-H17-O1	0.91	2.34	3.039(11)	134
N1-H17-O2	0.91	2.63	3.136(11)	116
N1-H18-O3	0.91	1.90	2.781(10)	161
O2-H1-O4	0.84	1.74	2.553(10)	164

Each gabapentin molecule interacts with three different oxalate dianion molecules and four different neighbouring gabapentin molecules as shown in figure 5.4.7 below.

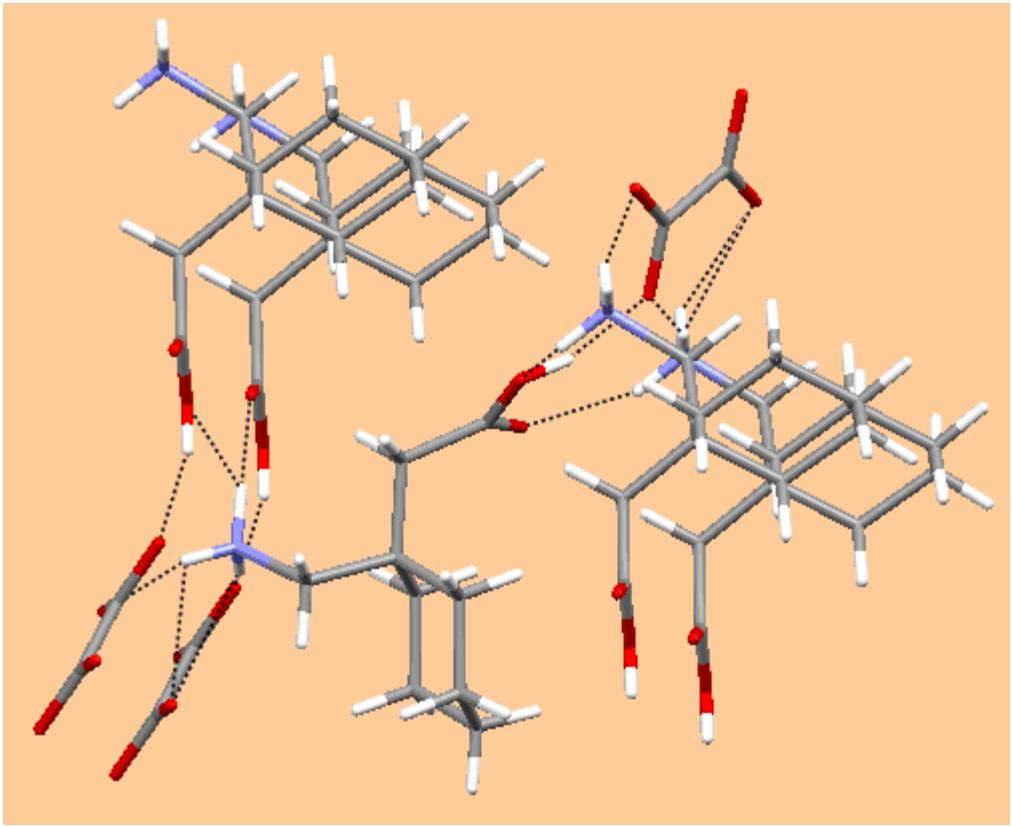


Figure 5.4.7 Hydrogen bonding interactions between gabapentin and oxalic acid.

In the hydrogen bonding network, the gabapentin molecules interact with each other to form a chain along the b-axis. This is indicated in figure 5.4.8.

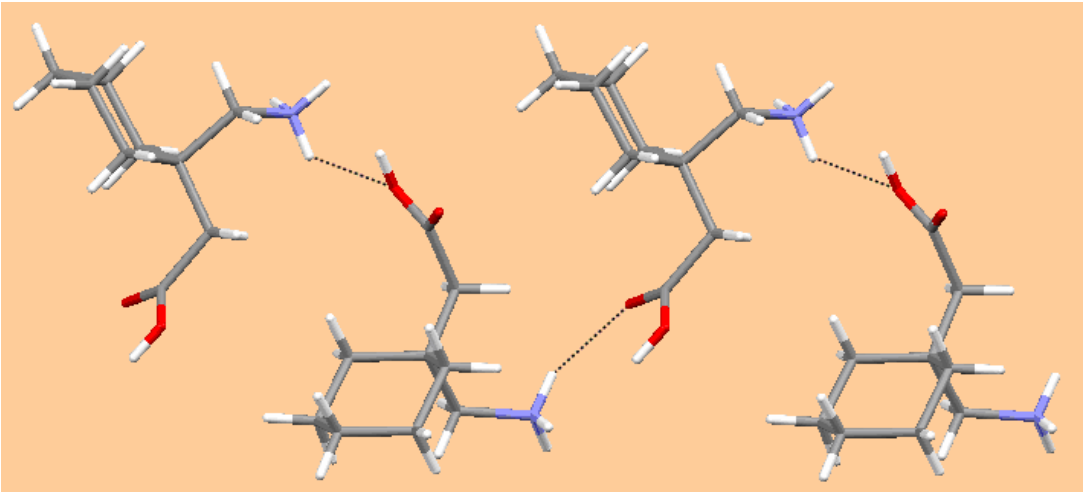


Figure 5.4.8 Hydrogen bonds linking the gabapentin molecules along the b-axis in the hydrogen bonding network.

These chains are then linked through various hydrogen bonding interactions with the oxalate dianion molecules.

The hydrogen bonding network can further be characterised by examining the graph sets present in the network. The first and second level hydrogen bond motifs which are present for the five strong hydrogen bonds were determined by RPLUTO (Motherwell *et al.*, 1999). A summary of the main graph sets is shown in matrix form in table 5.4.4 which corresponds to figure 5.4.9.

Table 5.4.4: Matrix of selected graph sets for the hydrogen bonding of the gabapentin-oxalic acid co-crystal.

	a	b	c	d	e
a	$D_2^2(6)$	-	-	-	-
b	$C_2^2(12)$	$D_2^2(6)$	-	-	-
c	$C_2^2(12)$	$R_4^2(8)$	$D_2^2(6)$	-	-
d	$C_2^2(12)$	$R_4^4(14)$	$R_2^4(8)$	$D_2^2(6)$	-
e	$C_3^3(16)$	$C_3^3(14)$	$C_3^3(14)$	$C_3^3(14)$	$C_1^1(7)$

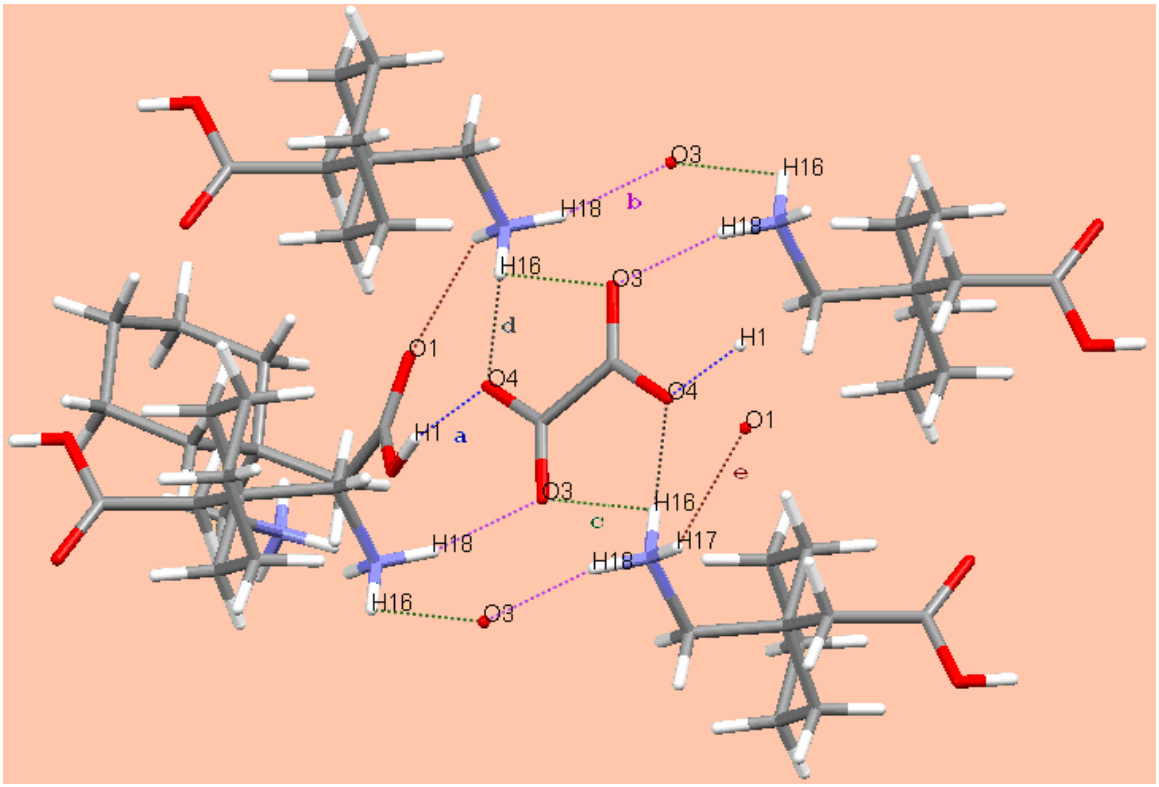


Figure 5.4.9 The letters **a** - **e** refer to five individual hydrogen bonds which are present, where some of the first and second level graph set motifs resulting from these bonds are indicated in table 5.4.4. The single red dots refer to the oxygen atoms where the remainder of the molecule has been deleted for visual clarity. Only a portion of the $C_1^1(7)$ chain motif is present.

Figure 5.4.9 shows the extensive hydrogen bonding present for the gabapentin-oxalic acid structure. The figure also shows the different ways in which the gabapentin molecules are linked to each other and to the oxalic acid molecules. The large number and variety of graph sets for this 2:1 gabapentin-oxalic acid co-crystal would have the effect of greatly increasing the stability of the compound.

5.4.7 Thermal Analysis

The melting point of the 2:1 gabapentin-oxalic acid co-crystal was initially determined by hot stage microscopy and this value verified by running a DSC scan. The melting point was determined to be approximately 157.5ºC from hot stage microscopy. The DSC of the 2:1 gabapentin-oxalic acid co-crystals produced the curve shown in figure 5.4.10.

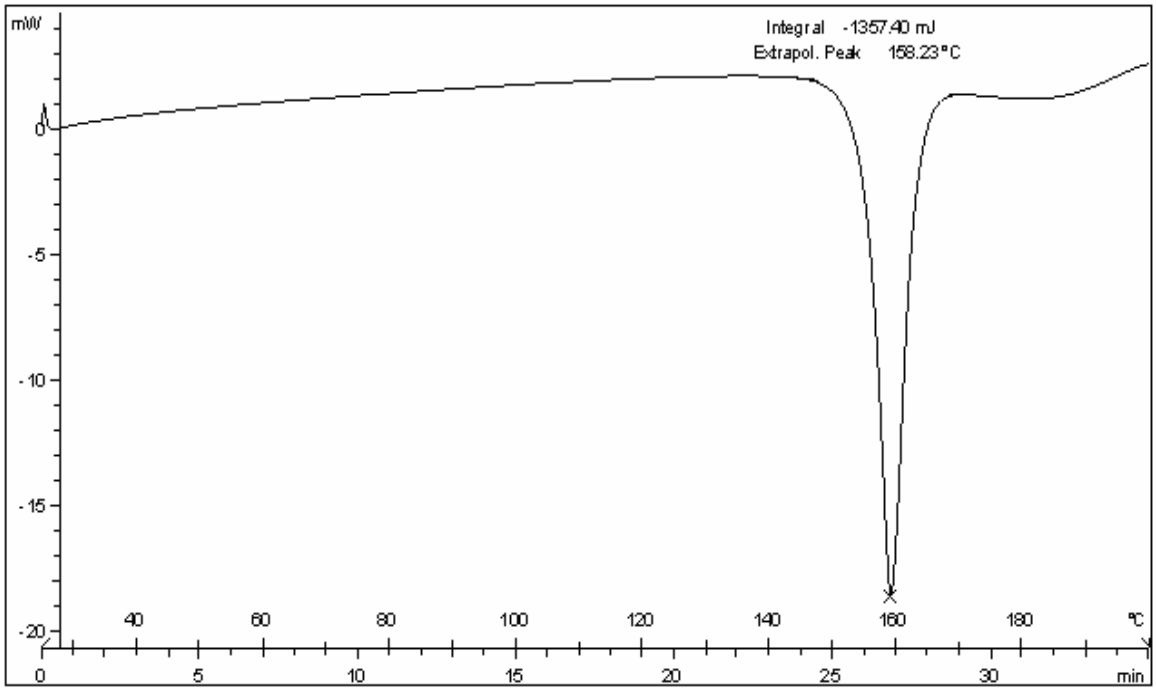


Figure 5.4.10 DSC curve of heat flow (mW) vs. temperature (°C) for the 2:1 gabapentin-oxalic acid co-crystals over the range of 25-200°C.

This curve shows a melting point of 158.2°C which is close to the value obtained from hot stage microscopy. The melting points of the starting materials, gabapentin and oxalic acid are 161°C and 101°C respectively. The plot also indicates that the melting of the crystalline substance is the only phase transition which takes place.

5.4.8 Discussion and Conclusion

Through visual examination of these crystals as well as the recording of an X-ray powder diffraction pattern, the crystalline substance which formed at pH 4 was found to be different from the starting materials and other gabapentin polymorphs, therefore indicating that a different crystalline phase had been formed. X-ray single crystal diffraction indicated that the crystalline phase is in fact the gabapentin-oxalic acid co-crystal. For these co-crystals gabapentin is protonated while oxalic acid is in the carboxylate dianion form.

The unit cell representation indicates the presence of four gabapentin molecules and two oxalic acid dianion molecules. Therefore, a 2:1 co-crystal of gabapentin-oxalic acid has formed. Again, as in the case of the GABA-oxalic acid co-crystal, the presence of the oxalate dianion clearly has an effect on the conformation of the gabapentin molecule as it has a very different conformation from all other gabapentin polymorphs and analogues. The hydrogen bonding network for this structure is also very extensive, indicated by a range of different graph sets. It is made up of gabapentin chains extended along the b-axis and linked together in different ways by the oxalate dianions.

The Cambridge Structural Database was searched in attempts to find out whether the 2:1 gabapentin-oxalic acid co-crystals had been previously reported. The structure of this co-crystal was not found and it has not yet been published and is therefore novel*.

* However, it is noted that after a private communication from Prof. J. Bernstein to Prof. D.C. Levendis, it appears that Wenger M. & Bernstein J. have recently submitted a paper on the same structure.

Chapter 5.5 Co-crystals of β-alanine and Oxalic acid

5.5.1 Introduction

β-alanine is the only beta amino acid which occurs naturally. It is a non-essential amino acid which can be found naturally in the body as well as in protein foods. The structure of β-alanine is closely related to the structure of the neurotransmitter GABA, where it simply contains one less carbon atom in the backbone.

The protonation constants of β-alanine are approximately 3.55 and 10.19 (www.research.chem.psu.edu/brpgroup/pka_compilation.pdf, 07/10/2007) and it can therefore exist in three different ionization states. A plot of the calculated molar fractions of β-alanine (determined from the protonation constants) against the pH, indicates the regions in which the different ionization states occur (figure 5.5.1).

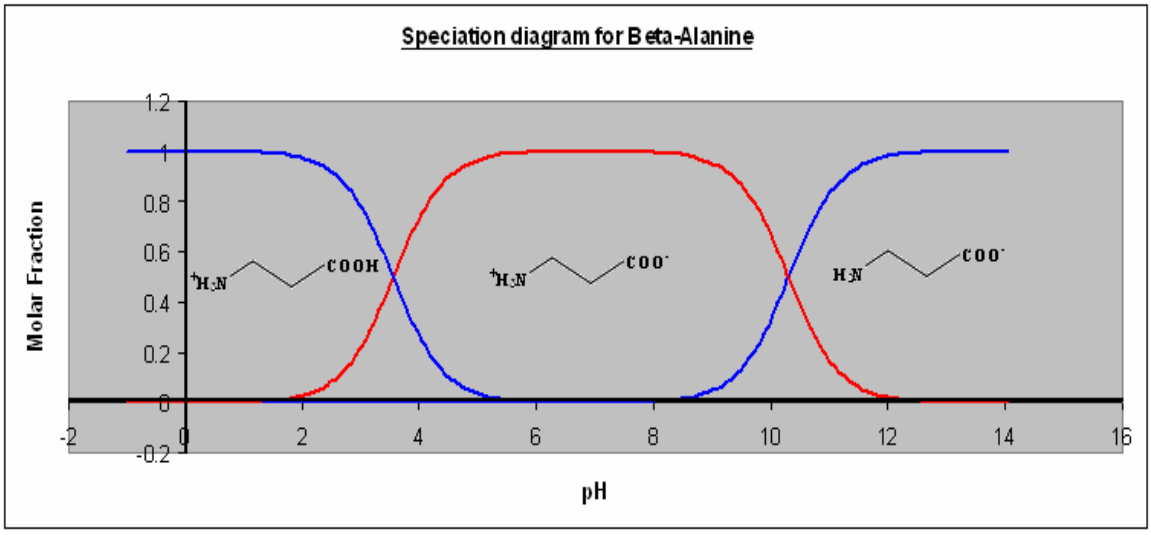


Figure 5.5.1 Speciation diagram of β-alanine.

At a pH of 3, β-alanine can exist as a mixture of zwitterionic and protonated species while oxalic acid exists in the semi-carboxylate anion form. For a pH of 6, β-alanine is a zwitterion and oxalic acid is in the carboxylate dianion form. At a pH of 12, β-alanine exists as an anion and oxalic acid again has the carboxylate dianion form.

5.5.2 Experimental

Equimolar amounts of β-alanine (Sigma Aldrich) and oxalic acid were dissolved in deionised water at room temperature. The solution was then adjusted to the desired pH using 1M hydrochloric acid and 2M sodium hydroxide solutions. Solutions of the compounds were adjusted to pH values of approximately 3, 6 and 12. The pH values were estimated using indicator paper. The solutions were then placed into vials and left in a fume hood in order for open-air evaporation to take place. For the solutions at pH 6 and 12, no suitable crystals were formed for X-ray single crystal diffraction analysis. In the pH 3 solution, block shaped crystals were obtained.

5.5.3 Microscopic analysis of the crystals formed

The crystals, which were formed at pH 3, were visually analyzed using an optical Micro Met Scientific microscope at a magnification of 45x. The images are shown in figure 5.5.2.

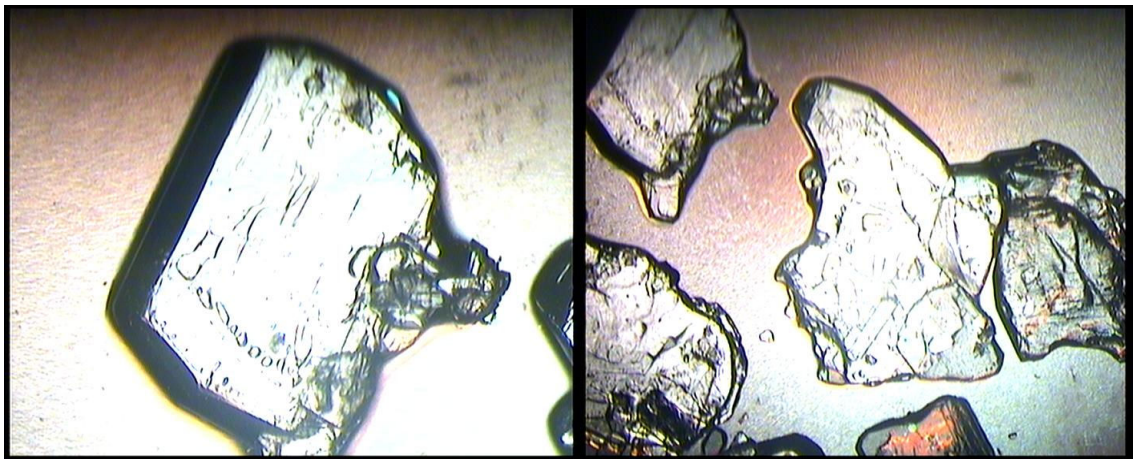


Figure 5.5.2 Optical microscope images of the crystals formed at pH 3 using a 45x magnification.

These images indicate that the crystals obtained are large blocks and suitable for X-ray single crystal diffraction analysis.

5.5.4 X-ray Powder diffraction

X-ray powder diffraction patterns for the three samples obtained at the pH values of 3, 6 and 12 were recorded in order to test for the presence of different crystalline phases when compared with the β-alanine and oxalic acid starting materials. Figure 5.5.3 shows the overlap of the powder diffraction patterns using Winplotr (Roisnel *et al.*, 2000).

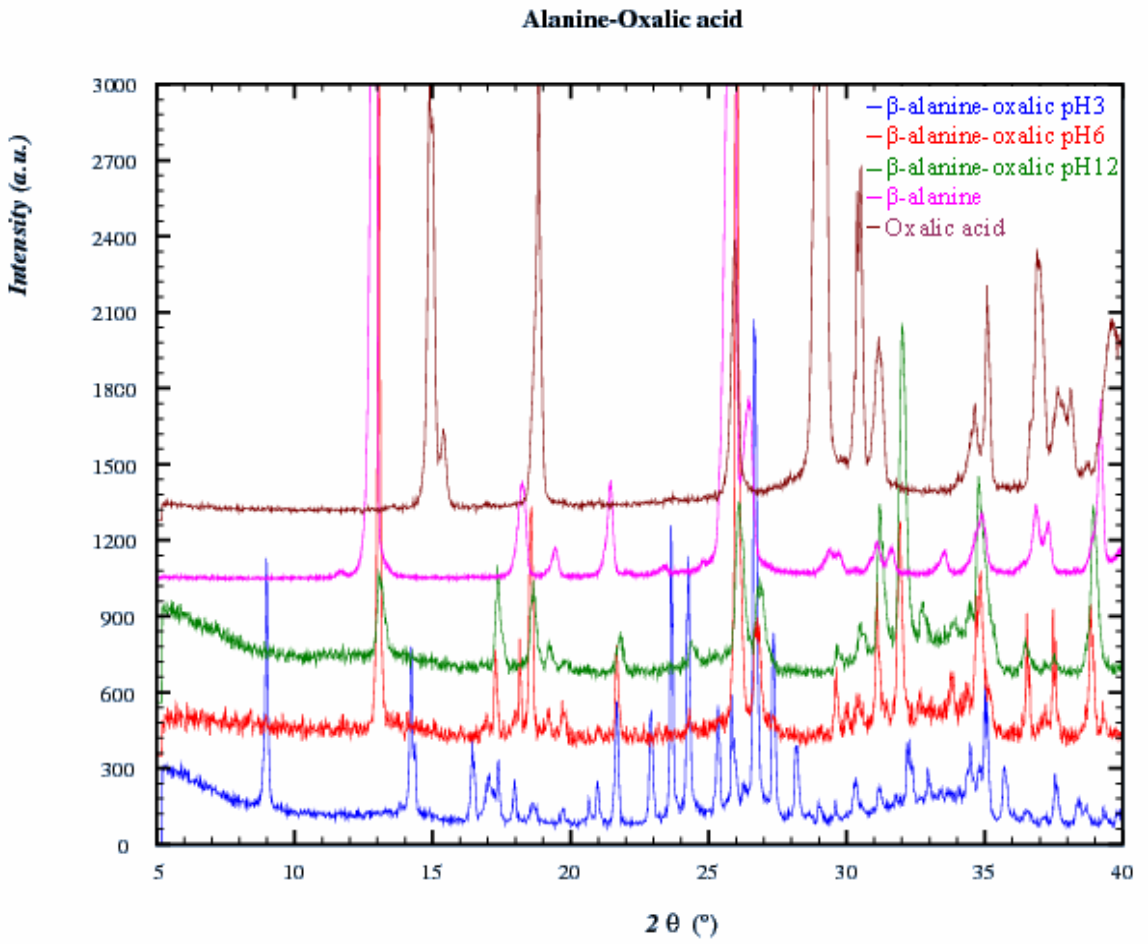


Figure 5.5.3 X-ray powder diffraction pattern comparison of the products obtained at the pH values of 3, 6 and 12 with the patterns of the starting materials, β-alanine and oxalic acid.

This comparison shows that the substances produced at pH 6 and 12 and the β-alanine powder diffraction patterns are all similar. However, the powder pattern of the pH 3 product is different from the other patterns. This indicates the presence of a different crystalline phase which can be further characterised by X-ray single crystal diffraction.

5.5.5 X-ray Single Crystal Diffraction

The block shaped crystals formed at pH 3, were examined by X-ray single crystal diffraction at 25°C on the Bruker, SMART 1K CCD area detector diffractometer. The crystallographic data is presented in table 5.5.1.

Table 5.5.1: Crystallographic data for the β-alanine-oxalic acid-water co-crystal.

Formula	$(C_3 H_8 N O_2),(C_2 O_4 H),(H_2O)$
Formula Weight	376.28g/mol
Temperature	298(2)K
Crystal System	Monoclinic
Space Group	C2/c
Description	Colourless, blocks
Unit cell dimensions	a= 22.419(5)
	b = 5.6992(11)
	c = 14.036(3)
	α = 90
	β =115.394(4)
	γ = 90
Volume	$V = 1620.1(6)A^3$
Z	4
Density	$1.543g/cm^{-3}$
Absorption coefficient	$0.145mm^{-1}$
Θ range for data col.	2.0-27.0°
Reflections collected	4882
Independent reflect.	1769
Final R indices	0.045

The molecular conformational diagram obtained through X-ray single crystal diffraction as well as the numbering scheme for this structure, is presented in figure 5.5.4.

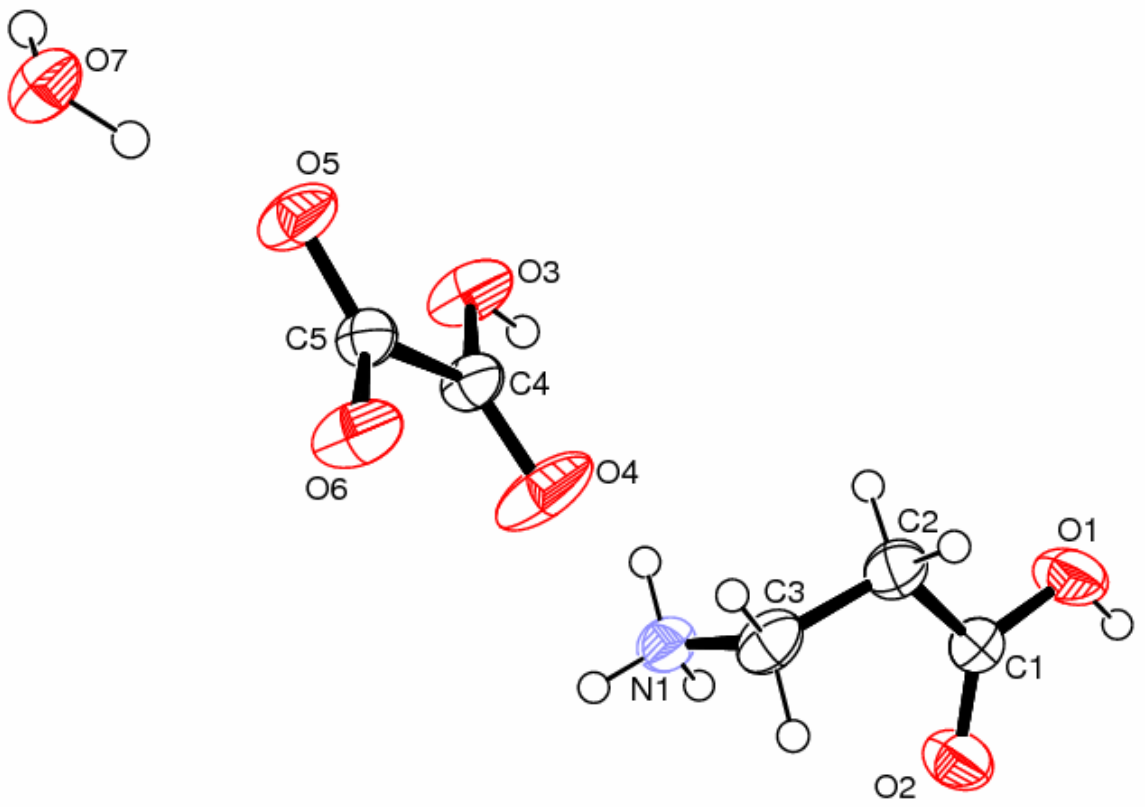


Figure 5.5.4 Ortep diagram of the molecular conformation of the β-alanine-oxalic acid-water structure with displacement ellipsoids at a 50% probability level.

It is evident from figure 5.5.4 that the crystals obtained at pH 3 are co-crystals of β-alanine, oxalic acid and water. By a comparison with other β-alanine conformations, it is evident that the molecular conformation of the β-alanine molecule is greatly affected by the presence of the oxalic acid and water molecules within this co-crystal. This would be due to the extensive hydrogen bonding interactions which are present between the three molecules. The β-alanine molecules in this case exist in a cationic form with the carboxyl group being neutral and the amino group positively charged. The oxalic acid molecule is a semi-oxalate anion.

The unit cell of the β-alanine-oxalic acid-water co-crystal is shown in figure 5.5.5.

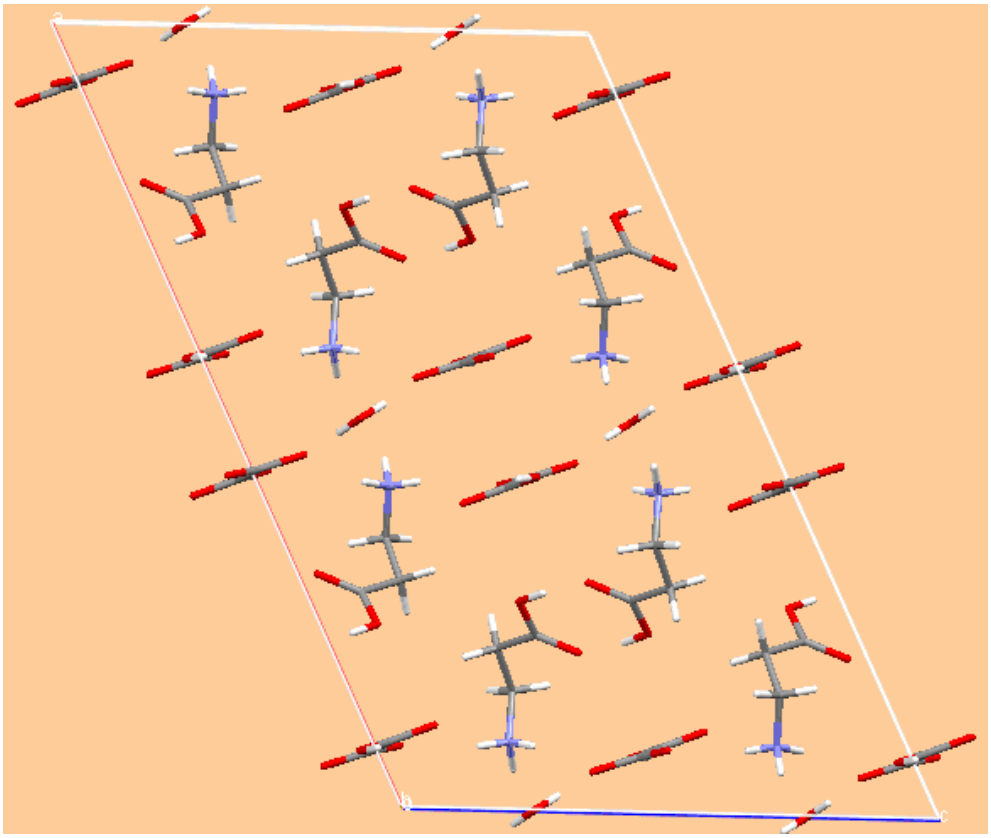


Figure 5.5.5 Unit cell of the β-alanine-oxalic acid-water co-crystal.

There are 8 β-alanine molecules, ((8 x 0.5) + 4) = 8 semi-oxalate anions and ((4 x 0.5)+2) = 4 water molecules. Therefore, this is a 2:2:1 β-alanine-oxalic acid-water co-crystal with the formula $2(C_3\ H_8\ N\ O_2)$, $2(C_2\ H\ O_4)$, H_2O.

5.5.6 Hydrogen bonding

The co-crystal of β-alanine-oxalic acid-water has an extensive hydrogen bonding network due to the presence of the NH_3^+ and COOH groups on the β-alanine molecules and the COO^- and COOH groups of the semi-oxalate anion as well as the H_2O molecule. The numbering scheme of the hydrogen atoms present on the molecules in the β-alanine-oxalic acid-water co-crystal is given in figure 5.5.6.

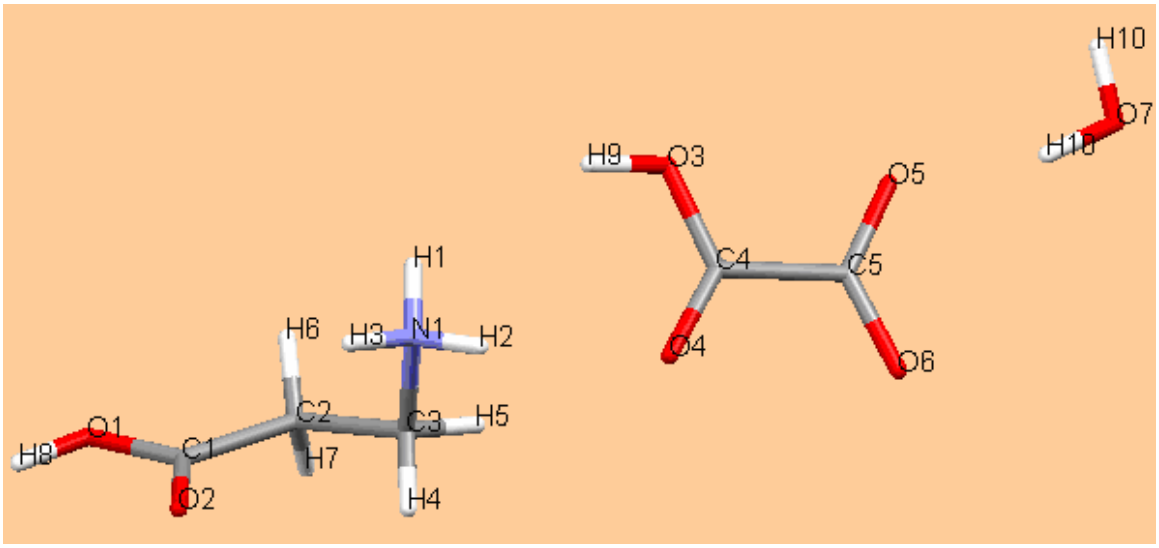


Figure 5.5.6 Numbering scheme for the hydrogen atoms present on the molecules within the β-alanine-oxalic acid-water co-crystal.

Each NH_3^+ group is involved in four hydrogen bonding interactions, where three of the interactions are with neighbouring oxalate dianion molecules and one of the interactions is with a neighbouring water molecule. Atom H1 acts as a bifurcated hydrogen bond donor and interacts with both the O4 and O6 atoms on a single neighbouring semi-oxalate anion ie. H1---O4 = 2.65Å and H1---O6 = 2.02Å. These two hydrogen bonding interactions are relatively weak. Atom H3 acts as a single hydrogen bond donor and interacts with an O7 atom on a neighbouring water molecule. The hydrogen bond length for the interaction is H3---O7 = 1.90Å (O7 has two different H3 atoms from different molecules interacting with it). Atom H2 acts as a single hydrogen bond donor and interacts with O5 on a neighouring semi-oxalate anion. The hydrogen bond length is H2---O5 = 2.06Å.

Atom H8, which is part of the OH group on the β-alanine molecule, interacts with O2 on a neighbouring β-alanine molecule. This interaction forms a dimer which is shown in figure 5.5.7.

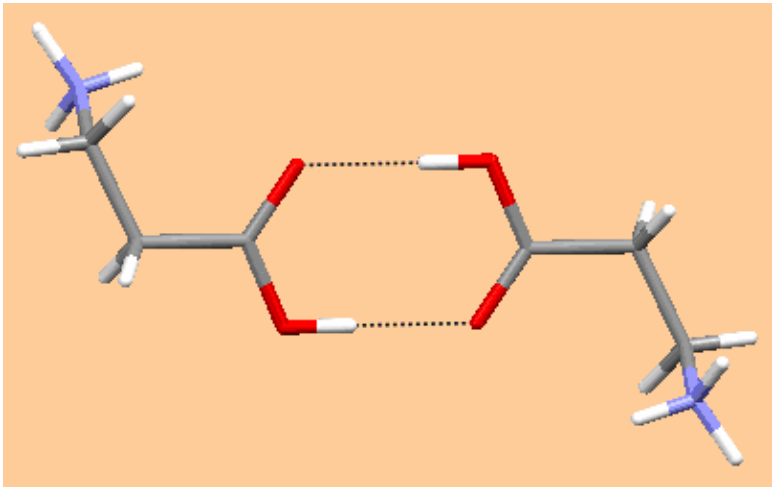


Figure 5.5.7 Hydrogen bonding interaction O1-H8---O2 forming a dimer.

The hydrogen bonding interaction has a length of H8---O2= 1.73Å, which is a relatively strong hydrogen bond. Atom H9 which is part of the OH group on the oxalate anion interacts with O6 on a neighbouring semi-oxalate anion (the same anion with which H1 interacted). The hydrogen bonding interaction has a length of H9---O6= 1.62Å and is very strong. Finally, atom H10, attached to the water molecule, interacts with O5 on a neighbouring semi-oxalate anion and has a bond length of H10---O5= 1.86Å.

A summary of the hydrogen bonding is presented in table 5.5.2.

Table 5.5.2: Hydrogen bonding parameters of the β-alanine-oxalic acid-water co-crystal(Å, °).

D-H---A	D-H	H---A	D---A	D-H---A
N1-H1-O6	0.89	2.02	2.852(2)	156
N1-H1-O4	0.89	2.65	3.274(2)	128
N1-H2-O5	0.89	2.06	2.866(2)	151
N1-H3-O7	0.89	1.90	2.790(2)	174
O1-H8-O2	0.93	1.73	2.663(2)	175
O3-H9-O6	0.98	1.62	2.584(2)	171
O7-H10-O5	0.88	1.86	2.717(2)	166

Each β-alanine molecule interacts with two different oxalate anion molecules, one different neighbouring β-alanine molecule and one water molecule as shown in figure 5.5.8.

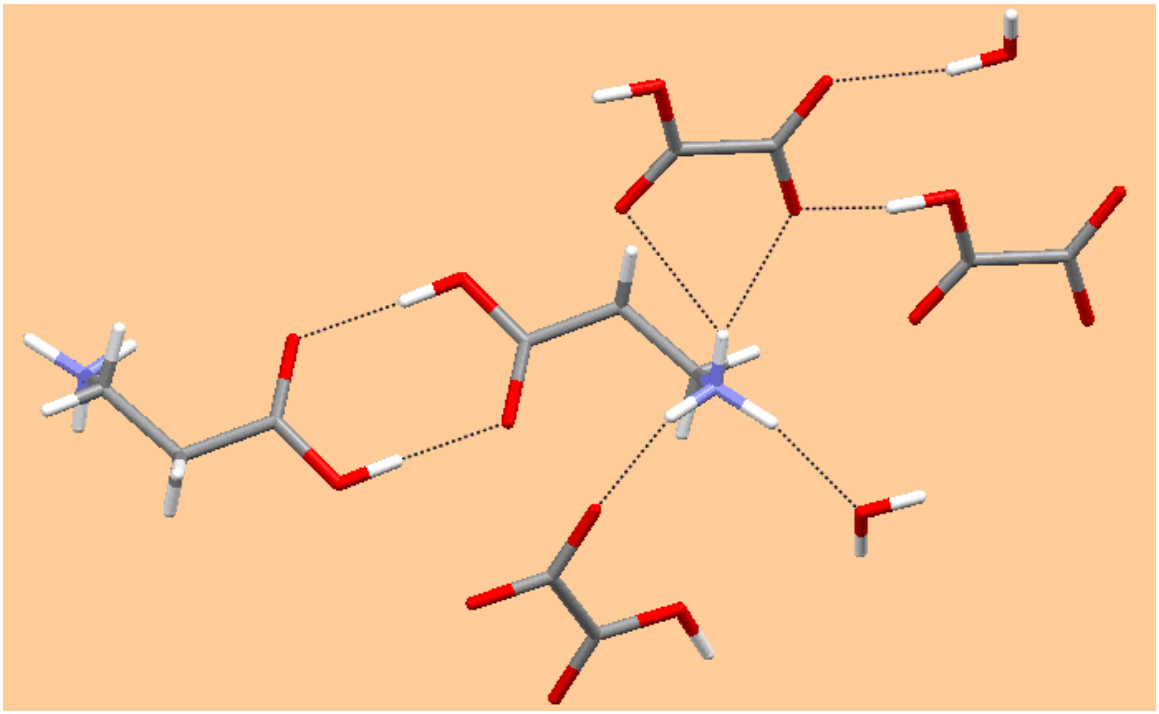


Figure 5.5.8 Hydrogen bonding interactions amongst the β-alanine, oxalic acid and water molecules.

Each semi-oxalate anion interacts with two β-alanine, two semi-oxalate anions and one water molecule, while each water molecule interacts with two β-alanine molecules and two semi-oxalate anions.

The hydrogen bonding network can be effectively characterised by examining the graph sets which are involved. The first and second level hydrogen bond motifs which are present for the seven hydrogen bonds were determined by RPLUTO (Motherwell *et al.*, 1999). A summary of the main graph sets is shown in matrix form in table 5.5.3 which corresponds to figure 5.5.9.

Table 5.5.3: Matrix of selected graph sets for the hydrogen bonding of the β-alanine-oxalic acid-water co-crystal.

	a	b	c	d	e	f
a	$R_2^2(8)$	-	-	-	-	-
b	$D_3^3(15)$	$D_1^1(2)$	-	-	-	-
c	$C_3^2(14)$	$D_2^2(5)$	$D_2^1(3)$	-	-	-
d	-	$D_2^2(5)$	$D_2^2(4)$	$D_1^1(2)$	-	-
e	-	$C_3^3(11)$	-	$D_3^3(10)$	$C_1^1(5)$	-
f	-	$C_2^2(6)$	$D_2^2(5)$	-	$D_3^2(8)$	$D_1^1(2)$

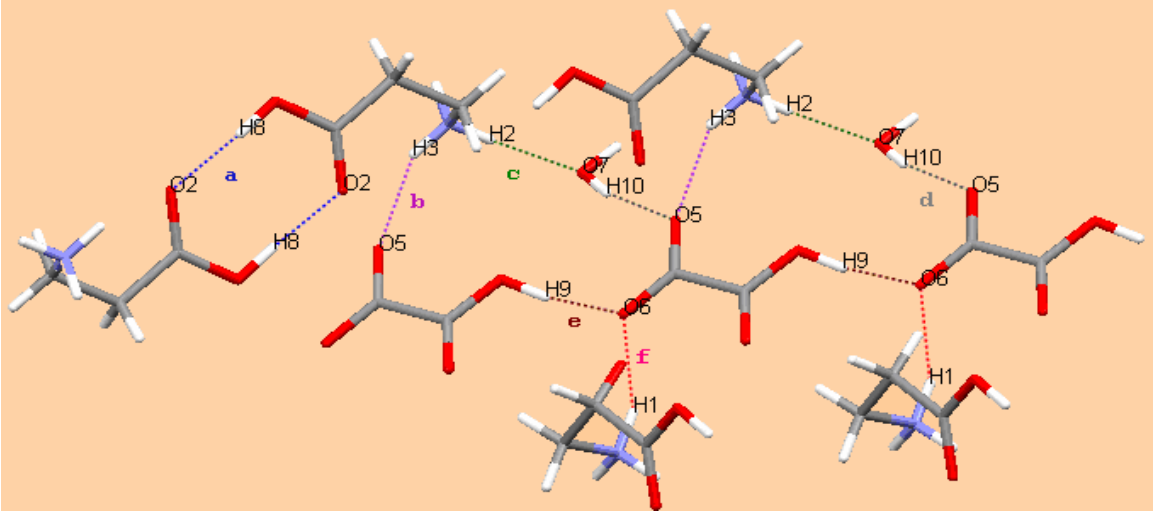


Figure 5.5.9 The letters **a** – **f** refer to the six strongest individual hydrogen bonds which are present, where some of the first and second level graph set motifs resulting from these bonds are indicated in table 5.5.3.

Figure 5.5.9 shows the extensive hydrogen bonding present for the β-alanine-oxalic acid-water co-crystal. There is also an additional weaker hydrogen bond (N1-H1-O4) which is not shown in this diagram, but is recorded in table 5.5.2. Figure 5.5.9 also shows the different ways in which the β-alanine, semi carboxylate anion and water molecules are linked to each other. The large number and variety of graph sets for this structure would have the effect of increasing the stability of the compound.

5.5.7 Thermal analysis

Again, for these β-alanine-oxalic acid-water co-crystals, the melting point was initially determined by hot stage microscopy. The value obtained was approximately 166°C. This value was verified by running a DSC scan. The DSC scan of these co-crystals produced the curve shown in figure 5.5.10.

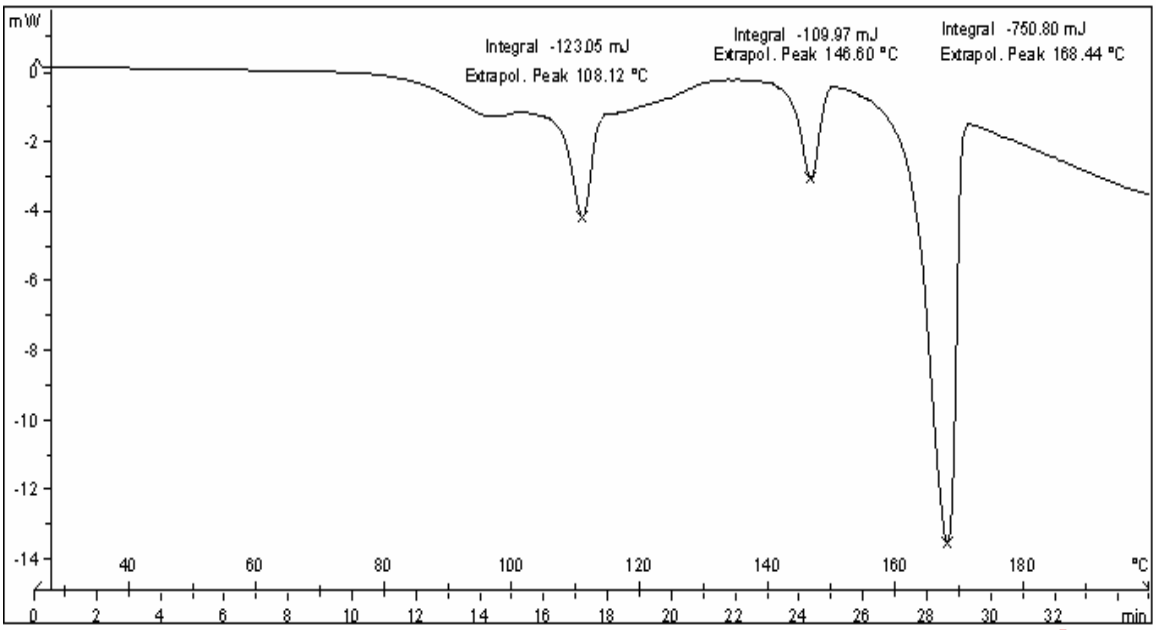


Figure 5.5.10 DSC scan of heat flow (mW) vs. temperature (°) for the 2:2:1 β-alanine-oxalic acid-water co-crystals over the range 25-200°C.

The curve in figure 5.5.10 indicates that the co-crystals melt at 168.4°C. This value is similar to the value obtained by hot stage microscopy. The melting points of the starting materials, β-alanine and oxalic acid are 196°C and 101°C respectively. Therefore, the melting point of the co-crystals is significantly different from that of the starting materials.

The DSC scan also contains two other peaks at 108.1°C and 146.6° which are different from the starting materials. This indicates that there are possibly phase transitions at these points. These possible phase transitions were further investigated by observing the changes which a crystal undergoes as the temperature changes. This was done under a microscope and snapshot images were taken at various temperatures. Figures 5.5.11

indicates the visible changes which the crystal undergoes at the above mentioned temperatures.

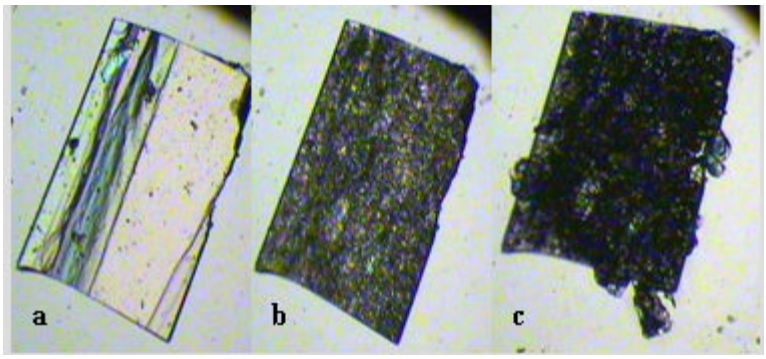


Figure 5.5.11 Images of the β-alanine-oxalic acid-water co-crystal: **a**.) Room temperature **b**.) 110°C **c**.) 147°C.

From figure 5.5.11(a) and (b), it is evident that the crystal undergoes a significant colour change from being clear to being darkened in colour. This could represent the first phase transition. When the temperature is increased further, the crystal appears to melt slightly and then re-crystallize to form a much darker black crystal as indicated in figure 5.5.11(**c**). This could possibly represent the second phase transition. When the crystal is heated further, it finally melts at approximately 168.4°C. The visual changes in the crystal could be as a result of phase transitions. They could also be due to the loss of water from the crystal. Single crystals of the **b** and **c** phases could not be isolated for analysis.

5.5.8 Discussion and Conclusion

Crystals were obtained at a pH of 3. The crystals obtained were compared visually in order to determine whether they differ in appearance. They were also examined using X-ray powder diffraction, comparing the powder patterns to those of the starting materials in order to investigate the presence of a different crystalline form. The visual differences and the difference in the powder pattern resulted in further characterisation being done. Through X-ray single crystal diffraction the crystals were identified as co-crystals of β-alanine, oxalic acid and water. Within the co-crystals, the β-alanine is in the cationic form and oxalic acid in the semi-carboxylate anion form.

The unit cell representation indicates the presence of eight β-alanine molecules, eight semi-oxalate anions and four water molecules, resulting in a 2:2:1 co-crystal of β-alanine-oxalic acid-water. The presence of the semi-oxalate anions and water molecules has a significant effect on the conformation of the β-alanine and this would be due to the extensive hydrogen bonding network which is present.

Within the hydrogen bonding network, there is the formation of a dimer between the β-alanine molecules. These dimers are linked together by forming hydrogen bonds with neighbouring semi-oxalate anions and water molecules. The complexity of the hydrogen bonding network can be seen by the large number of graph sets needed to represent the network.

The thermal analysis of the co-crystal indicated that its melting point is very different from the starting materials. The DSC scan also indicated the presence of possible phase changes which were also verified visually. These could not be explored further as single crystals of these phases could not be isolated.

The Cambridge Structural Database was again searched in attempts to find out whether the 2:2:1 β-alanine-oxalic acid-water co-crystal had previously been published. It was found that this structure had been published in an ACTA E paper by Krishnakumar and co-workers (Krishnakumar *et al.*, 2002). The unit cell parameters, conformation and hydrogen bonding networks of this structure were compared with the reported structure and they were found to be similar. Therefore, the co-crystals grown resemble the published structure of β-alaninium oxalate hemihydrate.

5.6 References

Aakeröy, C.B., Salmon, D.J. (2005). Cryst. Eng. Commun., Vol. 7, 439-448.

Alagar, M., Krishnakumar, R.V., Nandhini, M.S., Cameron, T.S., Natarajan, S. (2003). Acta Cryst., E59, 0108-0110.

Bond, A. (2007). Cryst. Eng. Commun., Vol. 9., 833-834.

Chandra, N. R., Prabu, M.M., Venkatraman, J., Suresh, S., Vijayan, M. (1998).Acta Cryst. B54, 257-263.

Childs, S.L., Stahly, G.P., Park, A. (2007). Molecular Pharmaceutics, Vol. 4, No. 3, 323 – 338.

Chitra, R., Choudhury, R. (2007). Acta Cryst., B63, 497-504.

Dobson, A.J., Gerkin, R.E. (1996). Acta Crystallogr., Sect.C:Cryst.Struct.Commun., 52, 3075.

Drebushchak, T.N.,Boldyreva, E.V., Shutova, E.S. (2002).Acta Cryst.,E58, 634-636.

Dunitz, J.D. (2003). Cryst. Eng. Commun., Vol. 5., 506.

Ibers, J. A. (2001). Acta Cryst. C57, 642-643.

Iitaka, Y. (1958). Acta Cryst., 11, 225-226.

Jonsson, P.G., Kvick, A. (1972). Acta Cryst., B28, 1827-1833.

Krishnakumar, R.V., Nandhini, M.S., Natarajan, S. (2002). Acta Cryst., E58, 117-119.

Motherwell, W.D.S, Shields, G.P., Allen, F.H. (1999). Acta Cryst., B55, 1044-1056.

Nandhini, M.S., Krishnakumar, V.R., Natarajan, S. (2001). Acta Cryst., C57, 115-116.

Rajagopal, K., Krishnakumar, R.V., Nandhini, M.S., Malthi, R., Rajan, S.S., Natarajan, S. (2003). Acta Cryst., E59, 878-880.

Roisnel, T., Rodrigues, J. (2000). Materials Science Forum, Proceeding of the seventh European powder diffraction conference, ed. R. Delhez and E.J. Mittenmeijer, 118-123.

Saraswathi, N.T., Vijayan, M. (2002). Acta Cryst., B58, 1051-1056.

Selvaraj, M., Thamotharan, S., Siddhartha, R, Vijayan, M. (2007). Acta Cryst., B63, 459-468.

Stahly, G.P. (2007). Crystal growth & design, Vol. 7, 1007 – 1026.

Suresh, S., Vijayan, M. (1995). Acta Cryst. B51, 353-358.

Thayer A.M. (2007). Form and Function, 85, 17-30.

Wenger, M., Bernstein, J. (2006). Angew.Chem. Int. Ed, 45, 7966-7969.

www.britannica.com, (15/06/2007).

www.cfsan.fda.gov/~rdb/opagras1.html, (30/10/2007).

www.drugs.com/mmx/gabapentin.html, (07/10/2007).

www.research.chem.psu.edu/brpgroup/pka_compilation.pdf, (07/10/2007).

www.web-books.com/moBio/Free/Ch2A4.htm, (30/10/2007).

Chapter 6
Conclusion

6.1 Conclusion

This research project, firstly allowed for the study of the neurotransmitter γ-aminobutyric acid (GABA). Through the experimental method of vapour diffusion, thin needle-like single crystals were formed which grew from the contact line of the solution. These could be analysed by X-ray powder and single crystal diffraction in order to compare this form with the two previously reported monoclinic and tetragonal polymorphs. The single crystal analysis allowed for these needle-like crystals to be identified as a hexagonal GABA pseudo polymorph which contains two different GABA molecules and disordered solvent molecules in the asymmetric unit. One type of GABA molecule (molecule 1) forms hexagonal channels down the c-axis and the other type of GABA molecule (molecule 2) forms 3-fold axis chains which coincide with 3-fold screw axis. It was discovered that this form resembles the dipeptide structures reported by Görbitz *et al.*, (2007), which contain hexagonally symmetric pores. The disorder of the solvent molecules could not be properly resolved, however, ^{1}H NMR allowed for the solvent to be identified as ethanol with a 1:10 ratio of EtOH : GABA molecules in the crystals.

A significant feature of this structure was found to be the release of the ethanol and other gases from the channels at a temperature which is significantly higher than the boiling temperature of ethanol. This therefore indicates the high stability of the hexagonal channels.

Thermal analysis was also carried out for all of the GABA polymorphs and it was found from the calculation of the enthalpy values that the hexagonal GABA solvate is significantly less thermodynamically stable than the two previously reported polymorphs.

A search of the Cambridge Structural Database indicates that this GABA solvate is unique, as it is the first single amino acid to be crystallized in this form, where there are

hexagonal GABA crystals containing a solvent. Further studies can be done on these crystals in order to examine their potential as microporous organic crystals.

The study of the neurotransmitter GABA was extended to the structurally related drug compound gabapentin. Through different experimental methods, two unreported gabapentin polymorphs were obtained and compared with an existing polymorph. The techniques of X-ray powder and single crystal diffraction allowed for a comparison of the three polymorphs. The conformations of the gabapentin polymorphs showed a number of differences, in particular with regard to the torsion angles related to the positioning of the NH_3^+ and COO^- groups in each structure. The hydrogen bonding networks also showed distinct differences which could be compared using graph set notation. β-gabapentin was the only polymorph which contained an intramolecular hydrogen bond.

A comparison of the densities and packing efficiencies of the three gabapentin polymorphs showed that the molecules are most efficiently packed in α-gabapentin. This is also the polymorph which is most easily crystallized. It is therefore evident that α-gabapentin is the most thermodynamically stable polymorph. Thermal analysis was carried our for these polymorphs and it was found that β-gabapentin had an additional endotherm at 87.5°C and γ-gabapentin had an additional exotherm at 89°C. Further X-ray single crystal diffraction experiments were carried out at temperatures below and above the endotherm and exotherm temperatures for β-gabapentin and γ-gabapentin respectively, in order to examine the possibility of phase transitions. However, there were no significant changes in the structures. It is possible that these peaks could represent the small changes which occur in the structures and hydrogen bonding networks.

Therefore, it is evident that two unpublished gabapentin polymorphs have been obtained and comparisons show significant differences amongst the three gabapentin polymorphs.

Further studies were carried out on the co-crystallization of neurotransmitter amino acids and analogues with oxalic acid. It was discovered that the conditions under which the experiments are carried out is significant due to the large number of crystalline forms

which can be produced for a particular substance. These different crystalline forms include polymorphs, salts, hydrates and solvates.

It was found that in order to produce co-crystals, the ionization states of the compounds at different pH values need to be examined. Experiments were set up at various pH values for each set of compounds, however, co-crystals were only formed for GABA-oxalic acid at pH 6, for gabapentin-oxalic acid at pH 4 and for β-alanine-oxalic acid-water at pH 3. In the GABA-oxalic acid co-crystal, GABA exists as a protonated species and oxalic acid as a carboxylate dianion. In the gabapentin-oxalic acid co-crystal, gabapentin is protonated while the oxalic acid is in the carboxylate dianion form. The β-alanine-oxalic acid-water co-crystal was formed with the β-alanine in a cationic form and oxalic acid in the semi-carboxylate anion form. This shows that in order for co-crystals to form, the amino acid needs to have an NH_3^+ group and the carboxylic acid must be in an anionic form where it is either a semi-carboxylate anion or a carboxylate dianion.

The crystal structures of the GABA-oxalic acid and gabapentin-oxalic acid co-crystals both have the amino acid protonated and the carboxylic acid in the carboxylate dianion form. The GABA-oxalic acid and gabapentin-oxalic acid co-crystals are also both present in the ratio of 2:1 for the amino acid: carboxylic acid molecules. The β-alanine-oxalic acid-water co-crystal has the amino acid in the protonated form and the carboxylic acid as a semi-carboxylate anion. This co-crystal has a ratio of 2:2:1 for the amino acid: carboxylic acid: water molecules. It is therefore a possibility that the 2:1 co-crystal of β-alanine-oxalic acid without the presence of water could be formed if the oxalic acid were in the carboxylate dianion form as was the case with the other two co-crystals.

It is evident for all the structures, that the presence of the oxalic acid greatly influences the conformation of the amino acid within the co-crystal. This would be due to the extensive hydrogen bonding present for all three structures.

The GABA-oxalic acid and gabapentin-oxalic acid structures have similarities in there hydrogen bonding networks. For both the structures, the amino acid molecules hydrogen

bond to form chains along the b-axis. These amino acid chains are then linked by forming hydrogen bonds in different ways with the oxalate dianions. The network of the β-alanine-oxalic acid-water structure is different due to the presence of the additional water molecule.

It is therefore evident that in order to obtain amino acid: carboxylic acid co-crystals, the ionization states of the involved compounds at specific pH values need to be examined in order to predict whether they will interact in a manner in which co-crystals will form.

Therefore, this research project allowed for the structural analysis and co-crystallization of neurotransmitter analogues.

6.2 Chapter 6 Reference

Görbitz, C.H. (2007). Chem. Eur. J., 13, 1022-1031.

Appendix

1.1 γ-aminobutyric acid

1.1.1.) DSC monoclinic GABA

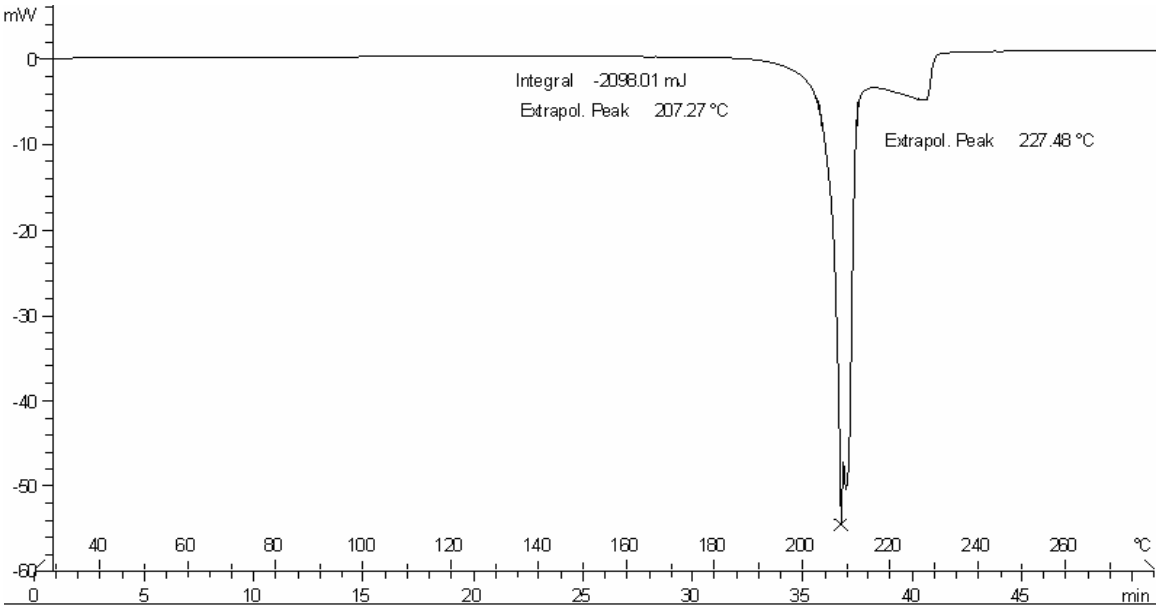


Figure A1.1 DSC curve of heat flow (mW) vs. temperature (°C) for monoclinic GABA from 30 to 280°C.

1.1.2) DSC Tetragonal GABA

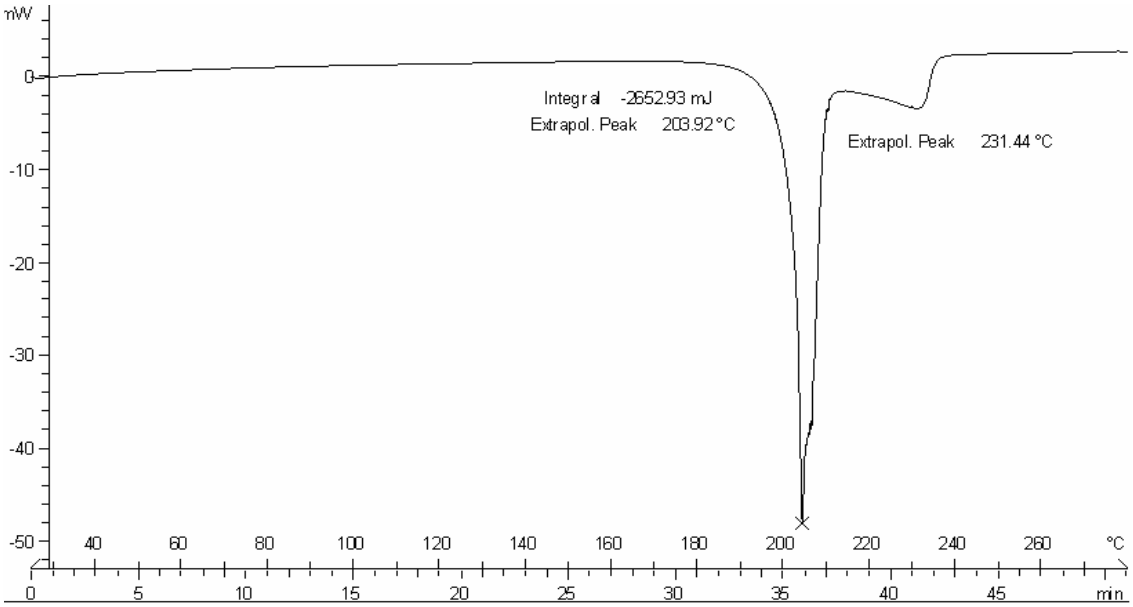


Figure A1.2 DSC curve of heat flow (mW) vs. temperature (°C) for tetragonal GABA from 30 to 280°C.

1.1.3.) Additional Crystallographic Data- Hexagonal GABA Solvate

Table A1.1.1: Fractional atomic coordinates and isotropic or equivalent isotropic displacement parameters for the hexagonal GABA solvate (Å^2).

	x	*y*	*z*	U_{iso}*/U_{eq}	Occ. (<1)
C1	0.2522 (3)	0.2905 (3)	0.8922 (5)	0.0312 (9)	
H4	0.2481	0.3477	0.9199	0.037*	
H5	0.1882	0.2340	0.9057	0.037*	
C2	0.2856 (3)	0.2967 (3)	0.7108 (4)	0.0316 (9)	
H6	0.3489	0.3543	0.6984	0.038*	
H7	0.2928	0.2409	0.6868	0.038*	
C1X	0.056 (3)	0.097 (3)	1.123 (8)	0.17 (2)*	0.36 (5)
C3	0.2179 (3)	0.3005 (3)	0.5831 (5)	0.0359 (9)	
H8	0.2119	0.3572	0.6060	0.043*	
H9	0.1543	0.2437	0.5978	0.043*	
C2X	0.0000	0.0000	0.54 (2)	0.200*	0.24 (5)
C4	0.2489 (3)	0.3045 (3)	0.4013 (4)	0.0316 (9)	
C3X	−0.007 (4)	0.035 (4)	0.729 (10)	0.200*	0.34 (3)
C5	0.5796 (3)	0.4242 (3)	0.4086 (4)	0.0332 (10)	
H13	0.6415	0.4281	0.4303	0.040*	
H14	0.5870	0.4875	0.4304	0.040*	
C6	0.5510 (3)	0.3965 (3)	0.2262 (5)	0.0335 (9)	
H15	0.5330	0.3290	0.2113	0.040*	
H16	0.4941	0.4019	0.2023	0.040*	
C5X	0.008 (5)	−0.061 (5)	0.577 (13)	0.200*	0.28 (4)
C7	0.6280 (3)	0.4563 (3)	0.0991 (5)	0.0408 (10)	
H17	0.6828	0.4466	0.1180	0.049*	
H18	0.6499	0.5241	0.1213	0.049*	

C8	0.5999 (3)	0.4365 (3)	−0.0850 (4)	0.0298 (8)	
N1	0.3213 (2)	0.2831 (2)	1.0076 (3)	0.0310 (8)	
H1	0.3817	0.3271	0.9786	0.046*	
H2	0.3140	0.2241	1.0000	0.046*	
H3	0.3099	0.2938	1.1138	0.046*	
N2	0.5050 (2)	0.3517 (2)	0.5234 (3)	0.0304 (7)	
H10	0.5161	0.3747	0.6290	0.046*	
H11	0.5075	0.2971	0.5201	0.046*	
H12	0.4466	0.3396	0.4902	0.046*	
O1	0.1916 (2)	0.2972 (2)	0.2850 (3)	0.0501 (8)	
O2	0.33175 (17)	0.31598 (19)	0.3682 (3)	0.0360 (7)	
O3	0.51131 (19)	0.3909 (2)	−0.1237 (3)	0.0412 (7)	
O4	0.66632 (18)	0.46627 (19)	−0.1932 (3)	0.0398 (7)	
O5	−0.067 (10)	−0.027 (8)	0.639 (19)	0.200*	0.10 (2)

Note: (1) U_{eq} = Equivalent isotropic atomic displacement parameter; (2) Atoms C1X, C2X, C3X, C5X and O5 are isotropic as they are part of the disordered solvent.

Table A1.1.2: Atomic displacement parameters for the hexagonal GABA solvate(Å^2).

	U^{11}	U^{22}	U^{33}	U^{12}	U^{13}	U^{23}
C1	0.035 (2)	0.031 (2)	0.031 (2)	0.0193 (19)	−0.0010 (17)	−0.0013 (18)
C2	0.037 (2)	0.041 (2)	0.023 (2)	0.0241 (19)	0.0015 (18)	−0.0011 (18)
C3	0.038 (2)	0.053 (2)	0.027 (2)	0.030 (2)	0.0027 (18)	0.0018 (19)
C4	0.039 (2)	0.039 (2)	0.022 (2)	0.023 (2)	−0.0010 (18)	−0.0028 (18)
C5	0.031 (2)	0.038 (2)	0.025 (2)	0.0137 (18)	−0.0016 (18)	0.0014 (19)
C6	0.037 (2)	0.036 (2)	0.025 (2)	0.0172 (19)	0.0011 (18)	0.0010 (18)
C7	0.035 (2)	0.049 (2)	0.032 (2)	0.016 (2)	0.0013 (19)	−0.003 (2)
C8	0.039 (2)	0.034 (2)	0.0204 (19)	0.0207 (19)	−0.0013 (19)	−0.0001 (18)
N1	0.0414 (19)	0.0357 (17)	0.0204 (16)	0.0226 (15)	0.0021 (15)	−0.0005 (14)

N2	0.0335 (18)	0.0389 (17)	0.0235 (16)	0.0217 (15)	−0.0024 (14)	−0.0030 (16)
O1	0.0440 (17)	0.092 (2)	0.0259 (15)	0.0423 (17)	−0.0066 (14)	−0.0043 (15)
O2	0.0304 (14)	0.0570 (17)	0.0266 (13)	0.0262 (13)	0.0023 (12)	−0.0015 (13)
O3	0.0307 (16)	0.0583 (18)	0.0296 (15)	0.0185 (14)	−0.0020 (12)	−0.0023 (14)
O4	0.0345 (15)	0.0564 (18)	0.0264 (15)	0.0212 (13)	0.0035 (12)	0.0007 (13)

Table A1.1.3: Bond length parameters for the hexagonal GABA solvate (Å).

C1—N1	1.476 (4)	C3X—C1X^{vi}	1.42 (6)
C1—C2	1.510 (5)	C3X—O5^{v}	1.44 (11)
C1—H4	0.9700	C3X—C5X^{ii}	1.68 (9)
C1—H5	0.9700	C3X—C1X^{vii}	1.69 (6)
C2—C3	1.498 (5)	C5—N2	1.480 (4)
C2—H6	0.9700	C5—C6	1.505 (5)
C2—H7	0.9700	C5—H13	0.9700
C1X—C5X^{i}	1.07 (8)	C5—H14	0.9700
C1X—O5^{ii}	1.26 (13)	C6—C7	1.497 (5)
C1X—C3X^{ii}	1.42 (6)	C6—H15	0.9700
C1X—C2X^{i}	1.50 (9)	C6—H16	0.9700
C1X—C3X^{iii}	1.69 (6)	C5X—C1X^{ix}	1.07 (8)
C1X—O5^{iv}	1.86 (12)	C5X—C3X^{v}	1.27 (11)
C3—C4	1.505 (5)	C5X—O5^{v}	1.34 (12)
C3—H8	0.9700	C5X—O5	1.62 (14)
C3—H9	0.9700	C5X—C3X^{vi}	1.68 (8)
C2X—C5X^{v}	1.09 (7)	C7—C8	1.503 (5)
C2X—C5X	1.09 (7)	C7—H17	0.9700
C2X—O5^{v}	1.21 (15)	C7—H18	0.9700
C2X—O5	1.21 (15)	C8—O4	1.252 (4)
C2X—C3X^{vi}	1.31 (13)	C8—O3	1.259 (5)
C2X—C3X^{vii}	1.31 (13)	N1—H1	0.8900

C2X—C1X^{viii}	1.50 (9)	N1—H2	0.8900
C2X—C1X^{ix}	1.50 (9)	N1—H3	0.8900
C2X—C3X	1.61 (15)	N2—H10	0.8900
C2X—C3X^{v}	1.61 (15)	N2—H11	0.8900
C4—O1	1.257 (4)	N2—H12	0.8900
C4—O2	1.265 (4)	O5—C1X^{vi}	1.26 (13)
C3X—O5	1.21 (11)	O5—C5X^{v}	1.34 (12)
C3X—C3X^{v}	1.26 (8)	O5—C3X^{v}	1.44 (11)
C3X—C5X^{v}	1.27 (11)	O5—C1X^{viii}	1.86 (12)
C3X—C2X^{ii}	1.31 (13)		

Symmetry codes: (i) −*y*, *x*−*y*, *z*+2/3; (ii) −*x*+*y*, −*x*, *z*+1/3; (iii) *x*−*y*, *x*, *z*+1/3; (iv) *y*, −*x*+*y*, *z*+2/3; (v) −*x*, −*y*, *z*; (vi) −*y*, *x*−*y*, *z*−1/3; (vii) *y*, −*x*+*y*, *z*−1/3; (viii) *x*−*y*, *x*, *z*−2/3; (ix) −*x*+*y*, −*x*, *z*−2/3.

Table A1.1.4: Bond angle parameters for the hexagonal GABA solvate (°).

N1—C1—C2	109.6 (3)	C5X^{v}—C3X—O5^{v}	73 (6)
N1—C1—H4	109.7	C2X^{ii}—C3X—O5^{v}	98 (7)
C2—C1—H4	109.7	C1X^{vi}—C3X—O5^{v}	127 (7)
N1—C1—H5	109.7	O5—C3X—C2X	48 (7)
C2—C1—H5	109.7	C3X^{v}—C3X—C2X	67 (2)
H4—C1—H5	108.2	C5X^{v}—C3X—C2X	42 (4)
C3—C2—C1	113.6 (3)	C2X^{ii}—C3X—C2X	128 (3)
C3—C2—H6	108.8	C1X^{vi}—C3X—C2X	103 (4)
C1—C2—H6	108.8	O5^{v}—C3X—C2X	46 (6)
C3—C2—H7	108.8	O5—C3X—C5X^{ii}	96 (8)
C1—C2—H7	108.8	C3X^{v}—C3X—C5X^{ii}	88 (4)
H6—C2—H7	107.7	C5X^{v}—C3X—C5X^{ii}	147 (7)
C5X^{i}—C1X—O5^{ii}	136 (9)	C2X^{ii}—C3X—C5X^{ii}	40 (3)
C5X^{i}—C1X—C3X^{ii}	83 (5)	C1X^{vi}—C3X—C5X^{ii}	39 (3)

O5^{ii}—C1X—C3X^{ii}	53 (6)	O5^{v}—C3X—C5X^{ii}	136 (6)
C5X^{i}—C1X—C2X^{i}	46 (6)	C2X—C3X—C5X^{ii}	140 (5)
O5^{ii}—C1X—C2X^{i}	97 (10)	O5—C3X—C1X^{vii}	124 (7)
C3X^{ii}—C1X—C2X^{i}	53 (5)	C3X^{v}—C3X—C1X^{vii}	55 (3)
C5X^{i}—C1X—C3X^{iii}	94 (6)	C5X^{v}—C3X—C1X^{vii}	115 (4)
O5^{ii}—C1X—C3X^{iii}	56 (6)	C2X^{ii}—C3X—C1X^{vii}	58 (4)
C3X^{ii}—C1X—C3X^{iii}	47 (3)	C1X^{vi}—C3X—C1X^{vii}	120 (5)
C2X^{i}—C1X—C3X^{iii}	48 (5)	O5^{v}—C3X—C1X^{vii}	46 (6)
C5X^{i}—C1X—O5^{iv}	45 (6)	C2X—C3X—C1X^{vii}	92 (3)
O5^{ii}—C1X—O5^{iv}	126 (8)	C5X^{ii}—C3X—C1X^{vii}	98 (5)
C3X^{ii}—C1X—O5^{iv}	93 (6)	N2—C5—C6	110.4 (3)
C2X^{i}—C1X—O5^{iv}	41 (5)	N2—C5—H13	109.6
C3X^{iii}—C1X—O5^{iv}	70 (5)	C6—C5—H13	109.6
C2—C3—C4	114.4 (3)	N2—C5—H14	109.6
C2—C3—H8	108.7	C6—C5—H14	109.6
C4—C3—H8	108.7	H13—C5—H14	108.1
C2—C3—H9	108.7	C7—C6—C5	114.9 (3)
C4—C3—H9	108.7	C7—C6—H15	108.6
H8—C3—H9	107.6	C5—C6—H15	108.6
C5X^{v}—C2X—C5X	150 (10)	C7—C6—H16	108.6
C5X^{v}—C2X—O5^{v}	89 (10)	C5—C6—H16	108.6
C5X—C2X—O5^{v}	71 (7)	H15—C6—H16	107.5
C5X^{v}—C2X—O5	71 (7)	C1X^{ix}—C5X—C2X	88 (10)
C5X—C2X—O5	89 (10)	C1X^{ix}—C5X—C3X^{v}	154 (8)
O5^{v}—C2X—O5	101 (10)	C2X—C5X—C3X^{v}	86 (10)
C5X^{v}—C2X—C3X^{vi}	119 (10)	C1X^{ix}—C5X—O5^{v}	100 (8)
C5X—C2X—C3X^{vi}	89 (8)	C2X—C5X—O5^{v}	59 (7)
O5^{v}—C2X—C3X^{vi}	145 (10)	C3X^{v}—C5X—O5^{v}	55 (6)
O5—C2X—C3X^{vi}	107 (6)	C1X^{ix}—C5X—O5	131 (9)
C5X^{v}—C2X—C3X^{vii}	89 (8)	C2X—C5X—O5	48 (8)

C5X—C2X—C3X^{vii}	119 (10)	C3X^{v}—C5X—O5	59 (6)
O5^{v}—C2X—C3X^{vii}	107 (6)	O5^{v}—C5X—O5	78 (10)
O5—C2X—C3X^{vii}	145 (10)	C1X^{ix}—C5X—C3X^{vi}	57 (5)
C3X^{vi}—C2X—C3X^{vii}	58 (8)	C2X—C5X—C3X^{vi}	51 (8)
C5X^{v}—C2X—C1X^{viii}	45 (5)	C3X^{v}—C5X—C3X^{vi}	133 (6)
C5X—C2X—C1X^{viii}	159 (9)	O5^{v}—C5X—C3X^{vi}	105 (7)
O5^{v}—C2X—C1X^{viii}	130 (6)	O5—C5X—C3X^{vi}	76 (6)
O5—C2X—C1X^{viii}	86 (5)	C6—C7—C8	116.7 (3)
C3X^{vi}—C2X—C1X^{viii}	74 (8)	C6—C7—H17	108.1
C3X^{vii}—C2X—C1X^{viii}	60 (6)	C8—C7—H17	108.1
C5X^{v}—C2X—C1X^{ix}	159 (9)	C6—C7—H18	108.1
C5X—C2X—C1X^{ix}	45 (5)	C8—C7—H18	108.1
O5^{v}—C2X—C1X^{ix}	86 (5)	H17—C7—H18	107.3
O5—C2X—C1X^{ix}	130 (6)	O4—C8—O3	122.9 (3)
C3X^{vi}—C2X—C1X^{ix}	60 (6)	O4—C8—C7	118.1 (3)
C3X^{vii}—C2X—C1X^{ix}	74 (8)	O3—C8—C7	118.9 (3)
C1X^{viii}—C2X—C1X^{ix}	127 (10)	C1—N1—H1	109.5
C5X^{v}—C2X—C3X	52 (9)	C1—N1—H2	109.5
C5X—C2X—C3X	98 (10)	H1—N1—H2	109.5
O5^{v}—C2X—C3X	60 (10)	C1—N1—H3	109.5
O5—C2X—C3X	48 (9)	H1—N1—H3	109.5
C3X^{vi}—C2X—C3X	154 (2)	H2—N1—H3	109.5
C3X^{vii}—C2X—C3X	135 (3)	C5—N2—H10	109.5
C1X^{viii}—C2X—C3X	94 (5)	C5—N2—H11	109.5
C1X^{ix}—C2X—C3X	138 (8)	H10—N2—H11	109.5
C5X^{v}—C2X—C3X^{v}	98 (10)	C5—N2—H12	109.5
C5X—C2X—C3X^{v}	52 (9)	H10—N2—H12	109.5
O5^{v}—C2X—C3X^{v}	48 (9)	H11—N2—H12	109.5
O5—C2X—C3X^{v}	60 (10)	C3X—O5—C2X	84 (10)
C3X^{vi}—C2X—C3X^{v}	135 (3)	C3X—O5—C1X^{vi}	70 (8)

C3X^{vii}—C2X—C3X^{v}	154 (2)	C2X—O5—C1X^{vi}	149 (10)
C1X^{viii}—C2X—C3X^{v}	138 (8)	C3X—O5—C5X^{v}	60 (7)
C1X^{ix}—C2X—C3X^{v}	94 (5)	C2X—O5—C5X^{v}	50 (6)
C3X—C2X—C3X^{v}	46 (5)	C1X^{vi}—O5—C5X^{v}	123 (10)
O1—C4—O2	121.3 (3)	C3X—O5—C3X^{v}	56 (8)
O1—C4—C3	118.9 (3)	C2X—O5—C3X^{v}	74 (10)
O2—C4—C3	119.9 (3)	C1X^{vi}—O5—C3X^{v}	77 (7)
O5—C3X—C3X^{v}	72 (7)	C5X^{v}—O5—C3X^{v}	96 (10)
O5—C3X—C5X^{v}	65 (7)	C3X—O5—C5X	93 (9)
C3X^{v}—C3X—C5X^{v}	109 (4)	C2X—O5—C5X	42 (6)
O5—C3X—C2X^{ii}	111 (8)	C1X^{vi}—O5—C5X	120 (9)
C3X^{v}—C3X—C2X^{ii}	61 (4)	C5X^{v}—O5—C5X	90 (9)
C5X^{v}—C3X—C2X^{ii}	170 (6)	C3X^{v}—O5—C5X	48 (5)
O5—C3X—C1X^{vi}	56 (7)	C3X—O5—C1X^{viii}	94 (8)
C3X^{v}—C3X—C1X^{vi}	78 (5)	C2X—O5—C1X^{viii}	54 (6)
C5X^{v}—C3X—C1X^{vi}	115 (7)	C1X^{vi}—O5—C1X^{viii}	142 (8)
C2X^{ii}—C3X—C1X^{vi}	67 (3)	C5X^{v}—O5—C1X^{viii}	35 (5)
O5—C3X—O5^{v}	89 (10)	C3X^{v}—O5—C1X^{viii}	123 (10)
C3X^{v}—C3X—O5^{v}	52 (4)	C5X—O5—C1X^{viii}	94 (7)

Symmetry codes: (i) $-y, x-y, z+2/3$; (ii) $-x+y, -x, z+1/3$; (iii) $x-y, x, z+1/3$; (iv) $y, -x+y, z+2/3$; (v) $-x, -y, z$; (vi) $-y, x-y, z-1/3$; (vii) $y, -x+y, z-1/3$; (viii) $x-y, x, z-2/3$; (ix) $-x+y, -x, z-2/3$.

Table A1.1.5: Torsion angle parameters for the hexagonal GABA solvate (°).

N1—C1—C2—C3	177.7 (3)	C1X^{vi}—C3X—O5—C2X	−163 (9)
C1—C2—C3—C4	−178.7 (3)	O5^{v}—C3X—O5—C2X	−25 (8)
C2—C3—C4—O1	172.4 (3)	C5X^{ii}—C3X—O5—C2X	−161 (4)
C2—C3—C4—O2	−8.3 (5)	C1X^{vii}—C3X—O5—C2X	−57 (10)
C5X^{v}—C2X—C3X—O5	99 (9)	C3X^{v}—C3X—O5—C1X^{vi}	87 (5)

C5X—C2X—C3X—O5	−82 (8)	C5X^{v}—C3X—O5—C1X^{vi}	−150 (8)
O5^{v}—C2X—C3X—O5	−145 (10)	C2X^{ii}—C3X—O5—C1X^{vi}	40 (8)
C3X^{vi}—C2X—C3X—O5	21 (10)	O5^{v}—C3X—O5—C1X^{vi}	138 (8)
C3X^{vii}—C2X—C3X—O5	131 (11)	C2X—C3X—O5—C1X^{vi}	163 (9)
C1X^{viii}—C2X—C3X—O5	81 (8)	C5X^{ii}—C3X—O5—C1X^{vi}	1(6)
C1X^{ix}—C2X—C3X—O5	−107 (10)	C1X^{vii}—C3X—O5—C1X^{vi}	105 (8)
C3X^{v}—C2X—C3X—O5	−85 (9)	C3X^{v}—C3X—O5—C5X^{v}	−122 (7)
C5X^{v}—C2X—C3X—C3X^{v}	−176 (8)	C2X^{ii}—C3X—O5—C5X^{v}	−170 (6)
C5X—C2X—C3X—C3X^{v}	3(6)	C1X^{vi}—C3X—O5—C5X^{v}	150 (8)
O5^{v}—C2X—C3X—C3X^{v}	−59 (6)	O5^{v}—C3X—O5—C5X^{v}	−72 (5)
O5—C2X—C3X—C3X^{v}	85 (9)	C2X—C3X—O5—C5X^{v}	−47 (7)
C3X^{vi}—C2X—C3X—C3X^{v}	106 (10)	C5X^{ii}—C3X—O5—C5X^{v}	152 (6)
C3X^{vii}—C2X—C3X—C3X^{v}	−143 (4)	C1X^{vii}—C3X—O5—C5X^{v}	−104 (7)
C1X^{viii}—C2X—C3X—C3X^{v}	166 (4)	C5X^{v}—C3X—O5—C3X^{v}	122 (7)
C1X^{ix}—C2X—C3X—C3X^{v}	−21 (7)	C2X^{ii}—C3X—O5—C3X^{v}	−47 (7)
C5X—C2X—C3X—C5X^{v}	179.2 (18)	C1X^{vi}—C3X—O5—C3X^{v}	−87 (5)
O5^{v}—C2X—C3X—C5X^{v}	117 (8)	O5^{v}—C3X—O5—C3X^{v}	50 (7)
O5—C2X—C3X—C5X^{v}	−99 (9)	C2X—C3X—O5—C3X^{v}	75 (7)
C3X^{vi}—C2X—C3X—C5X^{v}	−78 (13)	C5X^{ii}—C3X—O5—C3X^{v}	−86 (4)
C3X^{vii}—C2X—C3X—C5X^{v}	33 (8)	C1X^{vii}—C3X—O5—C3X^{v}	18 (9)
C1X^{viii}—C2X—C3X—C5X^{v}	−18 (6)	C3X^{v}—C3X—O5—C5X	−34 (5)
C1X^{ix}—C2X—C3X—C5X^{v}	155 (5)	C5X^{v}—C3X—O5—C5X	88 (8)
C3X^{v}—C2X—C3X—C5X^{v}	176 (8)	C2X^{ii}—C3X—O5—C5X	−81 (8)
C5X^{v}—C2X—C3X—C2X^{ii}	−176 (8)	C1X^{vi}—C3X—O5—C5X	−121 (8)
C5X—C2X—C3X—C2X^{ii}	3(6)	O5^{v}—C3X—O5—C5X	16 (9)
O5^{v}—C2X—C3X—C2X^{ii}	−59 (6)	C2X—C3X—O5—C5X	41 (6)
O5—C2X—C3X—C2X^{ii}	85 (9)	C5X^{ii}—C3X—O5—C5X	−120 (5)
C3X^{vi}—C2X—C3X—C2X^{ii}	106 (10)	C1X^{vii}—C3X—O5—C5X	−16 (11)
C3X^{vii}—C2X—C3X—C2X^{ii}	−143 (4)	C3X^{v}—C3X—O5—C1X^{viii}	−128 (7)
C1X^{viii}—C2X—C3X—C2X^{ii}	166 (4)	C5X^{v}—C3X—O5—C1X^{viii}	−6(4)

C1X^{ix}—C2X—C3X—C2X^{ii}	−21 (7)	C2X^{ii}—C3X—O5—C1X^{viii}	−176 (3)
C3X^{v}—C2X—C3X—C2X^{ii}	0.000 (17)	C1X^{vi}—C3X—O5—C1X^{viii}	145 (8)
C5X^{v}—C2X—C3X—C1X^{vi}	113 (6)	O5^{v}—C3X—O5—C1X^{viii}	−78 (5)
C5X—C2X—C3X—C1X^{vi}	−67 (5)	C2X—C3X—O5—C1X^{viii}	−53 (5)
O5^{v}—C2X—C3X—C1X^{vi}	−130 (8)	C5X^{ii}—C3X—O5—C1X^{viii}	146 (4)
O5—C2X—C3X—C1X^{vi}	15 (8)	C1X^{vii}—C3X—O5—C1X^{viii}	−110 (7)
C3X^{vi}—C2X—C3X—C1X^{vi}	36 (11)	C5X^{v}—C2X—O5—C3X	−55 (10)
C3X^{vii}—C2X—C3X—C1X^{vi}	146 (6)	C5X—C2X—O5—C3X	101 (8)
C1X^{viii}—C2X—C3X—C1X^{vi}	95 (3)	O5^{v}—C2X—O5—C3X	30 (4)
C1X^{ix}—C2X—C3X—C1X^{vi}	−92 (5)	C3X^{vi}—C2X—O5—C3X	−171 (4)
C3X^{v}—C2X—C3X—C1X^{vi}	−70 (4)	C3X^{vii}—C2X—O5—C3X	−112 (18)
C5X^{v}—C2X—C3X—O5^{v}	−117 (8)	C1X^{viii}—C2X—O5—C3X	−99 (8)
C5X—C2X—C3X—O5^{v}	62 (7)	C1X^{ix}—C2X—O5—C3X	124 (13)
O5—C2X—C3X—O5^{v}	145 (10)	C3X^{v}—C2X—O5—C3X	56 (7)
C3X^{vi}—C2X—C3X—O5^{v}	165 (14)	C5X^{v}—C2X—O5—C1X^{vi}	−88 (20)
C3X^{vii}—C2X—C3X—O5^{v}	−84 (6)	C5X—C2X—O5—C1X^{vi}	68 (17)
C1X^{viii}—C2X—C3X—O5^{v}	−135 (8)	O5^{v}—C2X—O5—C1X^{vi}	−3(14)
C1X^{ix}—C2X—C3X—O5^{v}	38 (8)	C3X^{vi}—C2X—O5—C1X^{vi}	156 (16)
C3X^{v}—C2X—C3X—O5^{v}	59 (6)	C3X^{vii}—C2X—O5—C1X^{vi}	−146 (19)
C5X^{v}—C2X—C3X—C5X^{ii}	129 (8)	C1X^{viii}—C2X—O5—C1X^{vi}	−132 (19)
C5X—C2X—C3X—C5X^{ii}	−52 (7)	C1X^{ix}—C2X—O5—C1X^{vi}	91 (23)
O5^{v}—C2X—C3X—C5X^{ii}	−114 (8)	C3X—C2X—O5—C1X^{vi}	−33 (15)
O5—C2X—C3X—C5X^{ii}	30 (8)	C3X^{v}—C2X—O5—C1X^{vi}	23 (15)
C3X^{vi}—C2X—C3X—C5X^{ii}	51 (11)	C5X—C2X—O5—C5X^{v}	156 (15)
C3X^{vii}—C2X—C3X—C5X^{ii}	162 (6)	O5^{v}—C2X—O5—C5X^{v}	86 (9)
C1X^{viii}—C2X—C3X—C5X^{ii}	111 (6)	C3X^{vi}—C2X—O5—C5X^{v}	−115 (11)
C1X^{ix}—C2X—C3X—C5X^{ii}	−76 (8)	C3X^{vii}—C2X—O5—C5X^{v}	−57 (14)
C3X^{v}—C2X—C3X—C5X^{ii}	−55 (5)	C1X^{viii}—C2X—O5—C5X^{v}	−44 (5)
C5X^{v}—C2X—C3X—C1X^{vii}	−126 (6)	C1X^{ix}—C2X—O5—C5X^{v}	179 (20)
C5X—C2X—C3X—C1X^{vii}	54 (4)	C3X—C2X—O5—C5X^{v}	55 (10)

O5^{v}—C2X—C3X—C1X^{vii}	−9(7)	C3X^{v}—C2X—O5—C5X^{v}	112 (10)
O5—C2X—C3X—C1X^{vii}	136 (9)	C5X^{v}—C2X—O5—C3X^{v}	−112 (10)
C3X^{vi}—C2X—C3X—C1X^{vii}	157 (11)	C5X—C2X—O5—C3X^{v}	45 (8)
C3X^{vii}—C2X—C3X—C1X^{vii}	−93 (5)	O5^{v}—C2X—O5—C3X^{v}	−26 (3)
C1X^{viii}—C2X—C3X—C1X^{vii}	−144 (2)	C3X^{vi}—C2X—O5—C3X^{v}	133 (5)
C1X^{ix}—C2X—C3X—C1X^{vii}	29 (4)	C3X^{vii}—C2X—O5—C3X^{v}	−169 (14)
C3X^{v}—C2X—C3X—C1X^{vii}	51 (4)	C1X^{viii}—C2X—O5—C3X^{v}	−156 (6)
N2—C5—C6—C7	−171.1 (3)	C1X^{ix}—C2X—O5—C3X^{v}	67 (16)
C5X^{v}—C2X—C5X—C1X^{ix}	−156 (5)	C3X—C2X—O5—C3X^{v}	−56 (7)
O5^{v}—C2X—C5X—C1X^{ix}	−103 (10)	C5X^{v}—C2X—O5—C5X	−156 (15)
O5—C2X—C5X—C1X^{ix}	155 (11)	O5^{v}—C2X—O5—C5X	−70 (8)
C3X^{vi}—C2X—C5X—C1X^{ix}	48 (6)	C3X^{vi}—C2X—O5—C5X	88 (5)
C3X^{vii}—C2X—C5X—C1X^{ix}	−3(9)	C3X^{vii}—C2X—O5—C5X	147 (21)
C1X^{viii}—C2X—C5X—C1X^{ix}	79 (41)	C1X^{viii}—C2X—O5—C5X	160 (12)
C3X—C2X—C5X—C1X^{ix}	−157 (4)	C1X^{ix}—C2X—O5—C5X	23 (10)
C3X^{v}—C2X—C5X—C1X^{ix}	−154 (7)	C3X—C2X—O5—C5X	−101 (8)
C5X^{v}—C2X—C5X—C3X^{v}	−2(3)	C3X^{v}—C2X—O5—C5X	−45 (8)
O5^{v}—C2X—C5X—C3X^{v}	51 (9)	C5X^{v}—C2X—O5—C1X^{viii}	44 (5)
O5—C2X—C5X—C3X^{v}	−50 (10)	C5X—C2X—O5—C1X^{viii}	−160 (12)
C3X^{vi}—C2X—C5X—C3X^{v}	−158 (6)	O5^{v}—C2X—O5—C1X^{viii}	130 (6)
C3X^{vii}—C2X—C5X—C3X^{v}	151 (7)	C3X^{vi}—C2X—O5—C1X^{viii}	−71 (8)
C1X^{viii}—C2X—C5X—C3X^{v}	−127 (39)	C3X^{vii}—C2X—O5—C1X^{viii}	−13 (13)
C1X^{ix}—C2X—C5X—C3X^{v}	154 (7)	C1X^{ix}—C2X—O5—C1X^{viii}	−137 (18)
C3X—C2X—C5X—C3X^{v}	−3(6)	C3X—C2X—O5—C1X^{viii}	99 (8)
C5X^{v}—C2X—C5X—O5^{v}	−53 (9)	C3X^{v}—C2X—O5—C1X^{viii}	156 (6)
O5—C2X—C5X—O5^{v}	−101 (18)	C1X^{ix}—C5X—O5—C3X	−111 (10)
C3X^{vi}—C2X—C5X—O5^{v}	151 (12)	C2X—C5X—O5—C3X	−78 (12)
C3X^{vii}—C2X—C5X—O5^{v}	100 (6)	C3X^{v}—C5X—O5—C3X	38 (7)
C1X^{viii}—C2X—C5X—O5^{v}	−178 (45)	O5^{v}—C5X—O5—C3X	−18 (11)
C1X^{ix}—C2X—C5X—O5^{v}	103 (10)	C3X^{vi}—C5X—O5—C3X	−128 (7)

C3X—C2X—C5X—O5^{v}	−54 (9)	C1X^{ix}—C5X—O5—C2X	−34 (14)
C3X^{v}—C2X—C5X—O5^{v}	−51 (9)	C3X^{v}—C5X—O5—C2X	116 (13)
C5X^{v}—C2X—C5X—O5	49 (9)	O5^{v}—C5X—O5—C2X	59 (13)
O5^{v}—C2X—C5X—O5	101 (18)	C3X^{vi}—C5X—O5—C2X	−50 (10)
C3X^{vi}—C2X—C5X—O5	−107 (7)	C1X^{ix}—C5X—O5—C1X^{vi}	180 (8)
C3X^{vii}—C2X—C5X—O5	−159 (15)	C2X—C5X—O5—C1X^{vi}	−146 (18)
C1X^{viii}—C2X—C5X—O5	−76 (34)	C3X^{v}—C5X—O5—C1X^{vi}	−31 (8)
C1X^{ix}—C2X—C5X—O5	−155 (11)	O5^{v}—C5X—O5—C1X^{vi}	−87 (9)
C3X—C2X—C5X—O5	47 (9)	C3X^{vi}—C5X—O5—C1X^{vi}	164 (11)
C3X^{v}—C2X—C5X—O5	50 (10)	C1X^{ix}—C5X—O5—C5X^{v}	−52 (13)
C5X^{v}—C2X—C5X—C3X^{vi}	156 (4)	C2X—C5X—O5—C5X^{v}	−18 (12)
O5^{v}—C2X—C5X—C3X^{vi}	−151 (12)	C3X^{v}—C5X—O5—C5X^{v}	98 (10)
O5—C2X—C5X—C3X^{vi}	107 (7)	O5^{v}—C5X—O5—C5X^{v}	41 (13)
C3X^{vii}—C2X—C5X—C3X^{vi}	−51 (10)	C3X^{vi}—C5X—O5—C5X^{v}	−68 (6)
C1X^{viii}—C2X—C5X—C3X^{vi}	31 (38)	C1X^{ix}—C5X—O5—C3X^{v}	−150 (10)
C1X^{ix}—C2X—C5X—C3X^{vi}	−48 (6)	C2X—C5X—O5—C3X^{v}	−116 (13)
C3X—C2X—C5X—C3X^{vi}	155 (3)	O5^{v}—C5X—O5—C3X^{v}	−56 (6)
C3X^{v}—C2X—C5X—C3X^{vi}	158(6)	C3X^{vi}—C5X—O5—C3X^{v}	−166 (7)
C5—C6—C7—C8	−175.2 (3)	C1X^{ix}—C5X—O5—C1X^{viii}	−18 (13)
C6—C7—C8—O4	−162.5 (3)	C2X—C5X—O5—C1X^{viii}	16 (10)
C6—C7—C8—O3	17.4 (6)	C3X^{v}—C5X—O5—C1X^{viii}	132 (8)
C3X^{v}—C3X—O5—C2X	−75 (7)	O5^{v}—C5X—O5—C1X^{viii}	76 (10)
C5X^{v}—C3X—O5—C2X	47 (7)	C3X^{vi}—C5X—O5—C1X^{viii}	−34 (4)
C2X^{ii}—C3X—O5—C2X	−123 (4)		

Symmetry codes: (i) −*y*, *x*−*y*, *z*+2/3; (ii) −*x*+*y*, −*x*, *z*+1/3; (iii) *x*−*y*, *x*, *z*+1/3; (iv) *y*, −*x*+*y*, *z*+2/3; (v) −*x*, −*y*, *z*; (vi) −*y*, *x*−*y*, *z*−1/3; (vii) *y*, −*x*+*y*, *z*−1/3; (viii) *x*−*y*, *x*, *z*−2/3; (ix) −*x*+*y*, −*x*, *z*−2/3.

Table A1.1.6: Hydrogen bonding parameters for the hexagonal GABA solvate (Å,°).

D*—H···*A	***D*—H**	**H···*A***	***D*···*A***	***D*—H···*A***
N1—H2···O1^{iv}	0.89	1.81	2.690 (4)	172
N1—H3···O2^{x}	0.89	2.03	2.878 (3)	158
N1—H3···O1^{x}	0.89	2.34	3.091 (4)	142
N1—H1···O3^{x}	0.89	1.96	2.823 (4)	163
N2—H10···O3^{x}	0.89	1.97	2.840 (4)	165
N2—H10···O4^{x}	0.89	2.51	3.197 (4)	134
N2—H11···O4^{xi}	0.89	1.83	2.701 (4)	166
N2—H12···O2	0.89	1.93	2.803 (4)	167

Symmetry codes: (iv) y, $-x+y$, $z+2/3$; (x) x, y, $z+1$; (xi) $-y+1$, $x-y$, $z+2/3$.

1.2 Gabapentin

1.2.1) DSC α-gabapentin

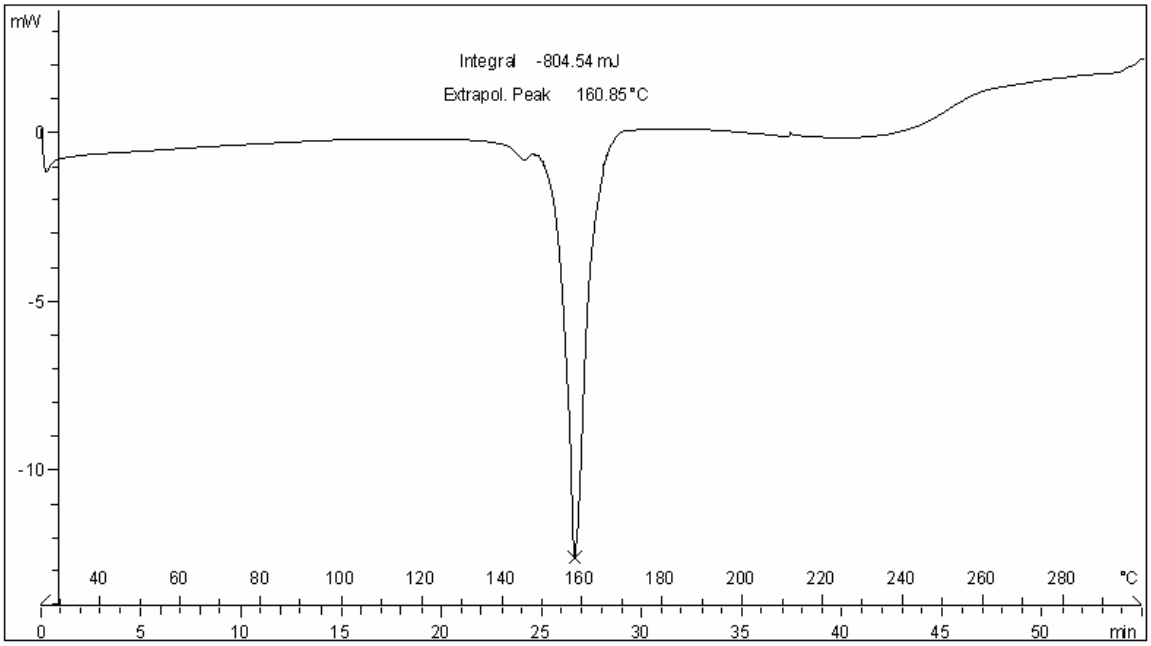


Figure A1.3: DSC curve of heat flow (mW) vs. temperature (°C) for α-gabapentin from 30 to 300°C.

1.2.2 Additional Crystallographic Data: β- and γ-gabapentin

1.2.2A β-gabapentin

Table A1.2.1: Fractional atomic coordinates and isotropic or equivalent isotropic displacement parameters for β-gabapentin (Å^2).

	x	*y*	*z*	U_{iso}*/U_{eq}
C2	0.10437 (13)	0.2698 (3)	0.47078 (19)	0.0237 (4)
C3	0.17104 (12)	0.1189 (3)	0.56450 (18)	0.0210 (4)
H1	0.1329	0.0230	0.6039	0.025*
H2	0.2148	0.1912	0.6446	0.025*
C4	0.16677 (12)	−0.0743 (3)	0.34216 (18)	0.0233 (4)
H3	0.1456	0.0435	0.2796	0.028*
H4	0.2053	−0.1615	0.2971	0.028*
C1	0.23067 (12)	0.0001 (3)	0.48329 (18)	0.0191 (4)

C5	0.28098 (12)	−0.1785 (3)	0.57268 (18)	0.0227 (4)
H7	0.2325	−0.2632	0.5990	0.027*
H8	0.3124	−0.2621	0.5150	0.027*
C7	0.35531 (13)	−0.1127 (3)	0.70615 (19)	0.0276 (5)
H9	0.3237	−0.0369	0.7675	0.033*
H10	0.3861	−0.2331	0.7588	0.033*
C8	0.43075 (13)	0.0192 (3)	0.6708 (2)	0.0365 (5)
H11	0.4678	−0.0620	0.6198	0.044*
H12	0.4755	0.0685	0.7595	0.044*
C9	0.38609 (12)	0.1983 (3)	0.5799 (2)	0.0318 (5)
H13	0.4365	0.2720	0.5501	0.038*
H14	0.3585	0.2915	0.6369	0.038*
C6	0.30796 (12)	0.1340 (3)	0.44909 (19)	0.0256 (4)
H5	0.3377	0.0596	0.3848	0.031*
H6	0.2771	0.2561	0.3987	0.031*
N1	0.08083 (10)	−0.1887 (2)	0.35151 (15)	0.0231 (4)
H15	0.0438	−0.1090	0.3904	0.035*
H16	0.0994	−0.2998	0.4065	0.035*
H17	0.0467	−0.2274	0.2633	0.035*
O1	0.01899 (8)	0.21326 (19)	0.41666 (13)	0.0272 (3)
O2	0.13809 (10)	0.4345 (2)	0.44863 (17)	0.0460 (4)

Table A1.2.2: Atomic displacement parameters for β-gabapentin (Å^2).

	U^{11}	U^{22}	U^{33}	U^{12}	U^{13}	U^{23}
C2	0.0269 (10)	0.0189 (11)	0.0256 (10)	0.0027 (9)	0.0076 (9)	−0.0044 (9)
C3	0.0203 (9)	0.0222 (10)	0.0199 (9)	−0.0010 (8)	0.0042 (8)	−0.0024 (8)
C4	0.0236 (9)	0.0254 (11)	0.0221 (10)	−0.0021 (8)	0.0080 (9)	−0.0004 (9)
C1	0.0204 (9)	0.0184 (10)	0.0187 (9)	−0.0006 (8)	0.0056 (8)	0.0014 (8)

C5	0.0228 (9)	0.0210 (11)	0.0250 (10)	0.0011 (8)	0.0075 (8)	0.0027 (9)
C7	0.0232 (9)	0.0288 (12)	0.0285 (11)	0.0020 (8)	0.0030 (9)	0.0054 (9)
C8	0.0238 (10)	0.0419 (14)	0.0393 (13)	−0.0034 (10)	0.0010 (10)	0.0051 (11)
C9	0.0261 (10)	0.0347 (13)	0.0341 (11)	−0.0093 (9)	0.0071 (10)	0.0037 (10)
C6	0.0241 (10)	0.0275 (11)	0.0266 (10)	−0.0017 (8)	0.0093 (9)	0.0034 (9)
N1	0.0223 (8)	0.0224 (9)	0.0238 (8)	−0.0001 (7)	0.0048 (7)	−0.0028 (7)
O1	0.0211 (6)	0.0296 (8)	0.0282 (7)	0.0020 (6)	0.0023 (6)	0.0032 (6)
O2	0.0380 (8)	0.0197 (8)	0.0761 (12)	−0.0020 (7)	0.0085 (8)	0.0084 (8)

Table A1.2.3: Bond lengths of β-gabapentin (Å).

C2—O2	1.241 (2)	C7—C8	1.516 (2)
C2—O1	1.266 (2)	C7—H9	0.9900
C2—C3	1.517 (2)	C7—H10	0.9900
C3—C1	1.546 (2)	C8—C9	1.521 (3)
C3—H1	0.9900	C8—H11	0.9900
C3—H2	0.9900	C8—H12	0.9900
C4—N1	1.486 (2)	C9—C6	1.525 (2)
C4—C1	1.525 (2)	C9—H13	0.9900
C4—H3	0.9900	C9—H14	0.9900
C4—H4	0.9900	C6—H5	0.9900
C1—C5	1.536 (2)	C6—H6	0.9900
C1—C6	1.540 (2)	N1—H15	0.9100
C5—C7	1.518 (2)	N1—H16	0.9100
C5—H7	0.9900	N1—H17	0.9100
C5—H8	0.9900		

Table A1.2.4: Bond angles of β-gabapentin (°).

O2—C2—O1	125.16 (17)	C5—C7—H9	109.5
O2—C2—C3	118.05 (16)	C8—C7—H10	109.5
O1—C2—C3	116.72 (16)	C5—C7—H10	109.5
C2—C3—C1	112.20 (14)	H9—C7—H10	108.1
C2—C3—H1	109.2	C7—C8—C9	111.49 (15)
C1—C3—H1	109.2	C7—C8—H11	109.3
C2—C3—H2	109.2	C9—C8—H11	109.3
C1—C3—H2	109.2	C7—C8—H12	109.3
H1—C3—H2	107.9	C9—C8—H12	109.3
N1—C4—C1	114.93 (13)	H11—C8—H12	108.0
N1—C4—H3	108.5	C8—C9—C6	112.13 (16)
C1—C4—H3	108.5	C8—C9—H13	109.2
N1—C4—H4	108.5	C6—C9—H13	109.2
C1—C4—H4	108.5	C8—C9—H14	109.2
H3—C4—H4	107.5	C6—C9—H14	109.2
C4—C1—C5	110.30 (15)	H13—C9—H14	107.9
C4—C1—C6	106.66 (13)	C9—C6—C1	113.34 (15)
C5—C1—C6	107.97 (14)	C9—C6—H5	108.9
C4—C1—C3	110.32 (14)	C1—C6—H5	108.9
C5—C1—C3	110.13 (14)	C9—C6—H6	108.9
C6—C1—C3	111.38 (15)	C1—C6—H6	108.9
C7—C5—C1	112.80 (15)	H5—C6—H6	107.7
C7—C5—H7	109.0	C4—N1—H15	109.5
C1—C5—H7	109.0	C4—N1—H16	109.5
C7—C5—H8	109.0	H15—N1—H16	109.5
C1—C5—H8	109.0	C4—N1—H17	109.5
H7—C5—H8	107.8	H15—N1—H17	109.5
C8—C7—C5	110.86 (15)	H16—N1—H17	109.5
C8—C7—H9	109.5		

Table A1.2.5: Torsion angles of β-gabapentin (°).

O2—C2—C3—C1	−81.3 (2)	C6—C1—C5—C7	56.37 (18)
O1—C2—C3—C1	95.97 (18)	C3—C1—C5—C7	−65.44 (18)
N1—C4—C1—C5	69.42 (18)	C1—C5—C7—C8	−58.3 (2)
N1—C4—C1—C6	−173.57 (14)	C5—C7—C8—C9	54.7 (2)
N1—C4—C1—C3	−52.5 (2)	C7—C8—C9—C6	−52.5 (2)
C2—C3—C1—C4	−46.4 (2)	C8—C9—C6—C1	53.3 (2)
C2—C3—C1—C5	−168.37 (14)	C4—C1—C6—C9	−172.22 (15)
C2—C3—C1—C6	71.87 (18)	C5—C1—C6—C9	−53.7 (2)
C4—C1—C5—C7	172.56 (13)	C3—C1—C6—C9	67.35 (19)

Table A1.2.6: Hydrogen bonding parameters of β-gabapentin (Å, °).

D*—H···*A	***D*—H**	**H···*A***	***D*···*A***	***D*—H···*A***
N1—H15···O1	0.91	2.19	2.9398 (19)	139
N1—H15···O1^{i}	0.91	2.42	3.0242 (18)	124
N1—H16···O2^{ii}	0.91	1.86	2.723 (2)	157
N1—H17···O1^{iii}	0.91	1.81	2.7174 (19)	176

Symmetry codes: (i) −*x*, −*y*, −*z*+1; (ii) *x*, *y*−1, *z*; (iii) −*x*, *y*−1/2, −*z*+1/2

1.2.2B : γ-gabapentin

Table A1.2.7: Fractional atomic coordinates and isotropic or equivalent isotropic displacement parameters for γ-gabapentin (Å^2).

	x	*y*	*z*	U_{iso}*/U_{eq}
C1	0.36190 (5)	0.2176 (3)	0.72157 (14)	0.0310 (3)
C2	0.30226 (5)	0.2639 (3)	0.48949 (14)	0.0311 (3)
C3	0.32851 (6)	0.1096 (3)	0.59961 (14)	0.0334 (4)
H3	0.3463	0.0014	0.5648	0.040*
H4	0.3056	0.0210	0.6265	0.040*
C4	0.33683 (5)	0.3708 (3)	0.79133 (15)	0.0331 (4)
H1	0.3587	0.4123	0.8767	0.040*
H2	0.3279	0.5115	0.7406	0.040*
C5	0.39772 (6)	0.3621 (3)	0.68455 (18)	0.0433 (4)
H5	0.4101	0.2736	0.6257	0.052*
H6	0.3821	0.4966	0.6365	0.052*
C6	0.38743 (6)	0.0247 (3)	0.81054 (16)	0.0389 (4)
H13	0.3651	−0.0573	0.8432	0.047*
H14	0.3991	−0.0827	0.7586	0.047*
C7	0.43791 (7)	0.4397 (4)	0.8004 (2)	0.0576 (5)
H7	0.4604	0.5230	0.7691	0.069*
H8	0.4263	0.5439	0.8542	0.069*
C8	0.46176 (7)	0.2409 (4)	0.8823 (2)	0.0649 (6)
H9	0.4763	0.1451	0.8314	0.078*
H10	0.4864	0.2968	0.9592	0.078*
C9	0.42760 (7)	0.1015 (4)	0.92549 (18)	0.0530 (5)
H11	0.4157	0.1925	0.9845	0.064*
H12	0.4435	−0.0322	0.9739	0.064*
N1	0.29507 (4)	0.2717 (2)	0.81185 (12)	0.0332 (3)

H15	0.2711	0.2793	0.7369	0.050*
H16	0.2879	0.3501	0.8748	0.050*
H17	0.3006	0.1249	0.8364	0.050*
O1	0.29105 (4)	0.1805 (2)	0.37705 (10)	0.0381 (3)
O2	0.29272 (4)	0.4596 (2)	0.51366 (11)	0.0418 (3)

Table A1.2.8: Atomic displacement parameters for γ-gabapentin (Å^2).

	U^{11}	U^{22}	U^{33}	U^{12}	U^{13}	U^{23}
C1	0.0362 (8)	0.0254 (7)	0.0307 (7)	0.0041 (6)	0.0093 (6)	0.0027 (6)
C2	0.0329 (8)	0.0308 (8)	0.0302 (7)	0.0003 (6)	0.0108 (6)	0.0034 (6)
C3	0.0449 (9)	0.0270 (8)	0.0289 (8)	0.0046 (6)	0.0122 (7)	0.0005 (6)
C4	0.0383 (8)	0.0261 (8)	0.0332 (8)	0.0011 (6)	0.0087 (6)	−0.0032 (6)
C5	0.0442 (9)	0.0379 (9)	0.0499 (10)	0.0016 (7)	0.0180 (8)	0.0069 (8)
C6	0.0438 (9)	0.0322 (8)	0.0385 (9)	0.0086 (7)	0.0099 (7)	0.0056 (7)
C7	0.0399 (10)	0.0500 (12)	0.0771 (14)	−0.0055 (9)	0.0102 (9)	0.0043 (11)
C8	0.0391 (10)	0.0626 (14)	0.0783 (15)	0.0056 (9)	−0.0026 (10)	0.0015 (12)
C9	0.0513 (11)	0.0503 (11)	0.0461 (11)	0.0142 (9)	−0.0006 (8)	0.0079 (9)
N1	0.0364 (7)	0.0308 (7)	0.0295 (6)	0.0048 (5)	0.0061 (5)	−0.0038 (5)
O1	0.0444 (7)	0.0380 (6)	0.0287 (6)	0.0000 (5)	0.0071 (5)	0.0001 (5)
O2	0.0570 (7)	0.0319 (6)	0.0369 (6)	0.0118 (5)	0.0154 (5)	0.0056 (5)

Table A1.2.9: Bond lengths of γ-gabapentin (Å).

C1—C4	1.534 (2)	C6—C9	1.521 (2)
C1—C3	1.537 (2)	C6—H13	0.9900
C1—C5	1.539 (2)	C6—H14	0.9900
C1—C6	1.542 (2)	C7—C8	1.518 (3)
C2—O2	1.2440 (19)	C7—H7	0.9900
C2—O1	1.2632 (19)	C7—H8	0.9900

C2—C3	1.520 (2)	C8—C9	1.517 (3)
C3—H3	0.9900	C8—H9	0.9900
C3—H4	0.9900	C8—H10	0.9900
C4—N1	1.484 (2)	C9—H11	0.9900
C4—H1	0.9900	C9—H12	0.9900
C4—H2	0.9900	N1—H15	0.9100
C5—C7	1.528 (3)	N1—H16	0.9100
C5—H5	0.9900	N1—H17	0.9100
C5—H6	0.9900		

Table A1.2.10: Bond angles of γ-gabapentin (°).

C4—C1—C3	112.05 (12)	C1—C6—H13	108.7
C4—C1—C5	107.87 (13)	C9—C6—H14	108.7
C3—C1—C5	109.82 (13)	C1—C6—H14	108.7
C4—C1—C6	111.14 (13)	H13—C6—H14	107.6
C3—C1—C6	107.51 (13)	C8—C7—C5	111.32 (17)
C5—C1—C6	108.42 (13)	C8—C7—H7	109.4
O2—C2—O1	124.01 (14)	C5—C7—H7	109.4
O2—C2—C3	119.65 (13)	C8—C7—H8	109.4
O1—C2—C3	116.34 (13)	C5—C7—H8	109.4
C2—C3—C1	118.21 (13)	H7—C7—H8	108.0
C2—C3—H3	107.8	C9—C8—C7	110.78 (16)
C1—C3—H3	107.8	C9—C8—H9	109.5
C2—C3—H4	107.8	C7—C8—H9	109.5
C1—C3—H4	107.8	C9—C8—H10	109.5
H3—C3—H4	107.1	C7—C8—H10	109.5
N1—C4—C1	115.27 (13)	H9—C8—H10	108.1
N1—C4—H1	108.5	C8—C9—C6	111.33 (16)

C1—C4—H1	108.5	C8—C9—H11	109.4
N1—C4—H2	108.5	C6—C9—H11	109.4
C1—C4—H2	108.5	C8—C9—H12	109.4
H1—C4—H2	107.5	C6—C9—H12	109.4
C7—C5—C1	113.85 (15)	H11—C9—H12	108.0
C7—C5—H5	108.8	C4—N1—H15	109.5
C1—C5—H5	108.8	C4—N1—H16	109.5
C7—C5—H6	108.8	H15—N1—H16	109.5
C1—C5—H6	108.8	C4—N1—H17	109.5
H5—C5—H6	107.7	H15—N1—H17	109.5
C9—C6—C1	114.37 (14)	H16—N1—H17	109.5
C9—C6—H13	108.7		

Table A1.2.11: Torsion angles of γ-gabapentin (°).

O2—C2—C3—C1	−29.1 (2)	C3—C1—C5—C7	−168.79 (15)
O1—C2—C3—C1	151.56 (14)	C6—C1—C5—C7	−51.60 (19)
C4—C1—C3—C2	63.47 (18)	C4—C1—C6—C9	−66.85 (19)
C5—C1—C3—C2	−56.38 (18)	C3—C1—C6—C9	170.20 (14)
C6—C1—C3—C2	−174.14 (14)	C5—C1—C6—C9	51.54 (19)
C3—C1—C4—N1	47.74 (17)	C1—C5—C7—C8	55.5 (2)
C5—C1—C4—N1	168.72 (13)	C5—C7—C8—C9	−55.8 (3)
C6—C1—C4—N1	−72.56 (17)	C7—C8—C9—C6	55.4 (2)
C4—C1—C5—C7	68.85 (18)	C1—C6—C9—C8	−55.0 (2)

Table A1.2.12: Hydrogen bonding parameters of γ-gabapentin (Å, °).

D—H···*A*	*D*—H	H···*A*	*D*···*A*	*D*—H···*A*
N1—H15···O1^{i}	0.91	1.93	2.7980 (16)	159
N1—H16···O2^{ii}	0.91	1.85	2.7324 (17)	161
N1—H17···O1^{iii}	0.91	1.91	2.7851 (18)	161

Symmetry codes: (i) −*x*+1/2, −*y*+1/2, −*z*+1; (ii) *x*, −*y*+1, *z*+1/2; (iii) *x*, −*y*, *z*+1/2

1.3 Co-crystals

1.3.1 GABA-oxalic acid co-crystal

Table A1.3.1: Fractional atomic coordinates and isotropic or equivalent isotropic displacement parameters of the GABA-oxalic acid co-crystal (Å^2).

	x	*y*	*z*	U_{iso}*/U_{eq}
C1	0.4548 (2)	0.76480 (15)	0.82536 (14)	0.0381 (3)
H4	0.5155	0.6807	0.8485	0.046*
H5	0.4626	0.8080	0.9149	0.046*
C2	0.5580 (2)	0.84471 (16)	0.74493 (14)	0.0414 (4)
H6	0.4963	0.9283	0.7208	0.050*
H7	0.5515	0.8010	0.6559	0.050*
C3	0.7653 (2)	0.86581 (17)	0.83354 (15)	0.0430 (4)
H8	0.8275	0.7823	0.8566	0.052*
H9	0.8276	0.9143	0.7768	0.052*
C4	0.78433 (18)	0.93869 (15)	0.97092 (14)	0.0342 (3)
N1	0.25376 (16)	0.74599 (12)	0.73996 (12)	0.0377 (3)
H1	0.1974	0.8229	0.7197	0.057*
H2	0.1970	0.6990	0.7904	0.057*
H3	0.2463	0.7048	0.6586	0.057*
O1	0.84502 (16)	0.86745 (10)	1.08670 (10)	0.0479 (3)
H10	0.8524	0.9121	1.1575	0.072*
O2	0.74580 (19)	1.05242 (12)	0.97406 (12)	0.0551 (3)
C5	0.9950 (2)	0.46330 (13)	1.06826 (13)	0.0321 (3)
O3	0.87406 (17)	0.37922 (11)	1.05383 (11)	0.0498 (3)
O4	1.11624 (17)	0.49738 (11)	1.18478 (10)	0.0497 (3)

Table A1.3.2: Atomic displacement parameters of the GABA-oxalic acid co-crystal (Å^2).

	U^{11}	U^{22}	U^{33}	U^{12}	U^{13}	U^{23}
C1	0.0406 (8)	0.0404 (8)	0.0299 (7)	−0.0014 (6)	0.0060 (6)	0.0008 (6)
C2	0.0428 (8)	0.0557 (9)	0.0250 (6)	−0.0062 (7)	0.0097 (6)	−0.0022 (6)
C3	0.0370 (8)	0.0626 (10)	0.0314 (7)	−0.0026 (7)	0.0135 (6)	−0.0094 (7)
C4	0.0301 (6)	0.0429 (8)	0.0291 (6)	−0.0040 (6)	0.0087 (5)	−0.0028 (6)
N1	0.0406 (7)	0.0397 (7)	0.0311 (6)	−0.0068 (5)	0.0091 (5)	0.0017 (5)
O1	0.0670 (8)	0.0447 (6)	0.0285 (5)	0.0070 (5)	0.0103 (5)	−0.0027 (4)
O2	0.0807 (9)	0.0439 (7)	0.0427 (6)	0.0094 (6)	0.0222 (6)	0.0047 (5)
C5	0.0395 (7)	0.0336 (7)	0.0237 (6)	−0.0004 (6)	0.0110 (5)	0.0011 (5)
O3	0.0589 (7)	0.0568 (7)	0.0324 (5)	−0.0227 (6)	0.0125 (5)	0.0049 (5)
O4	0.0631 (7)	0.0557 (7)	0.0225 (5)	−0.0179 (6)	0.0026 (5)	0.0043 (4)

Table A1.3.3: Bond lengths of the GABA-oxalic acid co-crystal (Å).

C1—N1	1.4835 (17)	C4—O2	1.2087 (18)
C1—C2	1.510 (2)	C4—O1	1.3068 (17)
C1—H4	0.9700	N1—H1	0.8900
C1—H5	0.9700	N1—H2	0.8900
C2—C3	1.533 (2)	N1—H3	0.8900
C2—H6	0.9700	O1—H10	0.8200
C2—H7	0.9700	C5—O3	1.2272 (17)
C3—C4	1.5097 (19)	C5—O4	1.2629 (16)
C3—H8	0.9700	C5—C5^{i}	1.560 (2)
C3—H9	0.9700		

Symmetry codes: (i) −*x*+2, −*y*+1, −*z*+2.

Table A1.3.4: Bond angles of the GABA-oxalic acid co-crystal (°).

N1—C1—C2	111.71 (11)	C2—C3—H9	109.3
N1—C1—H4	109.3	H8—C3—H9	107.9
C2—C1—H4	109.3	O2—C4—O1	122.80 (13)
N1—C1—H5	109.3	O2—C4—C3	123.27 (13)
C2—C1—H5	109.3	O1—C4—C3	113.93 (13)
H4—C1—H5	107.9	C1—N1—H1	109.5
C1—C2—C3	111.88 (12)	C1—N1—H2	109.5
C1—C2—H6	109.2	H1—N1—H2	109.5
C3—C2—H6	109.2	C1—N1—H3	109.5
C1—C2—H7	109.2	H1—N1—H3	109.5
C3—C2—H7	109.2	H2—N1—H3	109.5
H6—C2—H7	107.9	C4—O1—H10	109.5
C4—C3—C2	111.66 (11)	O3—C5—O4	126.27 (12)
C4—C3—H8	109.3	O3—C5—C5^{i}	118.47 (14)
C2—C3—H8	109.3	O4—C5—C5^{i}	115.26 (15)
C4—C3—H9	109.3		

Symmetry codes: (i) −*x*+2, −*y*+1, −*z*+2.

Table A1.3.5: Torsion angles of the GABA-oxalic acid co-crystal (°).

N1—C1—C2—C3	179.30 (12)	C2—C3—C4—O2	−70.69 (19)
C1—C2—C3—C4	−61.31 (18)	C2—C3—C4—O1	108.80 (15)

Table A1.3.6: Hydrogen bonding parameters of the GABA-oxalic acid co-crystal (Å,°).

D—H···*A*	*D*—H	H···*A*	*D*···*A*	*D*—H···*A*
N1—H1···O4^{ii}	0.89	1.94	2.8250 (17)	171
N1—H1···O3^{iii}	0.89	2.63	3.0592 (16)	111
N1—H2···O3^{iv}	0.89	1.94	2.8096 (16)	164
N1—H3···O2^{v}	0.89	2.05	2.8961 (17)	158
O1—H10···O4^{vi}	0.82	1.73	2.5474 (14)	175

Symmetry codes: (ii) $x-1, -y+3/2, z-1/2$; (iii) $-x+1, y+1/2, -z+3/2$; (iv) $-x+1, -y+1, -z+2$; (v) $-x+1, y-1/2, -z+3/2$; (vi) $-x+2, y+1/2, -z+5/2$.

1.3.2 Gabapentin-oxalic acid co-crystal

Table A1.3.7: Fractional atomic coordinates and isotropic or equivalent isotropic displacement parameters of the gabapentin-oxalic acid co-crystal(Å^2).

	x	*y*	*z*	U_{iso}*/U_{eq}
C1	0.53866 (15)	0.33665 (11)	0.34173 (4)	0.01608 (19)
C2	0.55374 (17)	0.35792 (12)	0.22119 (4)	0.0195 (2)
C3	0.48751 (18)	0.25931 (13)	0.27636 (4)	0.0219 (2)
H2	0.5626	0.1523	0.2758	0.026*
H3	0.3272	0.2386	0.2706	0.026*
C4	0.43706 (16)	0.22436 (11)	0.38927 (4)	0.0171 (2)
H14	0.4606	0.2740	0.4314	0.020*
H15	0.2763	0.2185	0.3787	0.020*
C5	0.42340 (18)	0.50372 (12)	0.34443 (5)	0.0226 (2)
H12	0.4708	0.5733	0.3101	0.027*
H13	0.2624	0.4877	0.3374	0.027*
C6	0.78643 (16)	0.36136 (13)	0.35730 (5)	0.0211 (2)
H4	0.8606	0.2539	0.3581	0.025*

H5	0.8466	0.4273	0.3238	0.025*
C7	0.4734 (2)	0.59204 (13)	0.40700 (6)	0.0314 (3)
H10	0.4045	0.7014	0.4049	0.038*
H11	0.4089	0.5300	0.4408	0.038*
C8	0.7204 (2)	0.60985 (15)	0.42232 (6)	0.0363 (3)
H8	0.7812	0.6851	0.3918	0.044*
H9	0.7476	0.6581	0.4646	0.044*
C9	0.83818 (19)	0.44632 (15)	0.42036 (5)	0.0298 (3)
H6	0.7916	0.3757	0.4545	0.036*
H7	0.9989	0.4637	0.4272	0.036*
C10	0.42935 (15)	0.48529 (11)	0.02839 (4)	0.01434 (18)
N1	0.52690 (13)	0.05509 (10)	0.39208 (4)	0.01588 (17)
H16	0.6720	0.0580	0.4056	0.024*
H17	0.5115	0.0094	0.3532	0.024*
H18	0.4520	−0.0055	0.4191	0.024*
O1	0.74308 (13)	0.38932 (11)	0.21192 (3)	0.0292 (2)
O2	0.38491 (12)	0.40120 (11)	0.18245 (3)	0.0291 (2)
H1	0.4302	0.4555	0.1527	0.044*
O3	0.23776 (11)	0.43727 (9)	0.01761 (3)	0.02081 (17)
O4	0.52499 (11)	0.51447 (9)	0.08163 (3)	0.02048 (17)

Table A1.3.8: Atomic displacement parameters of the gabapentin-oxalic acid co-crystal (Å^2).

	U^{11}	U^{22}	U^{33}	U^{12}	U^{13}	U^{23}
C1	0.0177 (4)	0.0176 (4)	0.0132 (4)	−0.0012 (3)	0.0024 (3)	0.0019 (3)
C2	0.0245 (5)	0.0209 (5)	0.0132 (4)	−0.0020 (4)	0.0030 (4)	−0.0009 (3)
C3	0.0291 (5)	0.0226 (5)	0.0143 (4)	−0.0069 (4)	0.0026 (4)	0.0012 (4)
C4	0.0178 (4)	0.0177 (4)	0.0163 (4)	0.0006 (3)	0.0051 (3)	0.0019 (3)
C5	0.0254 (5)	0.0196 (5)	0.0230 (5)	0.0026 (4)	0.0037 (4)	0.0037 (4)

C6	0.0182 (5)	0.0263 (5)	0.0189 (5)	−0.0032 (4)	0.0024 (4)	0.0035 (4)
C7	0.0489 (7)	0.0188 (5)	0.0278 (6)	0.0012 (5)	0.0109 (5)	−0.0017 (4)
C8	0.0560 (8)	0.0306 (6)	0.0226 (5)	−0.0190 (5)	0.0045 (5)	−0.0051 (4)
C9	0.0267 (6)	0.0426 (7)	0.0196 (5)	−0.0128 (5)	−0.0021 (4)	0.0027 (4)
C10	0.0164 (4)	0.0144 (4)	0.0126 (4)	0.0022 (3)	0.0032 (3)	0.0004 (3)
N1	0.0166 (4)	0.0182 (4)	0.0130 (4)	−0.0001 (3)	0.0021 (3)	0.0023 (3)
O1	0.0247 (4)	0.0440 (5)	0.0190 (4)	−0.0053 (3)	0.0030 (3)	0.0066 (3)
O2	0.0230 (4)	0.0468 (5)	0.0177 (4)	−0.0005 (3)	0.0036 (3)	0.0113 (3)
O3	0.0165 (3)	0.0304 (4)	0.0160 (3)	−0.0033 (3)	0.0040 (3)	−0.0028 (3)
O4	0.0194 (3)	0.0310 (4)	0.0112 (3)	−0.0033 (3)	0.0022 (3)	−0.0004 (3)

Table A1.3.9: Bond lengths of the gabapentin-oxalic acid co-crystal (Å).

C1—C6	1.5351 (13)	C6—H5	0.9900
C1—C4	1.5361 (12)	C7—C8	1.5230 (19)
C1—C5	1.5425 (13)	C7—H10	0.9900
C1—C3	1.5458 (13)	C7—H11	0.9900
C2—O1	1.2130 (13)	C8—C9	1.5230 (19)
C2—O2	1.3205 (13)	C8—H8	0.9900
C2—C3	1.5104 (13)	C8—H9	0.9900
C3—H2	0.9900	C9—H6	0.9900
C3—H3	0.9900	C9—H7	0.9900
C4—N1	1.4915 (12)	C10—O3	1.2373 (12)
C4—H14	0.9900	C10—O4	1.2628 (11)
C4—H15	0.9900	C10—C10^{i}	1.5594 (17)
C5—C7	1.5324 (15)	N1—H16	0.9100
C5—H12	0.9900	N1—H17	0.9100
C5—H13	0.9900	N1—H18	0.9100
C6—C9	1.5301 (15)	O2—H1	0.8400
C6—H4	0.9900		

Symmetry codes: (i) −*x*+1, −*y*+1, −*z*.

Table A1.3.10: Bond angles of the gabapentin-oxalic acid co-crystal (°).

C6—C1—C4	111.97 (8)	C1—C6—H5	109.1
C6—C1—C5	108.54 (8)	H4—C6—H5	107.8
C4—C1—C5	107.47 (8)	C8—C7—C5	111.24 (9)
C6—C1—C3	112.27 (8)	C8—C7—H10	109.4
C4—C1—C3	106.80 (8)	C5—C7—H10	109.4
C5—C1—C3	109.67 (8)	C8—C7—H11	109.4
O1—C2—O2	123.12 (9)	C5—C7—H11	109.4
O1—C2—C3	123.68 (9)	H10—C7—H11	108.0
O2—C2—C3	113.15 (9)	C9—C8—C7	111.71 (9)
C2—C3—C1	116.09 (8)	C9—C8—H8	109.3
C2—C3—H2	108.3	C7—C8—H8	109.3
C1—C3—H2	108.3	C9—C8—H9	109.3
C2—C3—H3	108.3	C7—C8—H9	109.3
C1—C3—H3	108.3	H8—C8—H9	107.9
H2—C3—H3	107.4	C8—C9—C6	111.02 (9)
N1—C4—C1	114.81 (7)	C8—C9—H6	109.4
N1—C4—H14	108.6	C6—C9—H6	109.4
C1—C4—H14	108.6	C8—C9—H7	109.4
N1—C4—H15	108.6	C6—C9—H7	109.4
C1—C4—H15	108.6	H6—C9—H7	108.0
H14—C4—H15	107.5	O3—C10—O4	126.42 (8)
C7—C5—C1	113.02 (9)	O3—C10—C10^{i}	118.20 (10)
C7—C5—H12	109.0	O4—C10—C10^{i}	115.38 (10)
C1—C5—H12	109.0	C4—N1—H16	109.5
C7—C5—H13	109.0	C4—N1—H17	109.5
C1—C5—H13	109.0	H16—N1—H17	109.5
H12—C5—H13	107.8	C4—N1—H18	109.5
C9—C6—C1	112.70 (8)	H16—N1—H18	109.5
C9—C6—H4	109.1	H17—N1—H18	109.5
C1—C6—H4	109.1	C2—O2—H1	109.5

C9—C6—H5	109.1		

Symmetry codes: (i) −*x*+1, −*y*+1, −*z*.

Table A1.3.11: Torsion angles of the gabapentin-oxalic acid co-crystal (°).

O1—C2—C3—C1	65.25 (14)	C4—C1—C5—C7	66.60 (11)
O2—C2—C3—C1	−117.36 (10)	C3—C1—C5—C7	−177.66 (8)
C6—C1—C3—C2	−62.50 (12)	C4—C1—C6—C9	−63.00 (11)
C4—C1—C3—C2	174.41 (8)	C5—C1—C6—C9	55.48 (11)
C5—C1—C3—C2	58.24 (11)	C3—C1—C6—C9	176.88 (8)
C6—C1—C4—N1	−62.02 (10)	C1—C5—C7—C8	54.86 (12)
C5—C1—C4—N1	178.88 (8)	C5—C7—C8—C9	−53.86 (12)
C3—C1—C4—N1	61.25 (10)	C7—C8—C9—C6	54.69 (12)
C6—C1—C5—C7	−54.68 (11)	C1—C6—C9—C8	−56.58 (12)

Table A1.3.12: Hydrogen bonding parameters of the gabapentin-oxalic acid co-crystal (Å,°).

D*—H···*A	***D*—H**	**H···*A***	***D*···*A***	***D*—H···*A***
N1—H16···O4^{ii}	0.91	1.88	2.7668 (11)	164
N1—H16···O3^{iii}	0.91	2.40	2.8898 (11)	114
N1—H17···O1^{ii}	0.91	2.34	3.0380 (11)	134
N1—H17···O2^{iv}	0.91	2.63	3.1358 (11)	116
N1—H18···O3^{iv}	0.91	1.90	2.7810 (10)	161
O2—H1···O4	0.84	1.74	2.5533 (10)	164

Symmetry codes: (ii) −*x*+3/2, *y*−1/2, −*z*+1/2; (iii) *x*+1/2, −*y*+1/2, *z*+1/2; (iv) −*x*+1/2, *y*−1/2, −*z*+1/2.

1.3.3 β-alanine-oxalic acid-water co-crystal

Table A1.3.13: Fractional atomic coordinates and isotropic or equivalent isotropic displacement parameters of the β-alanine-oxalic acid-water co-crystal (Å^2).

	x	*y*	*z*	U_{iso}*/U_{eq}
C1	0.27443 (9)	−0.0044 (4)	0.60455 (15)	0.0354 (5)
C2	0.29133 (10)	0.1804 (4)	0.68747 (17)	0.0418 (5)
H6	0.3042	0.1039	0.7552	0.050*
H7	0.2519	0.2716	0.6735	0.050*
C3	0.34573 (10)	0.3462 (4)	0.69565 (16)	0.0392 (5)
H4	0.3375	0.4007	0.6256	0.047*
H5	0.3453	0.4817	0.7371	0.047*
C4	0.41515 (9)	0.7971 (3)	0.96368 (14)	0.0306 (4)
C5	0.42914 (9)	1.0422 (3)	1.01543 (14)	0.0284 (4)
N1	0.41161 (8)	0.2348 (3)	0.74478 (13)	0.0379 (4)
H1	0.4197	0.1872	0.8096	0.057*
H2	0.4422	0.3382	0.7481	0.057*
H3	0.4126	0.1121	0.7063	0.057*
O1	0.23235 (9)	−0.1580 (3)	0.60741 (13)	0.0604 (5)
O2	0.29607 (8)	−0.0082 (3)	0.53827 (12)	0.0535 (5)
O3	0.42921 (8)	0.6255 (2)	1.03091 (11)	0.0465 (4)
O4	0.39377 (10)	0.7744 (3)	0.86972 (12)	0.0631 (5)
O5	0.44872 (8)	1.0548 (2)	1.11208 (10)	0.0461 (4)
O6	0.41960 (8)	1.2091 (2)	0.95282 (11)	0.0446 (4)
O7	0.5000	1.4153 (3)	1.2500	0.0357 (5)
H8	0.2213 (13)	−0.269 (5)	0.554 (2)	0.069 (8)*
H9	0.4251 (14)	0.475 (6)	0.995 (2)	0.089 (10)*
H10	0.4811 (12)	1.317 (5)	1.1973 (18)	0.061 (8)*

Table A1.3.14: Atomic displacement parameters of the β-alanine-oxalic acid-water co-crystal (Å^2).

	U^{11}	U^{22}	U^{33}	U^{12}	U^{13}	U^{23}
C1	0.0346 (10)	0.0400 (11)	0.0309 (10)	−0.0034 (9)	0.0133 (8)	−0.0026 (8)
C2	0.0440 (12)	0.0485 (13)	0.0344 (11)	−0.0032 (9)	0.0181 (9)	−0.0106 (9)
C3	0.0512 (12)	0.0300 (10)	0.0324 (10)	−0.0009 (9)	0.0140 (9)	−0.0072 (8)
C4	0.0432 (11)	0.0212 (9)	0.0267 (10)	−0.0033 (7)	0.0143 (8)	−0.0021 (7)
C5	0.0369 (9)	0.0212 (9)	0.0282 (9)	−0.0032 (7)	0.0150 (8)	−0.0034 (7)
N1	0.0440 (10)	0.0400 (9)	0.0295 (9)	−0.0067 (8)	0.0155 (7)	−0.0046 (7)
O1	0.0784 (12)	0.0665 (11)	0.0541 (11)	−0.0393 (10)	0.0452 (10)	−0.0249 (9)
O2	0.0672 (10)	0.0557 (10)	0.0527 (10)	−0.0278 (8)	0.0401 (9)	−0.0241 (8)
O3	0.0858 (12)	0.0195 (7)	0.0316 (8)	0.0001 (7)	0.0227 (7)	0.0001 (6)
O4	0.1184 (15)	0.0296 (8)	0.0257 (8)	−0.0073 (9)	0.0162 (9)	−0.0058 (6)
O5	0.0780 (11)	0.0303 (7)	0.0277 (8)	−0.0135 (7)	0.0205 (7)	−0.0061 (6)
O6	0.0814 (11)	0.0201 (7)	0.0337 (8)	−0.0012 (6)	0.0262 (8)	0.0004 (6)
O7	0.0492 (12)	0.0242 (10)	0.0264 (10)	0.000	0.0092 (9)	0.000

Table A1.3.15: Bond lengths of the β-alanine-oxalic acid-water co-crystal (Å).

C1—O2	1.220 (2)	C4—O3	1.301 (2)
C1—O1	1.300 (2)	C4—C5	1.543 (2)
C1—C2	1.493 (3)	C5—O5	1.236 (2)
C2—C3	1.508 (3)	C5—O6	1.249 (2)
C2—H6	0.9700	N1—H1	0.8900
C2—H7	0.9700	N1—H2	0.8900
C3—N1	1.479 (3)	N1—H3	0.8900
C3—H4	0.9700	O1—H8	0.93 (3)
C3—H5	0.9700	O3—H9	0.98 (3)
C4—O4	1.202 (2)	O7—H10	0.88 (2)

Table A1.3.16: Bond angles of the β-alanine-oxalic acid-water co-crystal (°).

O2—C1—O1	122.86 (18)	O4—C4—O3	125.02 (17)
O2—C1—C2	123.79 (18)	O4—C4—C5	121.25 (16)
O1—C1—C2	113.31 (17)	O3—C4—C5	113.72 (15)
C1—C2—C3	115.34 (17)	O5—C5—O6	126.93 (17)
C1—C2—H6	108.4	O5—C5—C4	118.28 (16)
C3—C2—H6	108.4	O6—C5—C4	114.78 (15)
C1—C2—H7	108.4	C3—N1—H1	109.5
C3—C2—H7	108.4	C3—N1—H2	109.5
H6—C2—H7	107.5	H1—N1—H2	109.5
N1—C3—C2	112.34 (17)	C3—N1—H3	109.5
N1—C3—H4	109.1	H1—N1—H3	109.5
C2—C3—H4	109.1	H2—N1—H3	109.5
N1—C3—H5	109.1	C1—O1—H8	112.1 (17)
C2—C3—H5	109.1	C4—O3—H9	110.3 (18)
H4—C3—H5	107.9		

Table A1.3.17: Torsion angles of the β-alanine-oxalic acid-water co-crystal (°).

O2—C1—C2—C3	−9.0 (3)	O3—C4—C5—O5	−3.3 (3)
O1—C1—C2—C3	173.20 (19)	O4—C4—C5—O6	−3.3 (3)
C1—C2—C3—N1	−73.8 (2)	O3—C4—C5—O6	176.04 (17)
O4—C4—C5—O5	177.3 (2)		

Table A1.3.18: Hydrogen bonding parameters of the β-alanine-oxalic acid-water co-crystal (Å,°).

D—H···*A*	*D*—H	H···*A*	*D*···*A*	*D*—H···*A*
N1—H1···O6^{i}	0.89	2.02	2.852 (2)	156
N1—H1···O4^{i}	0.89	2.65	3.274 (2)	128
N1—H3···O5^{ii}	0.89	2.06	2.866 (2)	151
N1—H2···O7^{iii}	0.89	1.90	2.790 (2)	174
O1—H8···O2^{iv}	0.93	1.73	2.663 (2)	175
O3—H9···O6^{i}	0.98	1.62	2.584 (2)	171
O7—H10···O5	0.88	1.86	2.717 (2)	166

Symmetry codes: (i) *x*, *y*−1, *z*; (ii) *x*, −*y*+1, *z*−1/2; (iii) −*x*+1, −*y*+2, −*z*+2; (iv) −*x*+1/2, −*y*−1/2, −*z*+1.

1.4 Additional Experimental Work Performed

Experiments were set up in order to attempt the co-crystallization of different amino acids. Initially, attempts were made to reproduce the co-crystals grown by Görbitz *et al.,* (1999) which include the co-crystallization of hydrophobic D- and L-amino acids. Some of the crystals which have been produced by Görbitz *et al.,* (1999) include the co-crystals of L-isoleucine with the D-amino acids D-valine, D-leucine, D-alanine, D-methionine and D-norleucine.

In order to reproduce these crystals, the same experimental method was followed (Görbitz *et al.*, 1999) which involves gel diffusion. Crystals were formed in the gel for L-isoleucine and D-norleucine using 96% ethanol as the diffusion solvent. The crystals however, were too small and flat to obtain the unit cell and collect data. Therefore, they could not be characterised. The remaining co-crystallization attempts using this same method did not produce crystals.

Various methods were attempted to produce co-crystals of GABA and gabapentin with the amino acids D-valine, β-alanine, L-aspartic acid, L-glutamic acid, L-serine, L-glycine. The gel diffusion method was again attempted; however, no crystals were obtained. Equimolar amounts of each amino acid were then also dissolved in various solvents including water, ethanol, methanol and 2-propanol and left under open-air evaporation. In this case, only crystals of the starting materials were produced. Crystallizations were also attempted at 60°C and 100°C, again not producing co-crystals. Refluxing of the solutions was also carried out, but this did not aid in the formation of co-crystals.

In order to test for the possible co-crystallization of further amino acids such as L-valine, D-norleucine, L-isoleucine and D-methionine, the method of solvent grinding was used and X-ray powder diffraction patterns of the ground products and starting materials were recorded. These patterns again did not indicate the presence of any different crystalline phases.

1.5 References

Görbitz, C.H., Dalhus, B. (1999). Acta Cryst., B55, 424-431.